Universitat de Lleida

ROLE OF VOLTAGE GATED T-TYPE CALCIUM CHANNELS IN THE VIABILITY OF HUMAN MELANOMA CELLS

Arindam Das

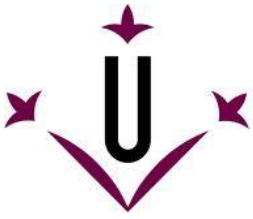

ROLE OF VOLTAGE GATED T-TYPE CALCIUM CHANNELS IN THE VIABILITY OF HUMAN MELANOMA CELLS

Arindam Das

Doctoral Thesis

Directors

Dr. Carles Cantí Nicolás

Dra. Rosa Maria Martí Laborda

Lleida, 2012

Universitat de Lleida

IRB Lleida
Institut de Recerca Biomèdica

Dr. **Carles Cantí Nicolás**, Principal Investigator of Calcium signalling and neuronal differentiation Laboratory at the Institute for Biomedical Research ,Lleida and Dr. **Rosa Maria Marti Laborda**, professor at the department of medicine at HUAV, university of Lleida ,as supervisors of the thesis

Hereby state that,

Arindam Das with a B.Sc. degree in Zoology and M.Sc. degree in Environmental Sciences both acquired from the University of Calcutta, India has performed under our direction and supervision, and within the Laboratory of Calcium signalling and neuronal differentiation of the Department of experimental medicine, the experiment work entitled "**Role of voltage gated T-type calcium channels in the viability of human melanoma cells** ".

The work accomplishes the adequate conditions in order to be defended in front of the corresponding Thesis Committee and, if it is case, to obtain the **Doctor degree** from the *University of Lleida.*

Signed

Carles Canti Nicolás **Rosa María Marti Laborda**

Lleida 2012

“I have a friend who's an artist and has sometimes taken a view which I don't agree with very well. He'll hold up a flower and say "look how beautiful it is," and I'll agree. Then he says "I as an artist can see how beautiful this is but you as a scientist takes this all apart and it becomes a dull thing," and I think that he's kind of nutty. First of all, the beauty that he sees is available to other people and to me too, I believe. Although I may not be quite as refined aesthetically as he is ... I can appreciate the beauty of a flower. At the same time, I see much more about the flower than he sees. I could imagine the cells in there, the complicated actions inside, which also have a beauty. I mean it's not just beauty at this dimension, at one centimeter; there's also beauty at smaller dimensions, the inner structure, also the processes. The fact that the colors in the flower evolved in order to attract insects to pollinate it is interesting; it means that insects can see the color. It adds a question: does this aesthetic sense also exist in the lower forms? Why is it aesthetic? All kinds of interesting questions which the science knowledge only adds to the excitement, the mystery and the awe of a flower. It only adds. I don't understand how it subtracts.”

Richard P Feynman

Acknowledgement

Standing at the end of my Ph.D. research work I feel good that I have the opportunity to express my gratitude to all people who have helped and inspired me during my doctoral study.

First I want to thank my supervisors Dr. Carles Cantí Nicolàs and Dra.Rosa Maria Martí Laborda for their constant encouragement and guidance with an open mind during the entire period of my work. I consider myself to be extremely fortunate to obtain an opportunity to work under the guidance of Dr. Carles Cantí Nicolàs and have him as the mentor of my Ph.D. He was always generous to provide me intellectual space, and taught me the value of good scientific work. I would also like to express my sincere gratitude to Dra.Rosa Maria Marti for her continuous support during my Ph.D study and research. Her patience, motivation, enthusiasm, and immense knowledge had motivated all her advisees, including me.

I wish to express my sincere appreciation to Dr. Xavier Matias Guiu for giving me an opportunity to be a member of IRB Lleida and a part of his group. Without his sound advice and constant selfless guidance the work presented in this thesis would not have been achieved. He was always there to guide me for every single step during the long four years of my Ph.D.

I especially want to thank Dra.Judith Herreros for her support and patient advice throughout my thesis. Her perpetual energy and enthusiasm in research, deep vision, in depth knowledge and enormous experience in the field of cell biology, had helped and inspired me a lot in my Ph.D study

I wish to thank Dr. Joseph Esquerda and Dr. Olga Tarabal for their sound advices during the long sessions of calcium imaging.

I am also grateful to Dr. Reinald Pamplona, Dra. Conchi Mora, Dr. Jose Valdivieso, Dra. Adriana Dusso, Dr. Xavier Dolcet, Dr. Mario Encinas, Dra. Judit Ribas, Dra. Andree Yeramian, Dra. Marta Llovera and Dr. Daniel Sanchis for their kindness and willingness to help each time they were asked.

I would also like to show my gratitude to Dr. Ramon Vilella from the department of immunology, hospital clinic of Barcelona for providing me wide variety of melanoma cell lines..

I would like to thank UDL, Government of Catalunya and Government of Spain for giving me the financial support during my Ph.D.

I am indebted to Dr. Nihar Ranjan Jana for giving me the opportunity to work for one year in National Brain research Centre, India. The associated experience broadened my perspective on the molecular biology techniques. I would like to thank late Dr. Swapan Kumar Das, Dr Aniruddha Mukherjee and Dr. Punarbasu Chowdhury for their continuous encouragement to do better science in my early university days.

I also thank members of the neuronal differentiation and calcium signalling laboratory - Charumathi, Mireia (the most wonderful person) and Deepshikha for their collaboration, humour and encouragement. Thank you guys and keep up the good work!!!

I would like to acknowledge my seniors Annabel, Nuria B and Milica for their immense support and assistance throughout all over my research work, publishing articles and preparation of thesis.

I would like to thank Monica D, David, Esteban, Maya, Jiseng, Omar, Dani, Hugo, Nuria E, ChristinaG Laura, Christina M, Anna macia, Myriam, Marta, Junemei, Ester, Berta, Estella, Petya, Montse, Noelia, AnnaV, Dolors, Azahar, Carme G, Paolo, Hiren, Bupesh, Venkat, Saravanan for their help and encouragement.I would like to thank especially Carlos, Lilliana, Alejandra and Disha for being my friend and the support you gave me. I treasure all precious moments we shared with you people in the Institute, hospital as well as in the caferetia!!!! It is a pleasure working with you people.

I am grateful to Dra.Anis Panosa for her enormous help to obtain best results and best quality images of flow cytometry studies.

I express full-hearted gratitude to my parents. Without their blessings and mental support, it would not be possible for me to cross the long way of Ph.D. To them I dedicate my thesis. No words are sufficient to express my heartfelt thanks to my sister, my brother in law and little Uttiyo for their encouragement and support especially during the tough times in my career. My deepest gratitude also goes to my parent in laws for their belief in me and whole hearted motivation for last couple of years.

Finally I thank my wonderful and patient wife Upasana for always standing by me, supporting and encouraging me to reach my fullest potential and always reassuring me that there is light at the end of the tunnel.

Arindam

Index

Abbreviations

AIF	Apoptosis-inducing factor
DNA	Deoxyribonucleic acid
VGCC	Voltage gated calcium channel
RNA	Ribonucleic acid
JNK	Jun N-terminal kinases
siRNA	Small interfering RNA
VDAC	Voltage dependent anion channel
Ca_v	Voltage gated calcium channel
DMSO	Dimethyl sulfoxide
dNTP	Deoxyribonucleotide
ER	Endoplasmic reticulum
FBS	Foetal bovine serum
mRNA	Messenger RNA
Q RT-PCR	Quantitative Real Time Polymerase Chain reaction
RT-PCR	Reverse Transcriptase Polymerase Chain Reaction
WB	Western Blott
XBP-1	X Box Binding Protein1
GADD153	Growth Arrest And DNA Damage Inducible Gene 153
GRP 78	Glucose Regulated Protein 78
ATG	Autophagy related gene
Bcl-2	B-cell lymphoma 2
ATF	Activating transcription factor
BiP	Binding immunoglobulin protein
nM	Nano molar
eIF2α	Eukaryotic initiation factor 2α
MTT	3-(4,5-dimethylthiazol-2-yl)-2,5-diphenyltetrazolium bromide
LC3	Light Chain 3
IRE1α	Inositol-requiring enzyme α
PERK	Protein kinase RNA-like endoplasmic reticulum kinase
UPR	Unfolded Protein Response
Tg	Thapsigargin
µM	Micromolar
Mib	Mibefradil
Pim	Pimozide
FURA2/AM	Fura-2-acetoxymethyl ester
Ca^{2+}	Calcium ion
IP_3	Inositol 1,4,5-trisphosphate
Kda	Kilo Dalton
kb	Kilobase
SDS-PAGE	Sodium dodecyl sulfate polyacrylamide gel electrophoresis

TBST-buffer	Tris Buffer saline in Tween 20
VOCC	Voltage operated Calcium channel
SERCA	Sarco / endoplasmic reticulum Ca^{2+}- ATPase
SOCC	Store operated calcium channel
AV	Autophagic Vacuole
eIF3e	Eukaryotic translation initiation factor 3, subunit e
GAPDH	Glyceraldehyde 3-phosphate dehydrogenase
PBS	Phosphate buffer saline
WST-1	4-[3-(4-iodophenyl)-2-(4-nitrophenyl)-2H-5-tetrazolio]-1,3-benzene disulfonate
cAMP	Cyclic adenosine monophosphate
CaMK	Calcium/Calmodulin-dependent protein kinase
shRNA	Small hairpin RNA
XBP-1	X Box Binding Protein
SDS	Sodium dodecyl sulphate
Sec.	Seconds
HRP	Horseradish peroxidase
Tween 20	Polyoxyethylene sorbitan monolaurate
Caspases	Cysteine-containing aspartate specific proteases
CQ	Chloroquine
BAX	BCL-2 associated X protein
PTEN	Phosphatase And Tensin Homologue Deleted On Chromosome 10
PI3K	Phosphatidylinositol-3-kinase
PCD	Programmed Cell Death
PTP	Permeability transition pore
PI	Propidium Iodide
RGP	Radial Growth Phase
VGP	Vertical growth phase
SSM	Superficial spreading melanoma
UV	Ultraviolet
PKC	Protein kinase C
PDGF	Platelet-derived growth factor
VEGF	Vascular endothelial growth factor
CDK	Cyclin dependent kinase
cDNA	Complementary deoxyribonucleic acid
dNTP	Deoxynucleotide triphosphate
ERSE	ER stress response element
UPRE	UPR promoter element
ERAD	ER-associated degradation
RT	Room temperature

Abstract

ABSTRACT

The expression of voltage-gated calcium channels (VGCCs) has not been reported previously in melanoma cells in spite of increasing evidence of a role of VGCCs in tumorigenesis and tumour progression. To address this issue we have performed an extensive RT-PCR analysis of VGCC expression in human melanocytes and a range of melanoma cell lines and biopsies. In addition, we have tested the functional expression of these channels using Ca^{2+} imaging techniques, and examined their relevance for the viability and proliferation of the melanoma cells. Our results show that control melanocytes and melanoma cells express channel isoforms belonging to the Ca_v1 and Ca_v2 gene families. Importantly, the expression of isoforms of low voltage-activated Ca_v3 (T-type) channel is restricted to melanoma. We have confirmed the function of T-type channels as mediators of constitutive divalent cations influx in melanoma cells. Additionally, pharmacological and gene silencing approaches demonstrate a role for T-type channels in melanoma viability and proliferation.

These results encourage the analysis of T-type VGCCs as targets for therapeutic intervention in melanoma tumorigenesis and ⁄or tumour progression. In this regard, we have found that Mibefradil and Pimozide, two structurally-unrelated, clinically-used T-type Ca^{2+} channel blockers, inhibit the growth of melanoma cells *in vitro*, and that this effect is due to both a reduction in the proliferation rate and an induction of caspase-dependent cell death. We have further explored the molecular pathways leading to T-type channels blockers-mediated apoptosis, and found that both drugs induce endoplasmic reticulum (ER) stress and a subsequent inhibition of the basal autophagy present in melanoma cells. Finally, we have demonstrated by gene silencing experiments that the $Ca_v3.1$ and $Ca_v3.2$ isoforms of T-type channels are the targets of T-type channel blockers, regarding their effects on melanoma ER-stress and autophagy.

Altogether, the results attained in this thesis point to T-type Ca^{2+} channels as putative prognosis markers and therapeutic targets to tackle melanoma metastasis.

RESUM

En aquest treball de tesi hem estudiat per primera vegada l'expressió funcional dels canals de calci dependents de voltatge (CCDV) en melanòcits humans i un ampli rang de línies cel.lulars i biòpsies de melanoma humà, mitjançant tècniques de biologia molecular i d'imatge. Els nostres resultats demostren que els melanòcits control i les cèl.lules de melanoma expréssen isoformes de les famílies de gens Ca_v1 i Ca_v2. De forma destacable, l'expressió d'isoformes de la família Ca_v3 (canals de tipus T) es troba restringida a les cèl.lules de melanoma, en les que promouen la progressió del cicle cel.lular.

Aquests resultats motiven l'anàlisi dels CCDV-T com a dianes terapèutiques contra la tumorigènesi i/o progressió tumoral del melanoma. En aquesta línea, hem trobat que mibefradil i pimozida, dos bloquejants de CCDV-T d'us clínic, inhibeixen el creixement de les cèl.lules de melanoma *in vitro*, i que aquest efecte és degut tant a una reducció de la proliferació cel.lular, com a una inducció de la mort dependent de caspases. Hem explorat les vies moleculars implicades en el procés apoptòtic i hem trobat que ambdues drogues indueixen estrés de reticle endoplasmàtic (RE) i la inhibició subsequent de l'autofàgia basal constitutiva present a les cèl.lules de melanoma. Finalment, hem demostrat, a través del seu silenciament gènic, que la isoforma $Ca_v3.2$ és la diana molecular dels bloquejants de CCDV-T, en el que respecta als seus efectes sobre l'estrés de RE i l'autofàgia.

Conjuntament, els resultats obtinguts en el decurs d'aquesta tesi apunten als canals de tipus T como a possibles marcadors de pronòstic i/o dianes terapèutiques contra la metastasi del melanoma.

RESUMEN

Hemos estudiado por primera vez la expresión funcional de los canales de calcio voltaje-dependientes (CCDV) en melanocitos humanos y un amplio rango de líneas celulares y biopsias de melanoma humano, mediante técnicas de biología molecular y de imagen. Nuestros resultados demuestran que los melanocitos control y las células de melanoma expresan isoformas pertenecientes a las famílias de genes Ca_v1 y Ca_v2. De forma destacable, la expresión de isoformas de la família Ca_v3 (canales de tipo T) se encuentra restringida a las células de melanoma, en las que promueven la progresión del ciclo celular.

Estos resultados motivan el análisis de los CCDV-T como dianas terapéuticas contra la tumorigénesis y/o progresión tumoral del melanoma. En esta línea, hemos encontrado que mibefradil y pimozida, dos bloqueantes de CCDV-T de uso clínico, inhiben el crecimiento de las células de melanoma *in vitro*, y que este efecto es debido tanto a una reducción de la proliferación celular como a una inducción de la muerte dependiente de caspasas. Hemos explorado las vías moleculares implicadas en el proceso apoptótico y hemos hallado que ambas drogas inducen estrés de retículo endoplasmático (RE) y la inhibición subsiguiente de la autofagia basal constitutiva presente en las células de melanoma. Finalmente, hemos demostrado, a través de su silenciamiento génico, que la isoforma $Ca_v3.2$ es la diana molecular de los bloqueantes de CCDV-T en lo concerniente a sus efectos sobre el estrés de retículo endoplasmático y la autofagia.

Conjuntamente, los resultados obtenidos en el curso de esta tesis apuntan a los canales de tipo T como posibles marcadores de pronóstico y/o dianas terapéuticas contra la metástasis del melanoma.

Introduction

1. Melanoma

1.1 Introduction:

Malignant melanoma is a neoplasm of the skin which arises primarily from transformed melanocytes *de novo* or from dysplastic, congenital, or common nevi[1-5]. As in many cancers, both genetic predisposition and exposure to environmental agents are risk factors for melanoma development. Researchers have identified a number of risk factors associated with melanoma. These risk factors are grouped into four categories: 1. Environmental. 2. Genetic. 3. Immunosuppresive. 4. Previous melanoma. Studies have shown that melanoma primarily affects fair-haired and fair-skinned individuals and those who burn easily or have a history of severe sunburn. The UV component of sunlight causes skin damage and increases the risk for skin cancers such as melanoma. The exact mechanism and wavelengths of UV light that are the most critical remain controversial, but both UV-A (wavelength 320–400 nm) and UV-B (290–320 nm) have been implicated[6].

Cutaneous melanoma can be subdivided into several subtypes, primarily based on anatomic location and patterns of growth. The majority of melanoma subtypes are observed to progress through distinct histological phases. As cutaneous melanomas progress from the radial growth phase (RGP) to the vertical growth phase (VGP), treatment options, cure rates, and survival rates decrease dramatically. Most melanoma subtypes demonstrate a slow RGP restricted to the epidermis, followed by a potentially more rapid VGP. RGP melanoma cells extend upward into the epidermis (pagetoid spread) but remain in situ and lack the capacity to invade the dermis and metastasize[6, 8, 9] (figure 1)

Although cutaneous melanoma only accounts for 5-7% of all skin malignancies, it is the most lethal, being responsible for about 75% of all skin tumour deaths[7, 11]. Once in advanced stage, the prognosis of patients with melanoma becomes very poor. Chemotherapy has failed to improve the survival of these patients[12]. Primary melanoma lesions may present various clinical subtypes, and within these may display wide diversity in characteristics of form and clinical progression. Such heterogeneity can make diagnosis difficult and, in the case of a confirmed melanoma, it can complicate prognostic

calculation[13]. Furthermore, recent cellular and molecular studies are continuing to reveal many additional variations, suggesting that such heterogeneity in melanoma may underlie the continued failure of current experimental therapy[14].

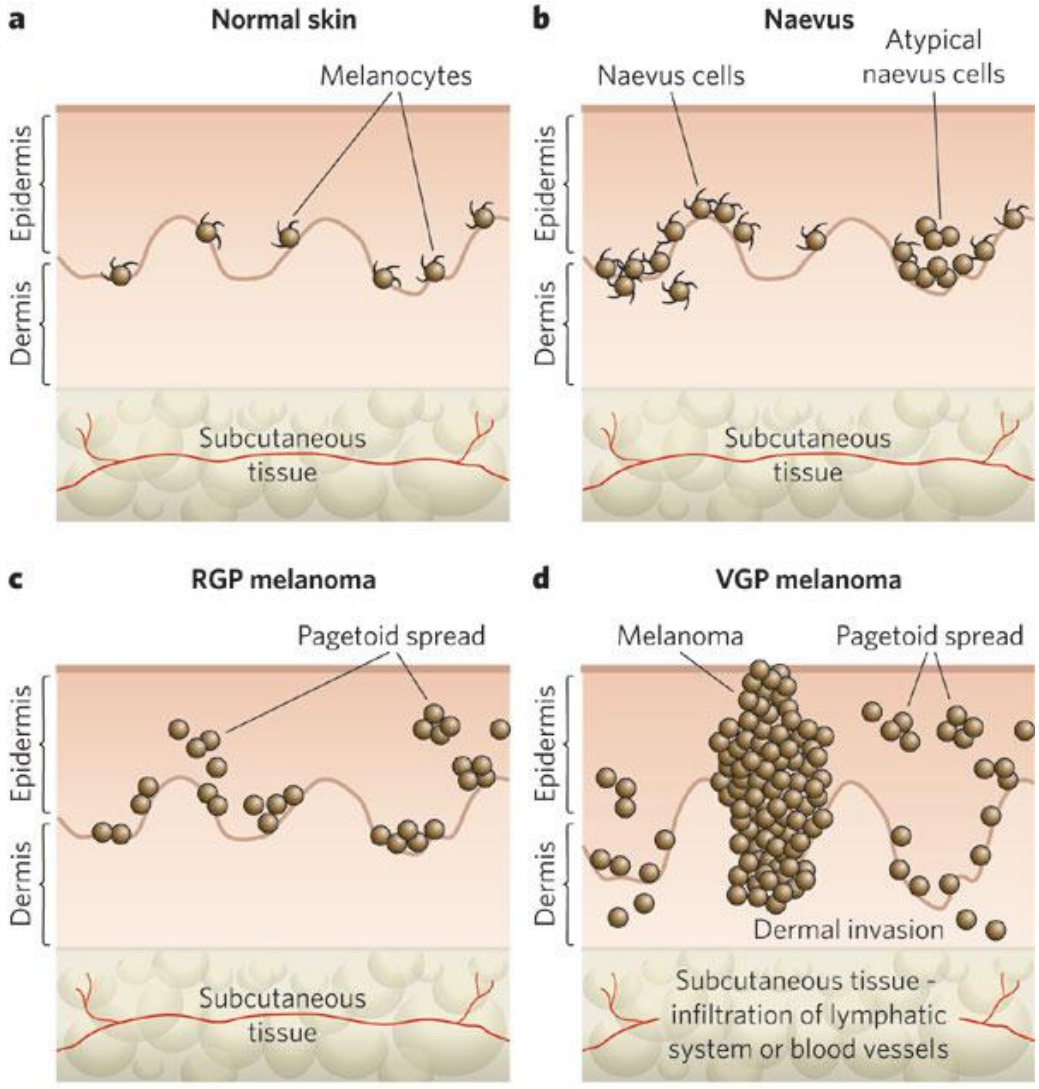

Figure 1. *Various stages of melanomagenesis and tumor progression for melanomas arising on a melanocytic nevi.* ***a.*** *Normal skin. This shows an even distribution of melanocytes within the basal layer of the epidermis.* ***b.*** *Naevus. In the early stages, benign melanocytic naevi occur with increased numbers of melanocytes.* ***c****. Radial-growth-phase (RGP) melanoma. This is considered to be the primary malignant stage.* ***d****. Vertical-growth-phase (VGP) melanoma. This is the first stage that is considered to have malignant potential and leads directly to metastatic malignant melanoma by infiltration of the vascular and lymphatic systems. Pagetoid spread describes the upward migration or vertical stacking of melanocytes that is a histological characteristic of melanoma (scheme adapted from Vanessa Gray-Schopfer 2007)*[12]

1.2 Melanoma epidemiology

Rising incidence rates of cutaneous melanoma have been observed during the last four decades in white populations worldwide. The cancer statistics in the United States have revealed 6 cases per 100,000 inhabitants and year at the beginning of the 1970s and 18 cases per 100,000 inhabitants and year at the beginning of 2000, demonstrating a three-fold increase in incidence rates. Incidence rates in central Europe increased in the same time period from 3 to 4 cases to 10 to 15 cases per 100,000 inhabitants and year, which is very similar to the increase in the United States. Cohort studies from several countries indicate that the trend of increasing incidence rates will continue in the future for at least the next 2 decades; thus, an additional doubling of incidence rates is expected. The highest incidence rates have been reported from Australia and New Zealand, from 40 to 60 cases per 100,000 inhabitants and year[15-17].

1.3 Melanoma and calcium signalling

Ca^{2+}-signaling of human cutaneous melanoma is in the focus of intensive research in recent years. Genomic and functional studies pointed to the important role of various Ca^{2+} channels in melanoma, but these data were contradictory. Ca^{2+}-signaling is suspected to play an important role in the development as well as in the viability and motility of melanoma cells[18-20]. The significance of Ca^{2+} in melanoma is supported by the fact that a Ca^{2+}-dependent isoform of protein kinase C is overexpressed in melanoma[21]. On the other hand, it is known that intracellular Ca^{2+} oscillations are critical for the survival and migration of melanoma cells[18, 19]. The melanocytic linage is characterized by a special resistance to apoptosis, which might be attenuated during malignant transformation. It is now well established that apoptosis regulatory proteins B-cell lymphoma/leukemia-2 gene/Bax are regulators of the endoplasmic reticulum Ca^{2+} stores, and that Ca^{2+} is a key mediator of apoptosis in a variety of cell types[22]. It has been claimed that the enhanced expression and/or function of Ca^{2+} channels in the plasma membrane of human melanoma cells may play an important role in their resistance to apoptosis[23].

2. Voltage-gated calcium channels

2.1 Introduction:

Ionized calcium (Ca^{2+}) is a ubiquitous second messenger, and temporally and spatially coded changes in the cytosolic Ca^{2+} levels are critical for linking external stimuli to cell physiology. Ca^{2+}-signaling directs a wide range of intracellular processes, ranging from short-term control of contraction, synaptic transmission, endo and exocytosis and modulation of enzyme function and metabolism, to longer-term control of gene expression, cell cycle progression, apoptosis, differentiation and proliferation[24-26]. The extracellular milieu is the ultimate source of Ca^{2+}, which flows into the cells through ion channels present in plasma membrane (figure 2).

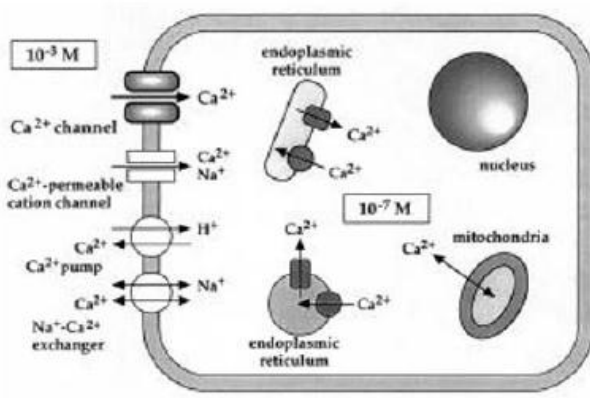

Figure 2. Regulation and distribution of intracellular concentration of free Ca^{2+}. The increase in intracellular concentration of free Ca^{2+} can be triggered by the release of Ca^{2+} from intracellular stores, especially the endoplasmic reticulum, and by influx from the extracellular space through voltage-dependent Ca^{2+} channels and Ca^{2+}-permeable cation channels (scheme taken from Michiaki Yamakage 2002)[27].

2.2 Primary Structure and Properties of Ca^{2+} Channel α1 Subunits

VGCCs were initially isolated as large heteromeric proteins from the skeletal muscle Ca^{2+} channel complex. The so-called DHP receptor complex contains 5 protein subunits, which were termed α_1 (170 kDa), α_2 (150 kDa), β (52 kDa), δ (17–25 kDa) and γ (32 kDa)[28, 29]. Up to 10 genes have been described to encode the pore-forming α1 subunit of VGCCs, being the most highly selective ion channels for Ca^{2+} (Table 1).

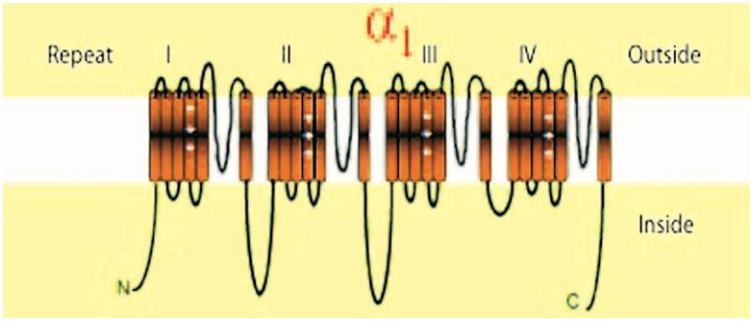

Figure 3. *α1 subunit of voltage-gated Ca^{2+} channels showing 4 homologous repeated domains (I-IV) with intracellular linkers, and N and C terminus. Each of the 4 homologous repeated domains is comprised of 6 membrane-spanning segments (S1-S6). The inward loop between the S5 and S6 transmembrane segments lines the pore, while the S4 transmembrane segment contains positively charged amino acids (Lys^+ or Arg^+) that move outwardly upon membrane depolarization, causing channel opening.*

The α_1 subunit is a large protein with 24 transmembrane segments arranged in 4 homologous repeated domains, with intracellular linkers and N and C terminus. The N and C-terminus exert important modulatory functions on the expression and function of the channels. Each of the 4 domains is comprised of 6 putative membrane-spanning segments (S1-S6). The inward dipping loop between S5 and S6 transmembrane segments form the channel pore, while the S4 transmembrane segments contain positively charged amino acids and act as voltage sensors, moving outwardly upon membrane depolarization and rendering the calcium channel open by an allosteric mechanism[28,29] (Figure 3). On the basis of sequence homology and functional properties, VGCCs are classified in two major groups: high voltage-activated calcium channels (HVAs), which activate at depolarized membrane potentials (usually - 40 mV or more positive), and low voltage-activated calcium channels (LVA or T-type) which open at more negative membrane potentials, closer to the typical cell resting membrane potentials (between -80 and -60 mV). HVA calcium channels include L-type, R-type, N-type and P/Q-type calcium channels. LVA calcium channels include the T-type calcium channels[30] (Figure 4). Some of the key features of high and low voltage-activated Ca^{2+} channels are displayed in Table 1, and their pharmacology is displayed in Table 2.

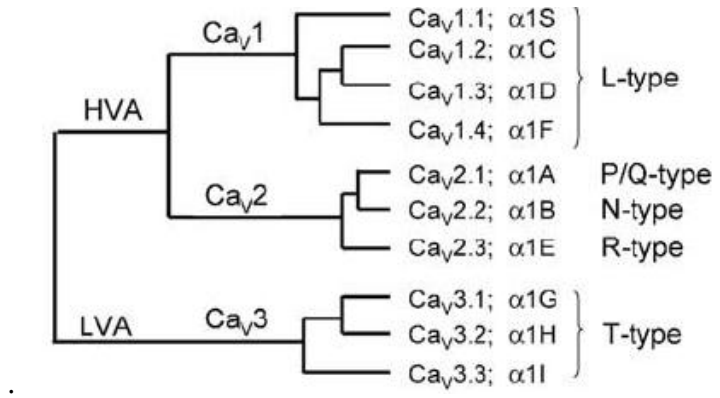

Figure 4. *Dendrogram showing the classification of VGCCs on the basis of their sequence homology and functional properties (scheme modified from Eric A.Ertel 2000)*[31]

Table 1: Summary of voltage-gated calcium channel classification

Electrophysiological nomenclature	**Molecular nomenclature**		**Main localization**
	old	**New**	
L-type calcium channel ("Long-Lasting")	α_{1S}	$Ca_v1.1$	skeletal muscle
	α_{1C}	$Ca_v1.2$	smooth and cardiac muscle, CNS
	α_{1D}	$Ca_v1.3$	Sinoatrial node, cochlear hair cells, neuronal (dendritic)
	α_{1F}	$Ca_v1.4$	Retina
P-type calcium channel ("Purkinje")/Q-type calcium channel	α_{1A}	$Ca_v2.1$	Purkinje neurons in the cerebellum/Cerebellar granule cells
N-type calcium channel ("Neural"/"Non-L")	α_{1B}	$Ca_v2.2$	Throughout the brain and peripheral nervous system.
R-type calcium channel ("Residual")	α_{1E}	$Ca_v2.3$	CNS; cell bodies, some distal dendrites and Presynaptic terminal

T-type calcium channel ("Transient")	α_{1G}	$Ca_v3.1$	Neuronal, cardiac
	α_{1H}	$Ca_v3.2$	Neuronal and many other tissues
	α_{1I}	$Ca_v3.3$	Neuronal

Table 2. Ca^{2+} channel antagonists and agonists (L, T, P/Q, N, R type)

Type	Activator	Inhibitor
T-type	NA	Mibefradil (dihydropyridine analogue), Pimozide (diphenylbutylpiperidine derivative), Penfluridol (diphenyl butylpiperidine derivative), Bepridil ,Flunarizine (piperazine derivatives), Kurtoxin (peptide)
L-type	BAY-K 8644(60,133)	Dihydropyridines (Nimodipine, Nifedipine, nitrendipine amlodipine, nicardipine Nifedipine , Nimodipine nitrendipine); Benzothiazapines (d-*cis*-diltiazem); Phenylalkylamines (verapamil)
P/Q-type	NA	ω-Agatoxin IVA (peptide)
N-type	NA	ω-CgTx GVIA (peptide)
R-type	NA	SNX-482 (peptide)

3. Involvement of voltage-gated Ca^{2+} channels in the control of cellular proliferation

Numerous studies have demonstrated that the Ca^{2+} influx through VGCCs, especially from the Ca_v1 (L-type) family, results in signalling that affects the expression of genes involved in cell proliferation, programmed cell death and apoptosis[32-36].

Dolmetsch et al (2001) showed that an isoleucine-glutamine motif in the carboxyl terminus of $Ca_v1.2$ L-type channels is essential for Ca^{2+}-calmodulin binding; Ca^{2+}- CaM in turn activates the Ras/mitogen activated protein kinase pathway and conveys the Ca^{2+} signal to the nucleus, stimulating the expression of genes essential for neuronal survival[37] In the nucleus, Ca^{2+} has been also involved in DNA replication through its role activating CaM-kinase II and IV, phosphatase like calcineurin, and regulating nuclear factors such as Ca^{2+}/cAMP response element binding protein and Ras, which control cyclins and Cyclin-dependent kinases[26].

Ca^{2+} seems to be particularly important for specific phases of the cell cycle; for example, the transition from the G1/S interphase (initiation of DNA synthesis) and the G2/M interphase (initiation of mitosis), is dependent upon CaM-kinase II[38]. In proliferating cells, these Ca^{2+} signals often form oscillatory patterns involving entry of external Ca^{2+} and release of Ca^{2+} from internal stores[39]; these oscillations play an important role in the ability of cells to reenter the cell cycle and initiate DNA synthesis at the G1/S phase transition, and for the initiation of mitosis during the M phase of the cell cycle; T-type Ca^{2+} channels are particular well suited to participate in such oscillations due to their unique biophysical properties, among them the ability to open with relatively small depolarizations, the rapid kinetics of inactivation and the overlapping of steady-state activation and inactivation curves[28].In fact, cells in the proliferative phase (G2/M) have been frequently reported to express T-type Ca^{2+} channels, whereas the same cells in the non-proliferative phases (G0/G1) express primarily L-type Ca^{2+} channels[40, 41]. That way, in vascular smooth muscle cells the percent of total Ca^{2+} channel current for T-type Ca^{2+} channels was 37% in the G1 phase and increased to 90% in the S and beginning of the M phases[42]. In human pulmonary artery myocytes, the gene silencing of α1G subunits of T-type Ca^{2+} channels inhibited proliferation and resulted in an increased number of cells in the G0/G1 (non-proliferative) cell cycle stage[43, 44]. Furthermore, Western blot analysis at various phases of the cell cycle has shown that an increased expression of the T-type

channels is associated with the G2/M phase of the cell cycle[40-45]. Taken together, these data strongly suggest that T-type Ca^{2+} channels play an important role in Ca^{2+}-signaling associated with S phase-related events, when DNA synthesis is increased in preparation for entry into the G2/M (proliferative) phase of the cell cycle[46].

4. Voltage-gated Ca^{2+} channels and cancer

Ca^{2+}-dependent signalling is frequently deregulated in cancer cells and, importantly, VGCCs may play a role in remodelling calcium homeostasis. The following sub-sections summarize the knowledge achieved for the different VGCC types up to date.

4.1 L-type Ca^{2+} channels and cancer

The expression of L-type Ca^{2+} channels in non-excitable cells is limited and, even if these channels are present, they require membrane depolarization to become activated. It has been shown that the cell membrane may be depolarized by the action of certain mitogens, giving a "chance" to L-type channels for modulating proliferation[47]. Indeed, Ca^{2+} influx through L-type channels has been implicated in the pro-proliferative action of endothelin-1 (ET-1) in the SPC-A1 human lung adenocarcinoma cell line[47-49]. In some cases, the cells have been shown to express a splice variant of L-type channels lacking voltage-sensing S4 transmembrane segments, which might explain the activation of L-type Ca^{2+} channels without depolarization[50]. There are pharmacological evidences for VGCC-mediated Ca^{2+} influx in colonic cell lines[54-56] and, interestingly, the up-regulation of the $Ca_v1.2$ L-type channel isoform has also been reported in colon cancer[57]. In a similar line, it has been suggested that the progression of colon cancer is often associated with enhanced mitogenic signals such as epidermal growth factor (EGF) and EGF receptors[58, 59] and their downstream signaling kinase c-src[60], which in turn increases the activity of L-type channels[61]. The up-regulation of $Ca_v1.1$ in colorectal carcinoma cell lines and biopsies has also been described[64] (table 3). Other works have unveiled uncommon coupling mechanisms of L-type channels to either cell survival or oncogenicity. For instance, Green et al. reported that a population of endosomes whose rapid trafficking is controlled by Ca^{2+}, contains $Ca_v1.2$ channels in their membranes; they further identified a protein domain in the II-III loop of $Ca_v1.2$ channels that binds Eukaryotic translation initiation factor 3 subunit (eIF3e), as essential for the activity dependence of both channel

internalization and endosome trafficking; this finding provides an interesting link between L-type calcium channel, calcium homeostasis and a mammalian oncogene[63].

4.2 T-type calcium channel and cancer

The $Ca_v3.1$ isoform of T-type voltage gated calcium channels has been reported to be overexpressed in glioma cells[67, 43]. The knock down of $Ca_v3.1$ in esophageal carcinoma cells can reduce cell proliferation via the p53 tumor-suppressing transcription factor-dependent pathway, leading to the up-regulation of the cell-cycle arrest protein p21[68]. The $Ca_v3.2$ isoform was reported to be over-expressed during neuroendocrine differentiation of prostate cancer cells[69]. Interestingly, a decreased function of T-channels also may play a role in cancer development and progression, as transformation of fibroblasts by *ras* oncogene reduces T-currents[70-72]. Hypermethylation of the CACNA1G gene in various human tumors (colon, colorectal, pancreatic and gastric cancers, as well as in acute myelogenous leukemias) results in silencing of $Ca_v3.1$ channels, indicating that CACNA1G may be a putative tumor suppressor gene[73-75]. Expressions of isoforms of T type calcium channel in various types of cancer are described in table 4.

4.3 P/Q, R-type calcium channels and cancer

P/Q and R-type VGCCs are involved in neuronal plasticity and survival, and mediate fast neurotransmission in the central and peripheral nervous systems. There are few evidences suggestive of a role of P/Q-type or R-type Ca^{2+} channels in cancer development. Nonetheless, the activity of $Ca_v2.3$ channels has been reported to promote chromogranin A secretion from neuroendocrine tumor cells[93]. It has also been shown that the enhanced proliferation of a tumorigenic mouse ovarian epithelial cell line by follicle stimulating hormone, involves a signalling pathway that includes the up-regulation of $Ca_v2.3$ channels[94]. Finally, several studies have reported that $Ca_v2.1$ antibodies play a pathogenic role in Lambert-Eaton myasthenic syndrome, which can be associated with small cell lung carcinoma[95, 96].

Table 3. L-type calcium channels and cancer

Cell type	L type isoform	Reference
Colon carcinoma	$Ca_v1.2$	57
Colorectal carcinoma	$Ca_v1.1$	64
lung adenocarcinoma	undefined	47-49
Human B lymphoma cells	$Ca_v1.2$	65
Human jurkat t cells	$Ca_v1.4$, $Ca_v1.1$	66,50

Table 4. T-type calcium channels and cancer

Cell type	T type isoform	Reference
breast carcinoma	$Ca_v3.1$, Ca_v 3.2	75-77,67
neuroblastoma	$Ca_v3.1$, $Ca_v3.2$	67,78-80,77,43
retinoblastoma	$Ca_v3.1$,$Ca_v3.2$, $Ca_v3.3$	81,82
glioma	$Ca_v3.1$, $Ca_v3.2$	67,43
Prostate carcinoma	$Ca_v3.1$, $Ca_v3.2$	69,83,75,77
Esophageal carcinoma	$Ca_v3.1$, $Ca_v3.2$, $Ca_v3.3$.	68
fibrosarcoma	$Ca_v3.1$	84
Colorectal carcinoma	$Ca_v3.1$	75
pheochromocytoma	$Ca_v3.1$, $Ca_v3.2$	85,86
adrenocarcinoma	$Ca_v3.2$	87
insulinoma	$Ca_v3.1$	88
Thyroid carcinoma	$Ca_v3.2$	89
Colon carcinoma	$Ca_v3.1$	75,90
Pancreatic carcinoma	$Ca_v3.1$	73
Hepatocellular carcinoma	$Ca_v3.1$, $Ca_v3.2$,$Ca_v3.3$	74
Gastric carcinoma	$Ca_v3.1$	75
Acute myelogenous leukemias	$Ca_v3.1$	75
Ovarian cancer	$Ca_v3.1$, $Ca_v3.2$	91,92

5. Effects of calcium channel blockers on cellular proliferation

In line with the relevance of the different VGCC families in cell proliferation summarized in the preceding sections (and with our own results attained during the development of this Thesis), only the blockade of L-type and T-type Ca^{2+} channels has shown to have an impact on cancer cell growth. L-type and T-type Ca^{2+} channel blocking agents are classified into broad groups according to their chemical structure like benzodiazepines, diphenylbutyl piperidines, phenylalkyl amines, piperazine derivatives and dihydro pyridines (Figure 2).

Although the main actions of the L-type and T-type channel blockers concern the cardiovascular system and include dilatation of coronary and peripheral arterial vasculature, reduction of heart rate and slowing of AV conduction, many articles have suggested antiproliferative effect of these drugs *in vivo* and *in vitro*. This relevant aspect is discussed in the following section.

5.1 Effect of T-type calcium channel blockers on cellular proliferation

There are a variety of agents that can affect T-type calcium current with varying degrees of specificity. Kurtoxin is a peptide purified from the *Parabuthus transvaalicus* scorpion venom and stands out like the most specific blocker of T-type channels available to date[97, 98]. Kurtoxin binds $Ca_v3.1$ and $Ca_v3.2$ T-type channels with high affinity (low nanomolar) and inhibits the T-type calcium currents by modifying the channel gating[98]. The antiproliferative properties of Kurtoxin have been documented *in vitro* in the rat *ductus arteriosus* smooth muscle cells[99].

Mibefradil, a benzimidazolyl-substituted tetraline derivative, is distinguished from other calcium channel antagonists because it preferentially blocks low-voltage-activated T-type calcium channels (T-channels) with 10 to 20 times more selectivity than high-voltage-activated (HVA) L-type Ca^{2+} channels[100, 101]. Mibefradil was introduced clinically in 1997 as an antianginal and antihypertensive agent, but was withdrawn from the market less than a year after its release due to potentially life-threatening interactions with β-blockers and hypolipidemic agents[102]. However, Mibefradil has been reintroduced in the clinical practice by earning the status as an orphan drug for treatment of pancreatic,

glioblastoma multiforme and ovarian cancer from the American Food and Drug administration in recent years[103]. Mibefradil has been recognized as an effective inhibitor of proliferation in many different cell types including blood mononuclear cells[104,] rat smooth muscle cells[105], human pulmonary artery myocytes[106], glioblastoma[43, 82, 106], retinoblastoma[82] and breast cancer[82] cell lines. Apart from its anti-proliferative properties, Mibefradil has been shown to suppress Ca^{2+} mediated spikes, waves, cell motility and invasive properties of HT1080 fibrosarcoma[84]. Anticancer effects of Mibefradil has also been investigated on tumor cells *in vivo*. Taylor et al. reported that the local injection of Mibefradil induces the death of human breast carcinoma cells implanted into subcutaneous adipose tissue in athymic nude mice[107].

The antipsychotic drug Pimozide has also been shown to be a potent inhibitor of T-type and L-type Ca^{2+} channels, but with less selectivity than Mibefradil[108]. In pituitary and heart cells, Pimozide proved to inhibit L-type channels[109], whereas in adrenal glomerulosa and spermatogenic cells, Pimozide prevented Ca^{2+} influx by blocking T-type channels[109, 110]. Pimozide has also been reported to inhibit proliferation of breast cancer cells[111] and astrocytoma cells[112]. In the latter, the apparent mechanism of action was through inhibition of CaM activity[112]. Pimozide had also been introduced in the clinical trial of patients suffering from melanoma, although its beneficial effects were attributed to the blockade of dopamine receptors[113, 93].

Using the structure-activity relationship of known T-type channel blockers, Gray et. al. synthesized two new inhibitors of Ca^{2+} entry, TH-1177 and TH-1211. These two compounds blocked T-type channels and capacitative Ca^{2+} entry and decreased the proliferation rate of breast and prostate cancer cell lines with a similar efficacy to that of Mibefradil[77]. Similarly, McCalmont et al. described the synthesis of several novel T- type channel antagonists that inhibited Ca^{2+} influx and exerted a negative effect on cellular proliferation[114]. Cyclic AMP[115], G-proteins[116], arachidonic acid metabolites including anandamide[106, 117] and nordihydroguariatetic acid[118], can also modulate T-type Ca^{2+} channels and inhibit cellular proliferation.

5.2 Effect of L-type calcium channel blockers on proliferation

It has been shown that dihydropyridine derivatives such as Nimodipine, Nifedipine, and amlodipine inhibit the proliferation and DNA synthesis of epidermoid carcinoma cells [119-122,161]. Verapamil, Nifedipine and Diltiazem have also been reported to inhibit the growth of human brain tumor cells *in vitro*[112, 123]. Interestingly, L-type channel blockers have also displayed tumor inhibition capabilities *in vivo*: verapamil and Diltiazem inhibited the growth of subcutaneous xenograft meningiomas in nude mice[124]; oral administration of amlodipine, Diltiazem or verapamil were demonstrated to inhibit the proliferation of human breast cancer cell in the athymic mouse, without any effect on mouse body weight or gross organ morphology[124].

6. Calcium signalling and cell death

Proliferation and apoptosis are two key processes determining normal tissue homeostasis. Apoptosis is a genetically determined self-destruction process that is characterized by membrane blebbing, DNA fragmentation and formation of apoptotic bodies[125]. Two major intracellular apoptosis pathways are the death receptor-mediated (extrinsic) pathway and the mitochondrion-initiated (intrinsic) pathway[126]. Central to these apoptotic processes are a group of caspases (a family of cysteine proteases) that rapidly demolish cellular structures and organelles in an orderly manner. Apoptotic Caspases include 'initiator Caspases' (Caspase 2, 8, 9 and 10) that start the apoptotic Caspase cascade, and 'effector Caspases' (Caspase 3, 6 and 7) that disassemble the cell [127]. De-regulated cell proliferation together with the suppression of apoptosis provides the condition for abnormal tissue growth, which ultimately can turn into the uncontrolled expansion and invasion characteristic of cancer. Although in molecular terms proliferation and apoptosis seem to be clearly delineated, both of them involve intense Ca^{2+} signaling and a remodelled Ca^{2+} homeostasis provides the critical environment for their unfolding[24]. The Ca^{2+}-dependent apoptotic mechanisms can be subdivided roughly into mitochondrial, cytoplasmic and endoplasmic reticulum mediated.

Mitochondria represent a central integration point for the signals regulating cells destiny. Ca^{2+} overload, which may be triggered by external stimuli, promotes mitochondrial uptake of Ca^{2+}. Excessive Ca^{2+} accumulation within the mitochondria is one of the

primary causes for mitochondrial permeability transition, which is at least partly mediated by the opening of permeability transition pore (PTP), a multi-protein complex located at the contact sites between the inner and the outer mitochondrial membranes. PTP opening permits releasing of mitochondrial apoptogenic factors, such as cytochrome c (Cyt-c) and apoptosis-inducing factor (AIF) into the cytoplasm where they in turn activate death-executing caspase cascade.

An initial cytosolic Ca^{2+} overload may also trigger apoptosis without directly involving Ca^{2+}-mediated mitochondrial permeability transition. It mainly relies on the activation of a Ca^{2+}-CaM-dependent phosphatase, namely calcineurin. Calcineurin-catalyzed dephosphorylation promotes apoptosis by regulating the activity of a number of downstream targets including pro-apoptotic Bcl-2 family member, Bad[122] and transcription factors from nuclear factor of activated T cell (NFAT) family[128]. There are also some other Ca^{2+}-dependent enzymes, which take part in the apoptotic events, among which of special note are several DNA-degrading endonucleases[123] and Ca^{2+} -activated cystein proteases of the calpain family, that are essential for the enzymatic activation of crucial pro-apoptotic effectors[124].

The endoplasmic reticulum is a principal site for protein synthesis and folding, Ca^{2+} storage and Ca^{2+} signalling. Ca^{2+} is pumped into the ER by SERCA adenosine triphosphatases (ATPases) and is released by inositol 1,4,5-trisphosphate (IP_3) or ryanodine receptor (RyR) Ca^{2+} release channel[25]. A significant fraction of the released Ca^{2+} is captured by mitochondria, which are strategically located near Ca^{2+}-release channels[129]. This close connection allows mitochondria to modulate, propagate, and synchronize Ca^{2+} signals and to prevent ER depletion by recycling Ca^{2+} to the ER. The ER-mitochondria connection enables Ca^{2+} signals not only to fine tune cellular metabolism but also to modulate the ability of mitochondria to undergo apoptosis. The switch from a life to a death signal involves the coincidental detection of Ca^{2+} and pro-apoptotic stimuli, and depends on the amplitude of the mitochondrial Ca^{2+} signal. The magnitude of mitochondrial Ca^{2+} signals, in turn, depends largely on the Ca^{2+} content of the ER, which is maintained by the balance between active Ca^{2+} pumping by SERCA and passive leakage through Ca^{2+}-release channels (Figure 5)[130-134].

7. Endoplasmic reticulum stress

The ER is highly sensitive to alterations in Ca^{2+} homeostasis. Ca^{2+} ionophores that deplete Ca^{2+} levels from the ER lumen, inhibitors of glycosylation, chemical toxicants, oxidative stress or the accumulation of misfolded proteins in the ER, can all disrupt ER function resulting in "ER stress". The ER responds by triggering specific signalling pathways, including unfolded protein response [UPR], the ER overload response [EOR], and the ER associated degradation [ERAD]. Overall activation of these pathways leads to a reduction in the amount of translocated proteins in ER lumen, augmentation of protein folding capacity of the ER, increased translocation and degradation of misfolded proteins in the ER.

The UPR is initiated when the unfolded proteins exceed the capacity of ER-resident chaperone proteins, such as glucose-regulated proteins 78 and 94 (GRP78 and GRP 94), to bind them. The principal chaperone protein is GRP78, which normally binds the N terminal ends of three transmembrane proteins referred to as interferon inducible protein kinase regulated by RNA like ER kinase (PERK), inositol requiring enzyme 1 alpha (IRE1α) and activating transcription factor 6 (ATF6). When the capacity of the sensor protein GRP78 to bind the unfolded proteins is exceeded, the individual ER transmembrane proteins undergo homodimerization and autophosphorylation, which trigger the UPR (Figure 6).

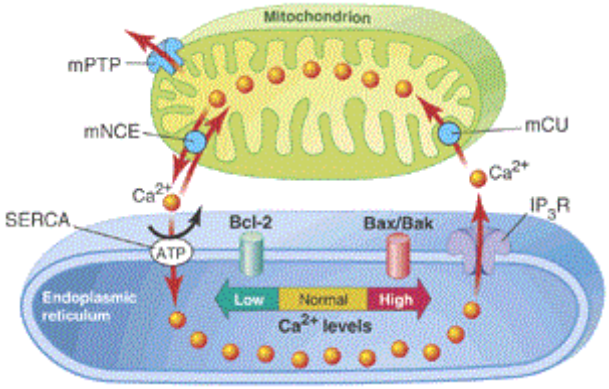

Figure 5.*Under normal conditions, Ca^{2+} continuously cycles between the ER and mitochondria. Ca^{2+} is pumped into the ER by Ca^{2+} ATPases (SERCA), and released by IP_3–gated channels*

(IP3R). Ca^{2+}enters mitochondria by a Ca^{2+}uniporter (mCU) and is released by a Na^{2+} /Ca^{2+} exchanger (mNCE) (scheme taken from Nicolas Demaurex 2009 [19].

PERK is a serine threonine kinase that has many targets. The kinase domain of activated phosphorylated PERK phosphorylates the alpha subunit of eukaryotic translation initiation factor 2 alpha (eIF2α), attenuating the initiation of translation and protein synthesis. PERK activation and eIF2α phosphorylation leads to: (a) a decrease in the protein folding capacity of the ER; (b) the induction of eIF2α phosphorylation- dependent ER stress genes; and (c) the promotion of cell survival. Phosphorylated eIF2α may also translate the transcription factor ATF4, that includes a target gene for a phosphatase growth arrest and DNA damage inducible gene 34 (GADD34) (which dephosphorylates eIF2α) and Growth Arrest and DNA damage inducible gene 153 (GADD153/CHOP). GADD153 is a member of CCAAT/enhancer binding proteins (C/EBPs). Generally expressed at low level in proliferating cells, GADD153 is strongly induced in response to stresses that result in growth arrest or cellular death including oxidative injury, genotoxic stress, anti cancer chemotherapy and ER stress. Recent studies suggest that overexpression of GADD153 plays a central role in the apoptotic process, including favouring the dephosphorylation of the proapoptotic protein Bad and the down-regulation of Bcl-2 expression.

IRE1α acts both as a serine/threonine kinase and an endoribonuclease. The latter activity results in splicing of the mRNA for X box-binding protein 1 (XBP-1), a transcription factor that binds both the ER stress response element (ERSE) and the UPR promoter element (UPRE). The UPRE is associated with the expression of genes involved in the transport of unfolded proteins out of the ER and their degradation by the ubiquitin proteasome system, a process referred to as ER-associated degradation (ERAD).

ATF6α shares many of the activities of IRE1α. In response to ER stress, p90ATF6 transits to the Golgi where it is cleaved by the proteases S1P and S2P, yielding a free cytoplasmic domain that is an active transcription factor, p50ATF6, which appears to be principally involved in induction of the chaperone proteins and to precede IREα1-mediated production of the ERAD pathway. ATF4, ATF6 and XBP-1 are transcription factors that up-regulate ER chaperone proteins, folding enzymes and protein degradation molecules, which in turn either prevent the aggregation of unfolded proteins, or aid in

their subsequent folding or in degradation of excessive misfolded proteins. Based on the current knowledge, the ATF6 and IRE1α-XBP1 pathways are generally regarded as anti-apoptotic UPR, and they are found to be attenuated when ER stress is persistent, whereas PERK activity is maintained, including GADD153 induction and inhibition of translation[135-142].

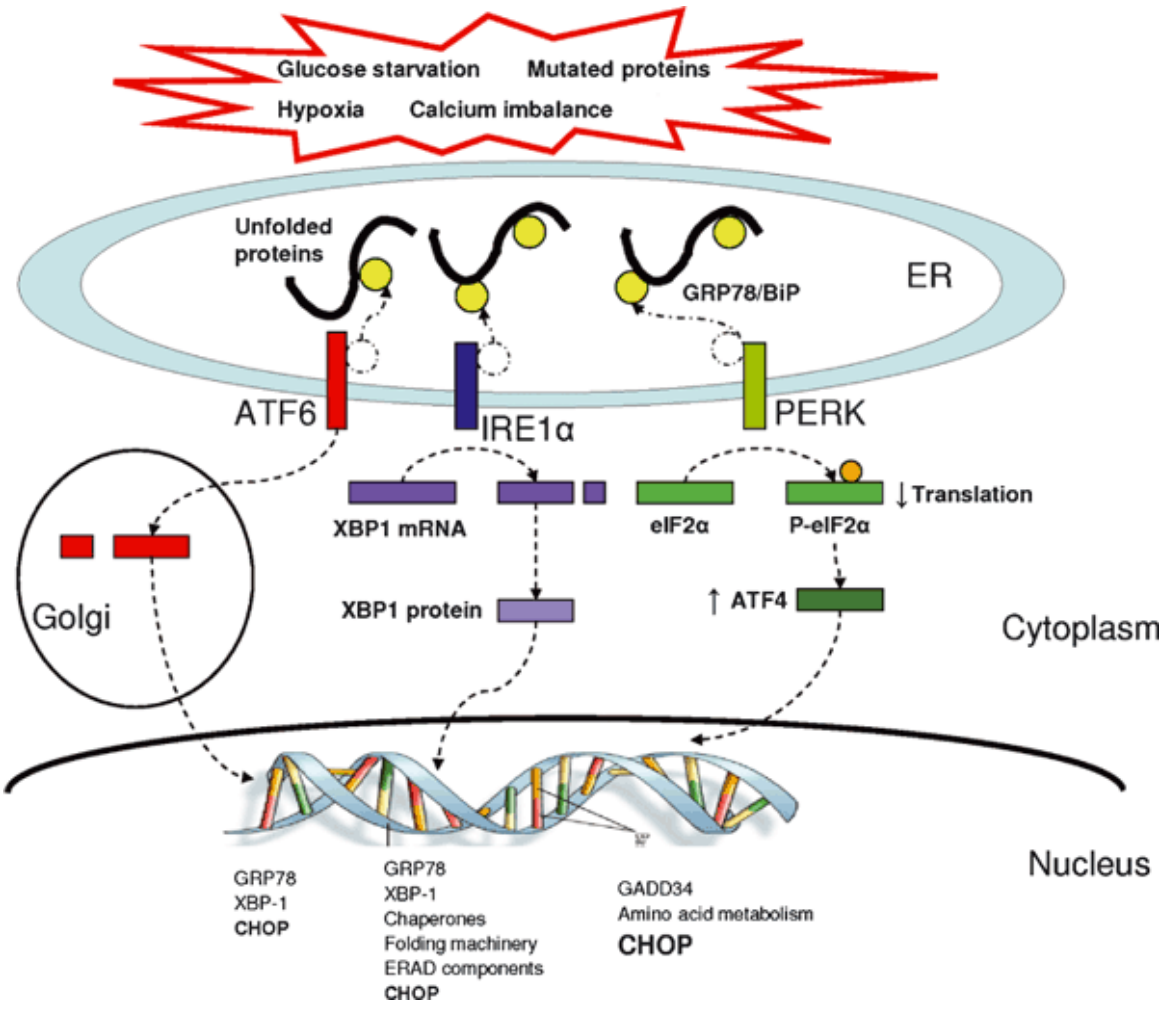

***Figure 6**. Schematic outline of key aspects of endoplasmic reticulum stress and unfolded protein response (scheme taken from Peter Hersey 2008)*[147].

In mammals and, depending on the state of the cell and the type of ER stress encountered, the outcome can be an increase in the capacity of the ER folding machinery, a reduction of the amount of proteins entering the ER, an enhanced clearance of the proteins from the ER, apoptosis or autophagy. PERK, IRE1α and increased Ca^{2+} levels have been implicated as mediators of ER stress-induced autophagy in mammalian cells[143-147]. In this regard, Kouroku et al. demonstrated that ER stress in response to ectopic expression of

polyQ72 upregulates the expression of autophagic gene Atg12, and induces autophagy through the PERK-eIF2α signaling pathway[145]. In contrast Imaizumi and co-workers showed that the activation of IRE1α was the linker between UPR and autophagy in mouse embryonic fibroblast cells[163].

8. Autophagy

When cells are under stress, they may adopt survival strategies or may undergo a programmed cell death. Autophagy (self-eating) is a lysosomal pathway involved in the turnover of cellular macromolecules and organelles that is essential to maintain cell homeostasis in a "normal" environment. In addition, autophagy is an adaptive, inducible survival strategy that allows cells to cope with different kinds of stress. At least three different types of autophagy exist: microautophagy, chaperone-mediated autophagy (CMA) and macroautophagy. The main differences between them concern the way by which endocytosed cargo is delivered to lysosomes. (1) Microautophagy implies direct delivery through invagination and fission of lysosomal membrane, and not much is known about the molecular machinery involved in the process[148].(2) CMA delivers certain proteins to lysosomes with the help of the cytosolic hsc70 chaperone, which recognizes a KFERQ-like motif in the target proteins[149].(3) Macroautophagy, commonly regarded as "autophagy", involves the envelopment of cytosol and/or organelles in the isolating membrane, which wraps around the cargo forming an autophagosome a vesicle surrounded by a double membrane. The autophagosome then undergoes a progressive maturation by fusion with endolysosomal vesicles creating an autolysosome, where the cargo is degraded (Figure 7). To date, more than 30 ATG (autophagy-related) genes required for autophagy and its related pathways have been identified in yeast and mammals. The Atg proteins required for autophagy are now classified into six functional groups: (1) the Atg1 kinase complex (Atg1-13-17-29-31), (2) Atg9, (3) the class III phosphatidylinositol (PI)3–kinase complex (Atg6 –Atg14–Vps15–Vps34), (4) the PI(3)P-binding Atg2–Atg18 complex, (5) the Atg12 conjugation system (Atg12–Atg5–Atg16), and (6) the Atg8 conjugation system (Atg8–PE)[162] .

In many cellular settings, the first regulatory process involves the de-repression of the mTOR Ser/Thr kinase, which inhibits autophagy by phosphorylating autophagy protein-13 (Atg13). This phosphorylation leads to the dissociation of Atg13 from a protein

complex that contains Atg1 kinase and Atg17, and thus attenuates the Atg1 kinase activity. When mTOR is inhibited, re-association of dephosphorylated Atg13 with Atg1 stimulates its catalytic activity and induces autophagy. Notably, the mammalian orthologue of the yeast Atg13 has not been identified to date.

Initially vesicle nucleation and assembly of the primary autophagosomal membrane starts with activation of mammalian Vps34, a class III phosphatidylinositol 3 kinase (PI3K) to generate phosphatidylinositol-3-phosphate (PtdIns3P). Vps34 activation depends on the formation of a multi protein complex in which Beclin-1 (Becn1; the mammalian orthologue of Atg6), UVRAG (UV irradiation resistance-associated tumour suppressor gene) and a myristylated kinase (Vps15, or p150 in humans). The isolation membrane chooses its cargo and elongates until the edges fuse forming a double-membrane structure called an autophagosome. Two ubiquitin-like conjugation systems are part of the vesicle elongation process. One pathway involves the covalent conjugation of Atg12 to Atg5, with the help of Atg7 and Atg10. The second pathway involves the conjugation of phosphatidylethanolamine (PE) to LC3/Atg8 (LC3 is one of the mammalian homologues of Atg8) by the sequential action of the protease Atg4, Atg7 and Atg3. Lipid conjugation leads to the conversion of the soluble form of microtubule-associated protein 1 light chain 3 (LC3; also know as Atg8 or LC3-I) to the autophagic vesicle-associated form (LC3-II). The mechanism of retrieval in which the Atg9 complex participates is poorly studied. The accumulation of LC3-II and its localization to vesicular structures are commonly used as markers of autophagy. Finally mature autophagosomes fuse with endosomes and lysosomes forming autolysosomes, where the final degradation of the cargo occurs.

Cells lacking nutrients suppress mTORC1 activity via a pathway involving AMP-activated protein kinase (AMPK), and activate the autophagy machinery that provides the starved cells with an alternative source of intracellular building blocks and energy, thereby enhancing the cell survival during the stress. Although as indicated above autophagy is a homeostatic mechanism, notably it does not always promote cell survival; under some circumstances autophagy can mediate non-apoptotic cell death or type II programmed cell death (PCD II), which is generally caspase-independent and morphologically distinct from apoptosis[150-153].

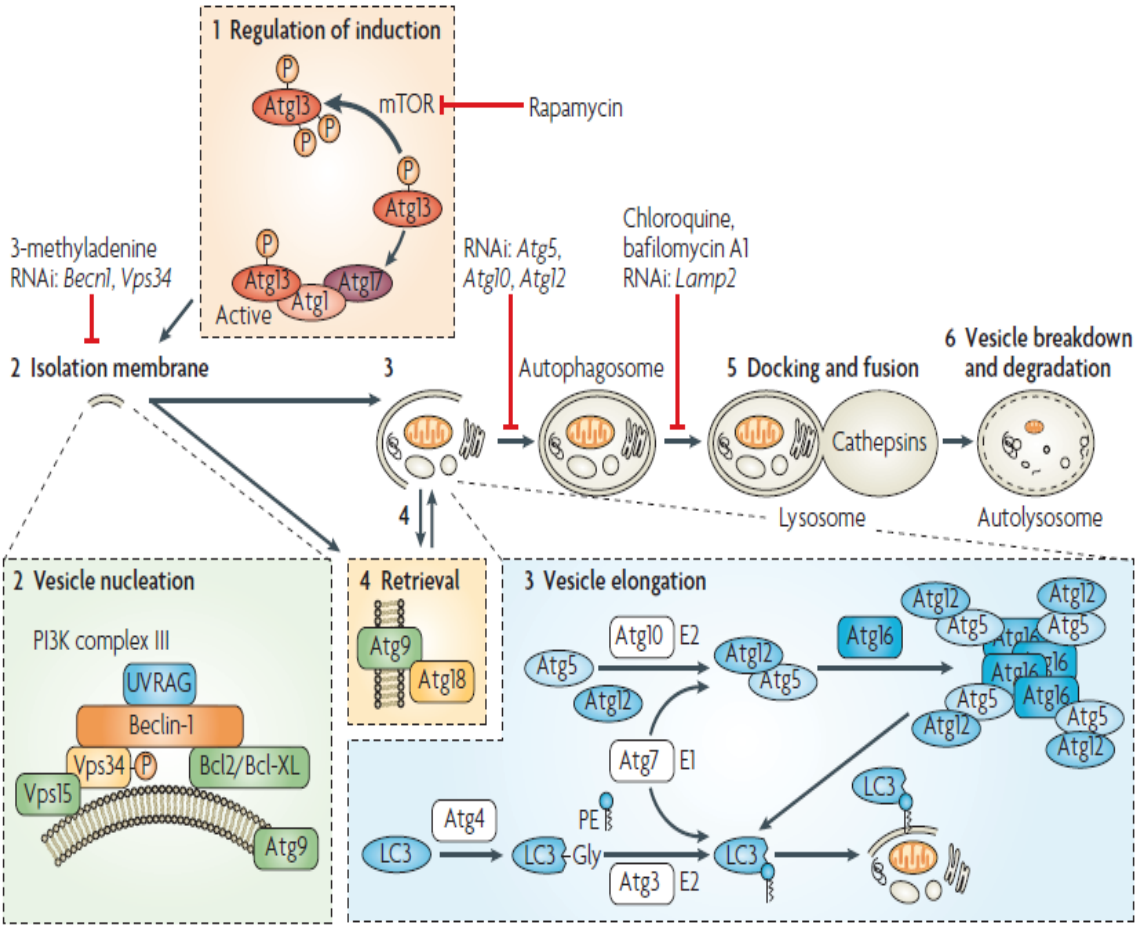

Figure 7. *Schematic depiction of macroautophagy in mammals (scheme taken from M. Chiara Maiuri 2007)* [175].

Intracellular Ca^{2+}-signalling regulates autophagy, but the exact mechanisms involved are still under debate. Removal of Ca^{2+} by chelation blocks autophagy at an early stage prior to LC3 conversion and autophagosome formation156. Ca^{2+} has previously been detected in LC3-positive structures154, and it is generally indispensable for membrane fusion events155. Ca^{2+} appears to have a dual role in autophagy regulation. Available evidences indicate that the IP3 receptors mediate a constitutive Ca^{2+} release which is taken up by mitochondria, promoting ATP production and in turn inhibiting AMPK and leading to autophagy suppression156. Several studies have also proposed that Ca^{2+} has a stimulatory function towards autophagy. When cells are under stress, Ca^{2+} signalling is refurbished and results in the elevation of cytosolic Ca^{2+}, in turn activating a variety of autophagy-stimulating proteins like calmodulin dependent kinase kinase-beta (CAMKK β), which causes AMPK-dependent inhibition of mTOR156. In addition, CaM also mediates the

phosphorylation of Beclin-1, causing its dissociation from Bcl-2156. Protein kinase C (PKC) and extracellular-regulated kinase (ERK) are also involved in Ca^{2+} dependent autophagy stimulation156. An increase in intracellular Ca^{2+} can also activate death associated protein kinase (DAPK) and calpain proteases, both Ca^{2+} dependent enzymes have recently been linked to both apoptosis and autophagy regulation[157, 158].

The p62/SQSTM1 (sequestosome 1) protein mediates diverse signalling pathways including cell stress, survival and death. The N-terminal PB1 domain of this protein exhibits self oligomerization, and the C-terminal UBA domain can bind to ubiquitinated proteins. p62 localizes in autophagosomes via LC3 interaction, and is continuously degraded by autophagy-lysosome system[167]. A growing line of evidence indicates that ubiquitinated proteins initially interacts with p62, then aggregation of the protein complex occurs in a p62-dependent manner and the aggregates are finally degraded by autophagy. Ablation of autophagy leads to marked accumulation of p62 resulting in the formation of p62-positive inclusions. Since p62 accumulates when autophagy is inhibited, and decreased levels can be observed when autophagy is induced, p62 may be used as a marker to quantify the autophagic flux[164-167].

9. Role of autophagy in cancer

The role of autophagy in cancer is a debatable topic. Autophagy serves as a protective role allowing the cells to survive in a changing environmental condition such as nutrient depreviation. Numerous line of evidence suggest an anticancer role of autophagy. The autophagy gene Beclin-1 is a haploinsufficient tumor suppressor gene in mice and is mono allelically lost in human breast, ovarian, and other tumors[168-170]. Moreover, p53 and PTEN, two of the most commonly mutated tumor suppressor genes, both induce autophagy[171, 172]. Together, these findings suggest that autophagy inhibits tumor formation, although the pathway is still not clear. On the other hand there are growing evidences indicating the predominant role of autophagy in tumor progression, suggesting that the role of autophagy may depend on the type of tumors, the stage of tumorigeneses, the nature and extent of the insults. For instance, autophagy has been found to be up-regulated during the later stages of cancer development; that would allow cell survival in the central areas of the tumour, which are usually poorly vascularized and lack of nutrient and oxygen[173-176].

9.1 Autophagy in melanoma progression

The presence of basal levels of autophagy in melanoma has been recognized for many years because some melanoma cells contain autophagosomes with melanized melanosomes, which are readily visible under the light microscope. Melanized autophagosomes are the underlying basis of 'coarse melanin,' a long-recognized phenomenon by pathologists that accounts for the dark areas of melanomas seen in clinical presentation[179]. Non-pigmented melanomas contained similar autophagosome like structure but without melanin[179]. Lazova et al. showed that superficial spreading cutaneous malignant melanoma, cells in florid melanoma *in situ* (MIS) and invasive cells in the dermis, all appeared to be undergoing autophagy; in all these cases, autophagosomes were detected through immunohistochemistry using the marker LC3B (microtubule-associated light chain 3B); normal melanocytes as well as keratinocytes did not stain for LC3B, suggesting that an association between autophagy and invasion is a significant factor in malignant melanoma progression[177-179]. In the same line of evidence, Ma et. al.[180] have recently found that patients, whose melanoma tumor had a higher number of autophagic vacuoles, are less likely to respond to Temozolomide and Sorafenib treatment and have a shorter life expectancy compared with those with a low autophagic index. Moreover, inhibition of autophagy by Atg5 shRNA or with chloroquine significantly increased temozolomide-driven cell death in cultured melanoma cells. In addition, they noted a high tumorigenicity in mouse xenografts and an increased invasive potential of cultured melanoma cells with high autophagic vesicle content. The widespread expression of autophagy in different melanoma cells suggests that maintaining an elevated autophagic flow may be important for the survival of melanoma cells, and thus that invasive and metastatic cells may be susceptible to anti-autophagic therapies[181].

9.2 Pharmacological inhibition of autophagy as an approach towards cancer treatment

Autophagic vacuolization is not always the result of enhanced autophagy, but may also result from the failed elimination of autophagic debris. Multiple studies have shown that pharmacological inhibition of autophagy can effectively enhance tumor cell death in preclinical models[182, 184, 185, 196-198]. In apoptosis-defective leukemic and colon cancer cell

lines, inhibition of autophagy was shown to sensitize resistant cells to TRAIL-mediated apoptosis[182].

Autophagy can be pharmacologically inhibited broadly in two ways, at an early stage or in late stage. Early-stage autophagy inhibitors like 3-methyadenine,Wortmannin and LY294002,target class III PI3K. Late-stage inhibitors like CQ, hydroxychloroquine (HCQ) or Bafilomycin A1, are lysosomotropic drugs that prevent the acidification of lysosomes whose digestive hydrolases depend on low pH[183].

The ability of autophagy inhibition to enhance chemosensitivity and tumor regression has been confirmed in a murine lymphoma model, a colon cancer xenograft model, and a prostate cancer xenograft mouse model[184, 185-189]. Several phase I/phase II trials have been conducted in order to evaluate the efficacy of a combination of HCQ with other cytotoxic drugs, on a variety of tumor types[188, 189]. A combined therapy with the proteasomal inhibitor bortezomib and CQ was shown to suppress tumor growth to a greater extent than did either drug alone in colon cancer xenografts[190]. Phase I/II clinical trials evaluating this combination are ongoing in patients with multiple myeloma[201]. In some tumor cell lines, when the fusion of autophagosomes and lysosomes is blocked by the addition of lysosomal inhibitors (such as CQ or Bafilomycin A1), autophagic vacuoles accumulate and the cells manifest a mixed type I -II morphology before they start to die[173,198]. This observation strongly suggests that the inhibition of autophagy, either at early or late stages of the process, may lead to apoptosis as a result of the failure to adapt to starvation.

A number of anticancer therapies, including DNA-damaging chemotherapeutic drugs, have been observed to induce the accumulation of autophagosomes in tumor cell lines and inhibition of autophagy. *In vivo* experiments confirmed that the inactivation of Beclin1, Atg5, Atg10 and Atg12 can cause apoptosis[191-194]. Although the mechanisms through which the inhibition of autophagy may favour cell death are not entirely clear, it is possible that the inhibition of autophagy results in the absence of redox equivalents, favouring oxidative reactions that trigger apoptosis, presumably through a direct effect on mitochondria[156,199,174]. Inhibition of autophagy may also reduce the capacity of cells to remove damaged organelles or to remove misfolded proteins which, in turn, would favour apoptosis[200].

Hypothesis

Hypothesis

The seminal hypothesis of the present study is that melanoma cells over-express certain types of voltage-gated calcium channels, which play a critical role in the progression of the cell cycle and, generally, in maintaining the homeostasis of these cells.

The experimental goals to rule this hypothesis are the following:

- To characterize the expression of genes encoding VGCCs in human melanoma cell lines, biopsies and control untransformed melanocytes.
- To demonstrate the function of the VGCCs which show a relevant expression, at the molecular level, in melanoma cell lines and untransformed melanocytes.
- To study the putative role of VGCCs in melanoma cell cycle progression and Ca^{2+}-homeostasis.
- To analyze the value of certain types of VGCCs as targets of pharmacological and/or genetic approach against melanoma. That is, to study the effects of specific VGCC blockers and VGCC gene-knockdown on the viability of melanoma cells grown *in vitro*.
- To explore the molecular pathways involved in VGCC-blockade/gene silencing-mediated alterations in melanoma cells homeostasis and viability.

Materials

Table 5. Reagents and cell culture materials

Company	Product
Applied Biosystems(New Jersey, USA)	TaqMan Universal PCR Mastermix First strand c DNA synthesis kit for RT-PCR
BD Biosciences (Bedford, MA, USA)	Plates (100X20) Serological pipettes
Biological Industries	EZ ECL Chemiluminescence Detection kit for HRP
Biorad Laboratories(CA,USA)	30% Acrylamide/Bis solution 29:1
Falcon(BD Labware , USA)	Serological pipet (different volume) Plates 100X 20 mm 6 well plates for cell culture 96 well plates for cell culture 24 well plates for cell culture
Fisher Scientific (Madrid ,Spain)	Centrifuge tubes (different volume) Methanol
GIBCO-Invitrogen(Carlsbad ,USA)	Dulbecco's modified Eagles medium (DMEM) 254 medium supplemented with human melanocyte growth supplement (HMGS-2) Fetal bovine serum (FBS) Fungizone amphotericin B OptiMEM® FURA-2/AM Lipofectamine™ RNAiMAX™ reagent HEPES Trypsin EDTA SYBR safe DNA gel stain Low molecular weight protein bench mark
Merck (Barcelona, Spain)	β Mercaptoethanol
Millipore (Bedford, MA)	Polyvinylidine fluoride (PVDF) membrane
Roche (Germany)	2-(2-Methoxy-4-nitrophenyl)-3-(4-nitrophenyl)-5-(2,4-disulfophenyl)- 2H-tetrazolium (WST-1)
Sigma Aldrich (Barcelona ,Spain)	Ammonium persulfate (APS) D-glucose Calcium chloride Sodium hydroxide Manganese chloride Magnesium chloride Potassium chloride Dimethyl sulfoxide (DMSO) Dodecyl sodium sulfate (SDS) Glycerol Glycine Hoechst (Bisbenzimide H) 33258 N,N,N',N'-tetramethyl-ethane-1,2-diamine (TEMED) Penicillin Sodium chloride (NaCl)

	Thapsigargin Tris base Triton X-100 TRIzol reagent Tween-20 Nimodipine Nifedipine (S)-())-Bay K 8644 Kurtoxin Mibefradil Poly-D-Lysine hydrobromide
Panreac (Barcelona, Spain)	Ethanol Hydrochloric acid (HCl) Isopropanol
Sakura Finetechnical (Tokyo, Japan)	Tissue Tek OCT
Cascade Biologicals Inc.(Portland ,OR,USA)	Neonatal human epidermal melanocytes(HEMn-Lp)
Alomone Labs Ltd (Jerusalem, Israel).	x-agatoxin IVA x-conotoxin GVIA rSNX-482
Gene Craft (Germany)	Taq DNA polymerase
GE healthcare	50 base pair DNA ladder
Thermo Scientific	SuperSignal® West Dura Extended Duration Substrate

Table 6. Sequence of short interfering RNA

Product name	Sequence	company
siRNA $Ca_v3.1$	5´- GCGAGGCAGUUUAUGAGUUtt-3´ 3´- AACUCAUAAACUGCCUCGCtg-5´	Applied Biosystems
siRNA $Ca_v3.2$	5´- GCAACUACGUCUUCACCAUtt-3´ 3´-AUGGUGAAGACGUAGUUGCag-5´	Applied Biosystems

Table 7. Oligonucleotides used to amplify transcripts of pore-forming Ca^{2+} channel subunits

Gene	Acc. no.	Sequence	length (bp)	Temp.
$Ca_v1.2$	NM_000719	Forward: GCCGAAGACATCGATCCTGA Reverse: GAAAATCACCAGCCAGTAGAAGA	267	58°C
$Ca_v1.3$	NM_000720	Forward: GCATTGGGAACCTTGAGCATGTGTCTG Reverse: GCGAGCTGTCATCCTCGTAGC	255	55°C
$Ca_v2.1$ *	NM_000068	Forward: CGATGCCTCAGGGAACACTTGG Reverse: CCATGTACCCATTGAGCTCACG	197	58°C
$Ca_v2.2$ *	NM_000718	Forward: CATCAACCGCCACAACAACT Reverse: ACATCAGAAAGGAGCACAGG	205	58°C
$Ca_v2.3$ *	NM_000721	Forward: GAGAAGATA ACATTGTC AGGAAATATGCCAAGAAGCTCAT Reverse: GCCACAATTTTGATCCC	218	55°C
$Ca_v3.1$	NM_018896	Forward GGTCCGGCACAAGTACAACT Reverse CACAATGAGCAGGAACGAGA	187	55°C
$Ca_v3.2$	NM_021098	Forward TCGAGGAGGACTTCCACAAG Reverse TGCATCCAGGAATGGTGAG	225	55°C
$Ca_v3.3$	NM_021096	Forward GGTGTCGTGGTGGAGAACTT Reverse GTGCACATGGAGTGGATGAG	173	58°C
GAPDH	AF_261085	Forward AGAAGGCTGGGGCTCATTTG Reverse AGGGGCCATCCACAGTCTTC	258	55°C
XBP-1	M31627	Forward AAACAGACTAGCAGCTCAGACTGC Reverse TCCTTCTGGGTAGACCTCTGGGAG	u-473 s-290 183	63°C

Acc. no.: Accession number of the amplified gene; Length: length in base-pairs of the PCR product; Temp.: annealing temperature used in the PCR

*Primer sets taken from available literature: for $Ca_v2.1$ as in Wimmers et al., 2008; for $Ca_v2.2$ as in Chiou et al., 2006; for $Ca_v2.3$ as in Pereverzev et al., 2002

Table 8. Antibodies

Name of primary antibody	Molecular weight (KDa)	dilutions	company
BrdU	-	1:150	Dako
Beta Actin	45	1:3000	Sigma
GRP-78/ BiP (ET-21)	78	1:3000	Sigma
GADD153(F-168):SC-575	28	1:1000	Santa Cruz Biotechnology
LC3	19 (LC3-I) 17 (LC3-II)	1:3000	Novus Biologicals
Beclin-1	60	1:1000	Santa Cruz Biotechnology
P62	47	1:4000	Novus Biologicals
Atg5	32 (ATG5) 54 (ATG5-ATG12)	1:2000	Sigma-Aldrich
Cyclin D1	36	1:1000	BD Pharmingen™
Caspase 3	19 (cleaved Caspase 3) 17 (cleaved Caspase 3)	1:1000	Cell Signaling technology
Caspase 9	47 (Procaspase 9) 35 (Cleaved Caspase 9)	1:1000	Cell Signaling Technology
Secondary anti mouse antibody	-	1:10,000	Sigma-Aldrich
Secondary anti rabbit antibody	-	1:5000	Sigma-Aldrich

Methods

1. Cell culture

Seven human malignant melanoma cell lines of cutaneous origin were obtained from the Department of Immunology of the Hospital Clinic de Barcelona (Spain). These cell lines were already being employed in human immunization protocols. M9 was derived from a primary tumour, whereas M16, M17, M28, M29, M36 and JG originated from malignant melanoma metastasis. The melanocytic lineage of these cell lines was previously confirmed by immunodetection of the specific melanoma cell markers S100 and HMB-45 (see Table 9, modified from Sorolla et al., 2008)[202]. Cell lines were classified as low, average, (medium) or high-proliferating, depending on the time needed to double the cell population (table 9). The cells were cultured in DMEM medium supplemented with 10% foetal calf serum, penicillin-streptomycin and fungizone amphotericin B (Invitrogen, Carlsbad, CA, USA) at 37°C and 5% CO2. Where indicated, hypoxia (2% O2, 93% N2, 5% CO2) was achieved using an In Vivo2 hypoxic workstation (Ruskin Technologies, Leeds, UK).The sampling of melanoma cells was completed by additional examination of three metastatic tumour biopsies (B1, B2 and B3), which were performed and diagnosed as melanoma tumours in the Hospital Universitari Arnau de Vilanova (Lleida, Spain) (Table 9).These samples were obtained with the approval of the local Ethical Committee and a specific informed consent was used. The biopsies were frozen embedded with Tissue Tek OCT (Sakura Fine technical Tokyo, Japan) for cryoprotection, and maintained at 80°C until use. Human epidermal melanocytes isolated from lightly pigmented neonatal foreskin (HEMn-LP) were purchased from Cascade Biologicals Inc. (Portland, OR, USA) and cultured according to the provider's instructions. Melanocytes were maintained in Medium 254 supplemented with human melanocyte growth supplemnent or HMGS-2 (hereafter referred as melanocyte growth media; Invitrogen) at 37°C and 5% CO2.

1.1 Trypsinization of adherent cells

In order to facilitate subculture or harvesting, cultured cells were trypsinized under the commonly used procedure for trypsinization of cells in a monolayer culture. Briefly after reaching an adequate confluency cells were rinsed with warm phosphate buffer saline (PBS, pH 7.4, 37°C) to eliminate traces of serum from the medium, and then incubated with 0.25% trypsin EDTA solution for 3-5 mins at 37°C).Trypsinization was stopped by dilution with serum supplemented high glucose DMEM medium and the resuspended

cells were centrifuged at 1000 rpm 5 minutes RT. The supernatant was discarded and the cell pellet was resuspended in 1 ml of fresh medium. From this cell suspension the cells were counted and subsequently seeded in adequate dishes depending on experimental design.

1.2 Freezing and thawing cultured cells

Cells were grown until approximately 80% confluency and fresh growth medium was added 24 hours before freezing. For freezing, the cells were trypsinized as previously described. After centrifugation the cell pellet was resuspended in special freezing medium composed of complete growth medium supplemented with 10% DMSO. The cell suspension was aseptically aliquoted into sterile cryovials which were placed in Styrofoam container. Cells underwent process of gradual freezing (48 hours at -80°C) to avoid formation of intracellular crystals and then were transferred to a liquid nitrogen freezer for long time storage. Thawing out cells was done in a 37°C water bath by gentle agitation for approximately 1-2 minutes. As soon as the content was thawed, the cryovial was removed from the water bath and decontaminated by spraying with 70% ethanol. All operations were carried out under strict aseptic conditions. The vial content was transferred to a centrifuge tube containing 9 ml of complete culture medium and centrifuged at 1000 rpm for 3 minutes. The cell pellet was resuspended with the complete medium and dispensed into a 100 x 20 mm culture dish for further propagation.

2. Cell viability assay

Cell viability was measured by the WST-1(4-[3-(4-iodophenyl)-2-(4-nitrophenyl)-2H-5-tetrazolio]-1,3-benzene disulfonate) colorimetric assay, which assesses the ability of metabolically active cells to reduce water soluble forms of tetrazolium. An expansion in the number of viable cells results in an increase in the overall activity of mitochondrial dehydrogenases in the sample. The augmentation of the enzyme activity leads to an increase in the amount of formazan dye formed, which directly correlates with the number of metabolically active cells in the culture. Human melanocytes and melanoma cells were plated on M96 well plates at a density of 4000 cells per well. After 24 h, the cells were treated with the Ca^{2+} channel modulators as appropriate for further 24 h. After treatment, the drugs were washed out and the cells were incubated for 60–120 min with

0.5 mg/ml of WST-1 reagent. Absorbance was measured at 440 nm wavelengths using a reference filter at 620 nm wavelengths in a microplate reader (Bio-Rad Laboratories Inc., Hercules, CA, USA). Viability assays were performed at least three times in independent experiments, using triplicate measurements in each.

Cell viability was also measured using MTT [3-(4,5-dimethylthiazol-2-yl)-2,5-diphenyltetrazolium bromide] (MTT), which assess the ability of metabolically active cells to reduce MTT. Melanoma cell lines were plated on M96 well plates at 4 x 10^3 cells per well. After the corresponding treatments, cells were incubated for 45 min with 0.5 mg/mL of MTT reagent and lysed with dimethyl sulphoxide. Absorbance was measured at 595 nm in a microplate reader (Bio-Rad, Richmond, CA, U.S.A.).

For calculation of the EC_{50} values we used the Graphpad Prism statistical software, and fitted a Hill's logistic equation to the concentration response data, using the following formula: Y= bottom + (top-bottom)/1+10 $^{(\log EC_{50}-X)\text{-Hillslope}}$ Where *x* is the logarithm of the concentration; and *y* is the response, and *y* starts at the bottom and goes to the top in a sigmoid curve.

3. Calcium imaging

Changes in the concentration of intracellular Ca^{2+} were measured using the membrane permeable acetoxymethylester form of the fluorescent dye FURA-2. The cells were grown on 10 μg/ml poly-L-lysine-coated glass coverslips for 24 h and incubated for 60 min at 37ºC in culture medium containing 10 μM of FURA-2/AM (Invitrogen). This procedure resulted in an even distribution of the fluorescent dye in the melanocytes and selected melanoma cells. The cells were rinsed with physiological solution to remove the extracellular dye and the coverslips were mounted on an inverted epifluorescence microscope Eclipse TE 200 (Nikon, Tokyo, Japan) equipped with a Spectramaster monochromator (Olympus, Tokyo, Japan) and a ORCA-AG CCD camera under the control of AQUACOSMOS software (Hamamatsu Photonics, Hamamatsu, Japan). In the experiments designed to measure Ca^{2+} influx, the FURA-2 dye was dually excited at wavelengths of 340 and 380 nm and emitted fluorescence was measured at 510 nm. Changes in Ca^{2+} were expressed as changes of the fluorescence ratio of F340/F380. In

the experiments designed to measure Mn^{2+} influx, the FURA-2 was excited at the isosbestic (Ca^{2+} insensitive) wavelength of 360 nm and the emitted fluorescence was measured at 510 nm. This approach is based on the abilities of Mn^{2+} to permeate through Ca^{2+} channels (and particularly T-type channels) and to quench the FURA-2 dye [203, 204].

3.1 Recording solutions

For FURA-2 recordings, cells were perfused at a rate of 4 ml/min with a Ringer physiological solution containing (in mM): 130 NaCl, 5 KCl, 2 $CaCl_2$ (except in Mn^{2+}-quenching experiments), 1 $MgCl_2$, 10 HEPES, 10 glucose, adjusted to pH 7.4 with NaOH. When indicated, cells were depolarized with an iso-osmotic solution in which NaCl was replaced by KCl up to a concentration of 130 mM. In the experiments of FURA-2 quenching by Mn^{2+}, 200 μM $MnCl_2$ was added to a Ca^{2+}-free Ringer solution. To demonstrate the participation of T-type channels in the constitutive Ca^{2+} entry, we applied the pharmacological T-type channel blocker Mibefradil, which was dissolved from frozen stocks to a working concentration of 10 μM in Ringer solution. In these experiments, which required high volumes of perfusion, we omitted the use of the highly specific T-type channel blocker Kurtoxin due to its limited availability.

4. Polymerase chain reaction (PCR)

The polymerase chain reaction is a rapid procedure for in vitro enzymatic amplification of a specific segment of DNA. In the present study, semi-quantitative and real time PCR techniques were employed.

4.1 Isolation of RNA and cDNA synthesis

Total RNA was prepared from each human melanoma cell line / biopsy and melanocyte cell culture using TRIzol reagent (Invitrogen) according to manufacturer's instructions. The final concentration of RNA in the sample was determined by a Nanodrop (ND-1000) spectrophotometer. Messenger RNA was reverse-transcribed (RT) to cDNA (42°C for1 h, 50°C for 1 h and 90°C for 10 min) using random hexamers and Superscript II reverse transcriptase (Applied Biosystems, Carlsbad, CA, USA). Negative control RT-minus

reactions were carried out to establish that the target RNA was not contaminated with DNA.

4.2 Semi-quantitative PCR

The cDNA product was used as a template for subsequent PCR amplifications for VGCC pore-forming subunits. Primers were designed to be complementary to the published human sequences for each of the pore-forming subunits of the VGCCs and to include as many known variants as possible. Where indicated, RT-PCR primer sequences were obtained from the available scientific literature. The housekeeping gene GAPDH was used as a loading control. Table 7 contains primer sequences, product sizes and PCR conditions. For each set of primers, RT-PCR was repeated a minimum 3 times in independent samples. 20μL of reaction mixture contained 10 x reaction buffer (2μL), 1.25μL $MgCl_2$ (25mM), 1μL dNTPs (10mM), sterile water (22.55μL) and Taq polymerase (0.2μL). The PCR reaction was run in a thermocycler (Gene Amp® PCR System 2700 from Applied Biosystems). 38 cycles of PCR amplification include initialization at 95°C for 5 minutes, denaturation at 94°C for 30 seconds, annealing (temperature as specified in table 7) for 30 seconds, elongation at 72°C for 30 seconds and final elongation at 72°C for 7 minutes. Equal volumes of PCR products (20μL) were loaded and electrophoresed in a SYBR Safe (Life Technologies)-stained 3% agarose gel. The images of agarose gel illuminated by UV light were taken using Kodak EDAS 290 imaging system with Kodak 1D 3.6 software. Experiments were performed in triplicates and representative images were presented.

4.3 XBP-1 splicing assay

The method used for detection of spliced and unspliced mRNAs transcribed from the XBP-1 was based on previous literature[205, 206]. Briefly the RT-PCR product of XBP-1 mRNA was synthesized primers using primers as described in table number 6 with the following PCR protocol: 35 cycles of PCR amplification including initialization at 94°C for 4 minutes, denaturation at 94°C for 10 seconds, annealing at 63°C for 30 seconds, elongation at 72°C for 30 seconds and final elongation at 72°C for 10 minutes[248, 249]. XBP-1 processing is characterized by excision of a 26-bp sequence from the coding region of

XBP-1 mRNA. The cleaved fragment contains a Pst-1 restriction site, and the extent of XBP-1 processing can be thus evaluated by restriction analysis. PCR products were then incubated with Pst-1 restriction enzyme for 2.5 hours at 37°C, and the resulting digests were separated in 3% agarose gels. The PCR products derived from nonspliced XBP-1 mRNA were digested in two bands of 290 bp and 183 bp. In contrast the products amplified from spliced XBP-1 mRNA were resistant to digestion and remained 473 bp long.

4.4. Quantitative PCR (Real Time PCR)

Real-time PCR amplification with gene specific primers for human voltage-gated calcium channel genes CACNA1C ($Ca_v1.2$), CACNA1D ($Ca_v1.3$), CACNA1G ($Ca_v3.1$), CACNA1H ($Ca_v3.2$), CACNA1I ($Ca_v3.3$) and an endogenous control (GAPDH) were performed with using a TaqMan universal PCR master mix in an ABI prism 7000 sequence detection system (Applied Biosystems). This detection system determines the absolute quantity of a target nucleic acid sequence in a test sample by analyzing the cycle to cycle change in fluorescent signal as a result of amplification during PCR. 20 cycles at 95ºC for 15 seconds and 60°C for 1 minutes were performed. All assays were based on TaqMan hydrolysis probes labelled with FAM (green fluorescent fluorophore 6-carboxyfluorescein). The results were obtained in the form of a Ct value (cycle threshold), which represents the cycle number of the PCR during which the exponential growth of PCR product starts. Therefore, the higher the expression of the gene in the sample, the lower Ct value will be obtained as a result. The relative quantity of mRNA for every gene was calculated in the following manner: ΔCt=Ct of the target gene - Ct of GAPDH gene; Δ(ΔCt) = ΔCt of sample - ΔCt of the control. Relative mRNA levels were calculated and expressed as fold induction over contralateral controls (value=1.0) following the formula $2^{-\Delta(\Delta Ct)}$. All samples were amplified in triplicate and data were normalized using GAPDH as endogenous control. Every experiment was carried out in triplicate.

5. Propidium iodide (PI) staining and flow cytometry

Following treatment, approximately $1x10^6$ cells were fixed in 70% ethanol for at least 1 hour on ice. The cells were then resuspended in 2 ml of cell cycle buffer (20µg/ml PI) in PBS, containing 0.1% Triton X-100 and 50 µg ml^{-1} RNase A for 1 h at 37°C. PI fluorescence emission was measured with a FACS Canto II flow cytometer (BD Biosciences, Franklin Lakes, NJ, USA), and cell cycle distribution was analysed with MODFIT LT (Verity Software House, Topsham, ME, USA) and WinMDI 2.9 software (The Scripps Research Institute, La Jolla, CA, U.S.A.).

6. 5-Bromodeoxyuridine incorporation

The BrdU Cell Proliferation Assay detects 5-bromo-2'-deoxyuridine (BrdU) incorporated into cellular DNA during cell proliferation using an anti-BrdU antibody. When cells are cultured with labelling medium that contains BrdU, this pyrimidine analog is incorporated in place of thymidine into the newly synthesized DNA of proliferating cells. For the determination of DNA, cells were incubated with 6 µmol L^{-1} of 5-Bromodeoxy- uridine (BrdU) (Sigma Aldrich) for 2 hours and then fixed with 4% paraformaldehyde. After DNA denaturing with 2 M HCl for 30 min and neutralization with 0.1 M $Na_2B_4O_7$ (pH 8.5) for 2 min, cells were blocked in phosphate-buffered saline (PBS) solution containing 5% horse serum, 5% foetal bovine serum, 0.2% glycine and 0.1% Triton X-100 for 1 hour. Subsequently, cells were subjected to indirect immunofluorescence with a mouse anti-BrdU monoclonal antibody (Dako, Glostrup, Denmark), and fluorescein isothiocyanate-conjugated antimouse secondary antibody (Molecular Probes, Eugene, OR, U.S.A.). Nuclei were counterstained with 5 µg mL^{-1} Hoechst 33258 and cells were visualized under an epifluorescence microscope (Leica Microsystems, Wetzlar, Germany). The magnitude of the absorbance for the developed colour is proportional to the quantity of BrdU incorporated into cells, which is a direct indication of cell proliferation.

7. Western blot analysis

At the end of the corresponding treatments, the melanoma cell lines were washed twice with cold PBS. The corresponding melanoma cell lysates were obtained by adding lysis

buffer [2% Sodium dodecyl sulphate (SDS), 125 mM Tris-HCl, pH 6.8]. Protein extracts were denatured by heat shock at 95ºC for 3 min and quantified by a Lowry assay (Bio-Rad). Equal amounts of proteins were subjected to SDS–polyacrylamide gel electrophoresis (PAGE) and transferred to polyvinylidene difluoride membranes (Millipore, Bedford, MA, U.S.A.). Non-specific binding was blocked by incubation with TBST (20 mM Tris-HCl, 150 mM NaCl, 0.1% Tween-20, pH 7.4) plus 5% nonfat milk. Immunodetection was performed using the appropriate primary antibodies. Immunoblots were developed with an appropriate secondary Peroxidase-conjugated antibody, and the bound antibody was visualized using the chemiluminescent substrate Super Signal (Thermo Scientific, Rockford, U.S.A.) and EZ-ECL (Biological Industries, Israel). Levels of β-actin signal were used to verify equal protein loading in each lane. Some of the images were digitally acquired by VersaDoc Imaging System Model 4000 (Bio-Rad).

8. Gene knockdown by siRNA

Briefly, M16 and JG melanoma cells were plated at 50 % confluence. Transfection was performed in OptiMEM® medium containing 50-100 nM siRNA and Lipofectamine™ RNAiMAX™ reagent (Invitrogen) following the manufacturer's instructions. After 8 h the medium was changed to regular culture medium. To increase the efficiency of the knockdown, a second transfection was performed the following day. Cells were processed 24 h after the second transfection. In each experiment, the knockdown efficiency was analyzed by real-time PCR.

9. LysoTracker® Red DND-99 staining

LysoTracker® Red DND-99 is a cell-permeant red-fluorescent dye for selective lysosomal staining with a minimum background. It consists of a fluorophore linked to a weak base that is only partially protonated at neutral pH. This allows LysoTracker® probes to freely permeate cell membranes enabling them to label live cells. The 70%-confluent cells were treated with calcium channel blockers. At the appropriate time points, the growth medium was removed and the cells were labelled with LysoTracker® Red DND-99 (100 nM) for 2 minutes, washed with HBSS and further labelled with Hoestch 33258 (5 μg mL^{-1}) for further 15 minutes, at 37ºC in a CO_2 incubator. After Hoechst counter-staining, the cells

were washed twice with HBSS at room temperature and visualized immediately under an epifluorescence microscope (Leica Microsystems, Wetzlar, Germany).

10. Hoestch 33258 staining

The cells were treated with drugs and, at the appropriate time, the growth medium was aspirated and the cells were washed twice with warm PBS 1X. The cells were then fixed with paraformaldehyde in PBS at RT and cold methanol was added for permeabilization. The cells were kept at room temperature for 20 minutes, rinsed thoroughly 3 times with PBS and 5 µg ml^{-1} of Hoechst staining were added for further 15 minutes at RT. Finally, the cells were rinsed 3 times with PBS and visualized under an epifluorescence microscope (Leica Microsystems, Wetzlar, Germany)

11. Statistical analysis

Statistical significance was checked, as appropriate, by application of a Shapiro–Wilk normality test followed by a two-sample Student t-test, or a Mann–Whitney rank sum test.

RESULTS

Chapter 1

Functional Expressions of Voltage Gated Calcium Channels in Human Melanoma

1. Expression of VGCCs in control normal melanocytes and melanoma cells

Standard reverse transcriptase PCR (RT-PCR) was performed to determine the expression of the three gene families encoding VGCCs in three fast-growing metastatic melanoma cell lines (M28, M36, JG), two average-growing metastatic cell lines (M16, M17), one slow-growing metastatic melanoma cell line (M29), one very slow growing primary tumour-derived cell line (M9) and three tumour biopsies (named B1, B2 and B3). In the first set of data, we compared the expression of VGCCs in control normal melanocytes and three selected melanoma cell lines (M16, M28 and JG) that were cultured in parallel, using melanocyte growth medium (see Methods) (Figure 8A). As the Ca^{2+} imaging experiments demonstrated the functional relevance of L-type and T-type channels in the melanoma cells (see below), we additionally checked up the expression of these channels by quantitative RT-PCR (Q-PCR) (Figure 9). Subsequently, we extended the analysis of VGCCs expression to all melanoma cell lines grown in standard high-glucose DMEM, and to the biopsies (Figure 8B).

1.1 L-type channels

We tested the expression of L-type Ca^{2+} channels by RT-PCR using specific primers for $Ca_v1.2$ and $Ca_v1.3$ pore-forming subunits. Both channel isoforms have been suggested recently to play a role in the Ca^{2+}-dependent events underlying mitotic progression in endocrine cells[207]. Expression of $Ca_v1.2$ channels was found to be widespread, with positive results in all melanoma cells but two metastatic cell lines (M17 and JG), whereas the channels were undetectable in control normal melanocytes. In contrast, $Ca_v1.3$ channels were ubiquitously expressed in all metastatic cell lines, the primary tumour and the biopsies, while showing the highest levels in control normal melanocytes (Figures 8 A-B, Figure 9).

1.2 N-type, P-Q-type and R-type channels

Melanocytes are specified from pluripotent neural crest cells that delaminate from the developing neural tube in the initial stages of development[208]. Because of the common embryological origin with peripheral nervous and neuroendocrine tissue, we examined the expression of Ca^{2+} channels belonging to the Ca_v2 family, which play a well known

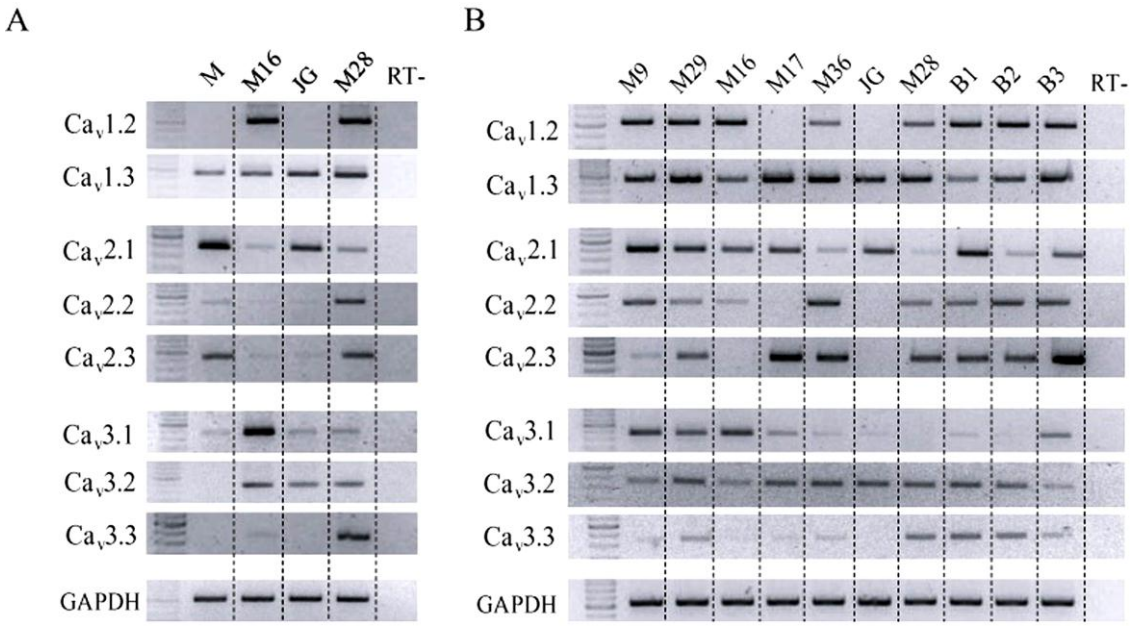

Figure 8. *RT-PCR expression analysis of human genes encoding VGCCs. (A) comparison of VGCC expression in control normal melanocytes(M) and three selected melanoma cell types (M16, JG and M28) cultured in melanocyte growth media. (B) Extended analysis for the same melanoma cell lines as in (A), plus M9, M29, M17 and M36, all cultured in melanoma standard high-glucose medium. The analysis included three biopsies taken from metastatic melanomas (B1, B2, B3). Results were validated at least three times from independent RT-PCR reactions. The first lane shows the MW markers, the 250-bps band being the most prominent.) RT- is the sample without reverse transcriptase.*

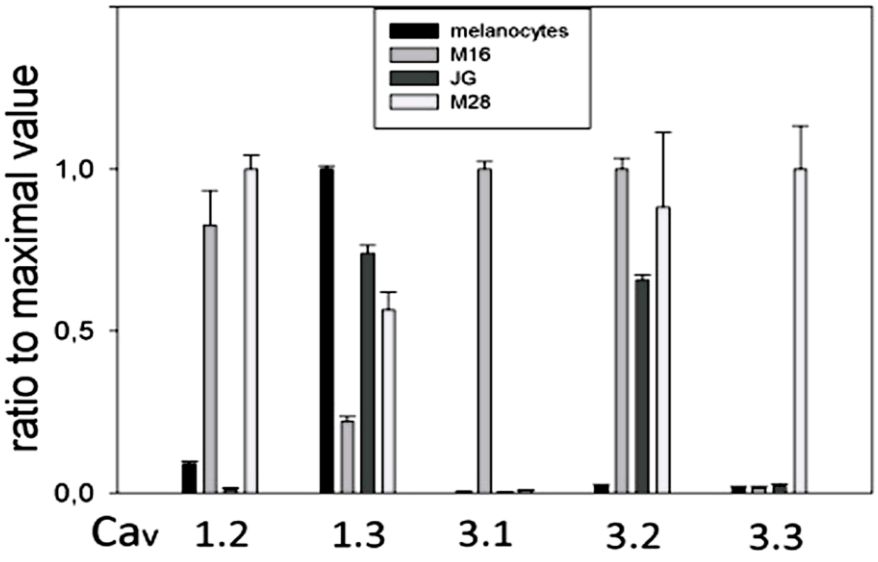

Figure 9*. Expression analysis of human genes encoding VGCCs by real time PCR*

Table 9. Classification of the melanoma-derived cell lines according to their origin and proliferation rate, and expression of VGCCs types

Origin	Samples	T-type	L-type	N, P-Q, R-type
Untransformed	Melanocytes	None	$Ca_v1.3$	$Ca_v2.1$ $Ca_v2.2$ (low) $Ca_v2.3$
Primary tumors	M9 (LPR)	$Ca_v3.1$ $Ca_v3.2$ (low)	$Ca_v1.2$ $Ca_v1.3$ (low)	$Ca_v2.1$ $Ca_v2.2$ $Ca_v2.3$ (low)
Metastasis (skin)	M29 (LPR)	$Ca_v3.1$ $Ca_v3.2$	$Ca_v1.2$ $Ca_v1.3$	$Ca_v2.1$ $Ca_v2.2$ (low) $Ca_v2.3$
	M16 (MPR)	$Ca_v3.1$ $Ca_v3.2$ (low)	$Ca_v1.2$	$Ca_v2.1$ $Ca_v2.2$ (low)
	M17 (MPR)	Cav3.1 (low) Cav3.2	$Ca_v1.3$	$Ca_v2.1$ $Ca_v2.3$
	JG (HPR)	$Ca_v3.2$ $Ca_v3.3$	None	$Ca_v2.1$
	M28 (HPR)	$Ca_v3.2$ $Ca_v3.3$	$Ca_v1.2$ $Ca_v1.3$	$Ca_v2.2$ $Ca_v2.3$
Metastasis (CSF)	M36 (HPR)	$Ca_v3.2$	$Ca_v1.2$ $Ca_v1.3$	$Ca_v2.1$ (low) $Ca_v2.2$ $Ca_v2.3$
Biopsies	B1	$Ca_v3.2$ $Ca_v3.3$	$Ca_v1.2$ $Ca_v1.3$	$Ca_v2.1$ $Ca_v2.2$ $Ca_v2.3$
	B2	$Ca_v3.1$ $Ca_v3.2$ $Ca_v3.3$	$Ca_v1.2$ $Ca_v1.3$	$Ca_v2.1$ (low) $Ca_v2.2$ $Ca_v2.3$
	B3	$Ca_v3.2$	$Ca_v1.2$ $Ca_v1.3$	Cav2.1 Cav2.2 Cav2.3

role in neurotransmitter release and neurosecretion[209]. Our results show that control normal melanocytes expressed transcripts for $Ca_v2.1$ and $Ca_v2.2$ (low expression) and $Ca_v2.3$ channels (figure 8A). Melanoma cells also expressed the three Ca_v2 isoforms, with the following exceptions: $Ca_v2.2$ was not amplified from M17 and JG metastatic cell lines; $Ca_v2.3$ was not amplified from M16 and JG metastatic cell lines or the M9 primary tumor cell line (figure 8B).

1.3 T-type channels

Low voltage-activated T-type channels are involved in cell proliferation and the expression of T-type channel isoforms is up-regulated in different tumours[43,76] . As shown in Figure 8B, the expression of T-type channels was detected in all melanoma cell lines and biopsies, although we found qualitative and quantitative differences in the expression of the different isoforms: the M9 primary tumour cells, the M29 and M16 metastatic cells and the B3 biopsy expressed the highest levels of $Ca_v3.1$, while showing lower levels of $Ca_v3.2$ transcripts. Interestingly, this pattern of expression was linked to a slower proliferation rate (Table 9, Figure 11). Only two cell lines derived from skin metastasis (M28 and M29) and two melanoma biopsy samples (B1, B2) expressed $Ca_v3.3$ channels, with no concomitant decrease in the level of $Ca_v3.2$ expression. Importantly, very low levels of $Ca_v3.1$ transcripts were detected as the only T-type channel isoform expressed in control normal melanocytes (Figures 8A and 9). As stated above, for these RT-PCR experiments we used three melanoma cell lines (M16, M28 and JG) as positive controls, cultured in parallel with control normal melanocytes in melanocyte growth medium, although in these conditions their proliferation rate was significantly lower than that attained in standard high-glucose medium (data not shown).

2. Moderate hypoxia induces the selective up-regulation of T-type and L-type channels

Physiological skin hypoxia has proved to be a relevant factor for melanocyte transformation and melanoma development[210]. It had been shown that $Ca_v3.2$ channels are upregulated via the activation of hypoxia inducible factor-2 (HIF-2) in PC12 cells[86] and that $Ca_v3.1$ channels are down-regulated by HIF-1 in neonatal cardiomyocytes[211] Therefore, we decided to test whether the expression of Ca_v3 channels was regulated by hypoxia in control normal melanocytes and melanoma cells.

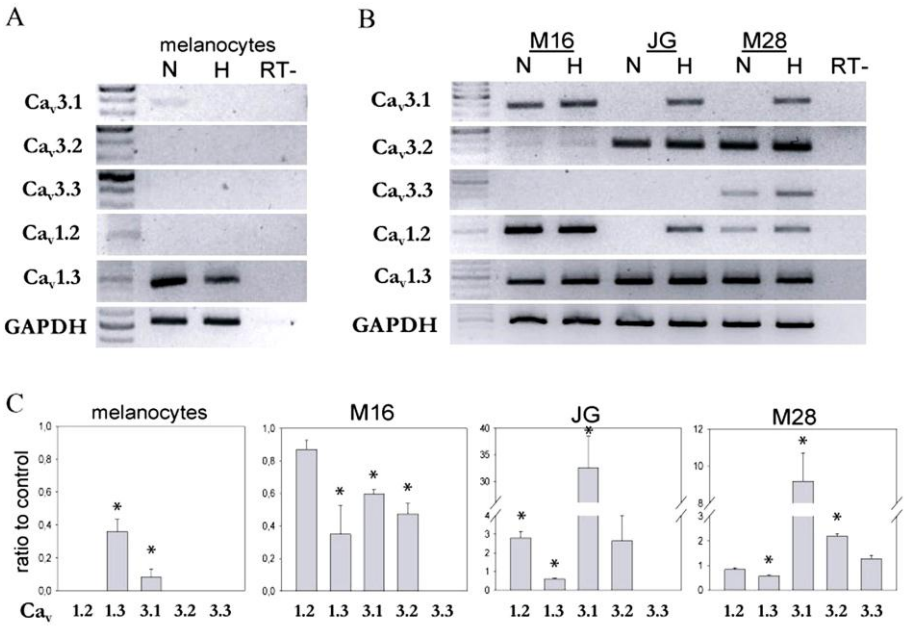

Figure 10. *Hypoxic up-regulation of T-type channel isoforms in control normal melanocytes and a selection of melanoma cell lines (M16, JG and M28). RT-PCR was performed to amplify T-type channel transcripts from the cells incubated in a normoxic (N) or hypoxic (H, 2% O_2) atmosphere for 24 h. (A) None of the transcripts for Ca_v3 channel isoforms was amplified from control normal melanocytes, irrespective of the O2 concentration. (B) Induction of $Ca_v3.1$ and $Ca_v3.2$ channel transcripts by hypoxia in fast-growing JG and M28 metastatic melanoma cells. (C) VGCC gene expression analysis by Q-PCR in the same cell lines as above. Histograms show mean fold expression in hypoxia related to the mean of the normoxic control ('ratio to control'). Absence of bars indicates undetectable levels in control conditions. Data was obtained from triplicate measurements in each of three to six independent experiments. *Significant differences related to control group ($P < 0.05$). RT-, minus reverse transcriptase*

JG, M16 and M28 cells at 70–80% confluence were placed in a hypoxic incubator and exposed to 2% O_2 for 24 h. Control plates were kept in a normoxic state and processed in parallel. RT-PCR data showed the up-regulation of selective T-type channels by hypoxia, which was specific to the cell type. Thus, $Ca_v3.1$ (and $Ca_v3.2$ to a minor extent) were up-regulated in fast-growing JG and M28 cells but not in average-growing M16 cells (Figure 10B). Hypoxia did not induce the up-regulation of any of the three T-type channel isoforms in control normal melanocytes but did induce a down-regulation of the already low levels of $Ca_v3.1$ (Figure 10A).

We also checked the effect of a moderate hypoxic environment on the expression levels of L-type channels, by RT-PCR. Under hypoxic conditions, the expression of L-type

$Ca_v1.2$ channels was increased in the JG cell line compared with normoxia conditions. In contrast, the expression of $Ca_v1.3$ channels was slightly reduced by hypoxia in control normal melanocytes (Figure 10A).We complemented these data by performing a series of Q-PCR experiments. This approach confirmed that the up-regulation of $Ca_v3.1$ (up to 60-fold) and $Ca_v3.2$ (≈two-fold) T-type channels by hypoxia was restricted to the fast-proliferating JG and M28 cell lines, whereas the expression of both isoforms was reduced by hypoxia in medium-proliferating M16 cells. Consistent with the RT-PCR data, these experiments also showed that the expression of the L-type $Ca_v1.2$ channels was increased by hypoxia in JG cells (≈three-fold), remaining unchanged in M16 and M28 cells, whereas $Ca_v1.3$ channels were down-regulated by hypoxia in all cell lines (Figure 10C).

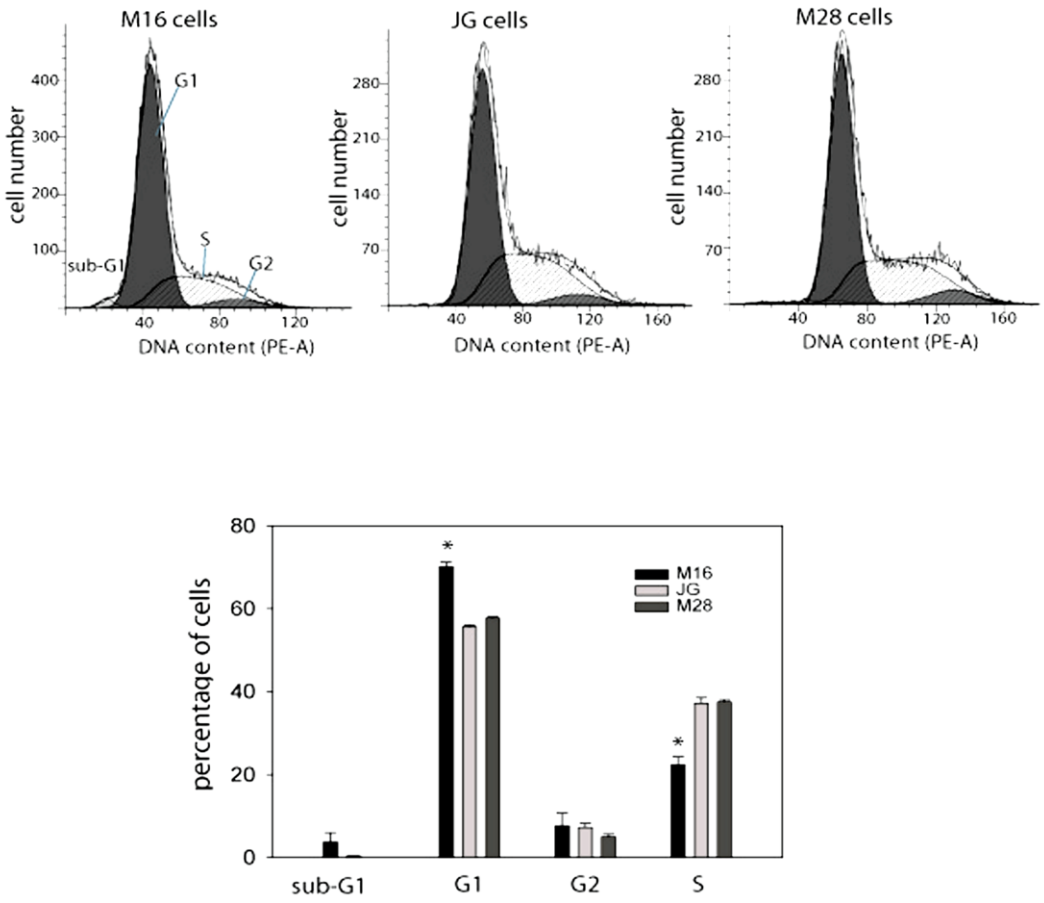

Figure 11. *Cell cycle analysis by flow cytometry (PI staining) of JG, M28 and M16 melanoma cells at 60–70% confluence.*

3. Functional expression by calcium imaging

To examine the functional expression of the VGCCs and their contribution to Ca^{2+} influx, we performed a series of Ca^{2+} imaging experiments using the membrane permeable acetoxymethylester (AM) form of the fluorescent dye FURA-2 in a dynamic fluorescence set-up in control normal melanocytes and a selection of melanoma cells.

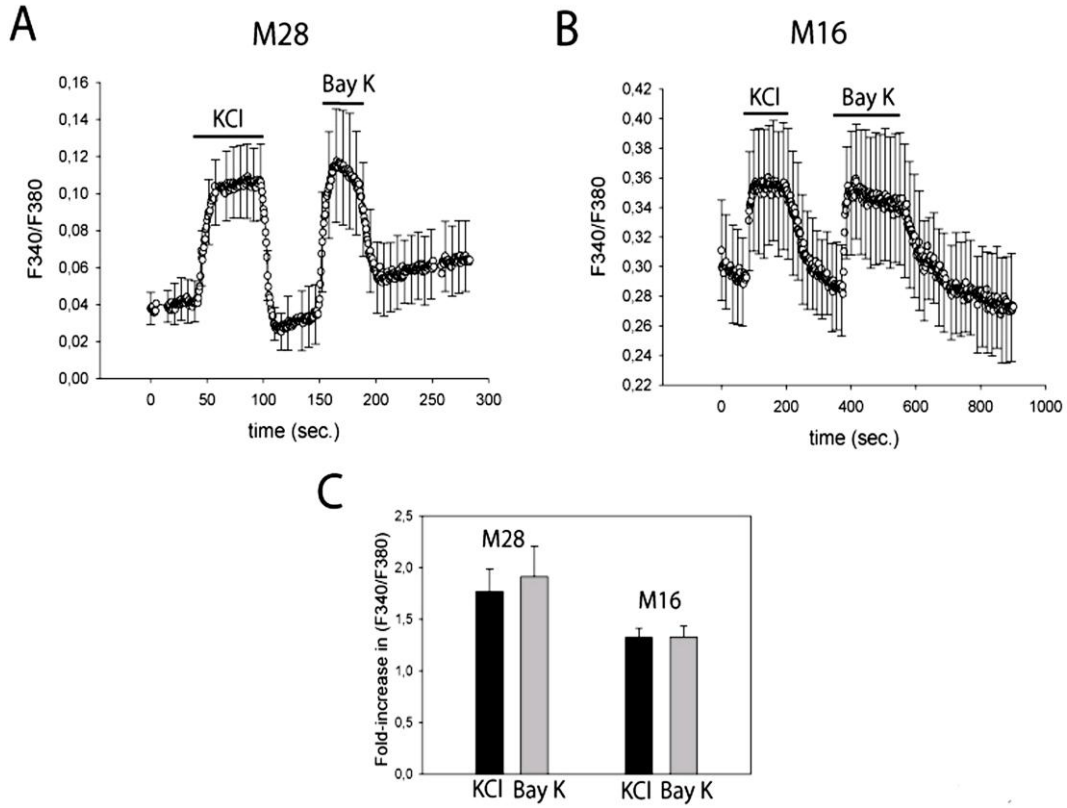

Figure 12. *Increases of cytosolic Ca^{2+} in response to sequential membrane depolarization, and pharmacological activation of L-type channels in control melanocytes (M) and melanoma cells (JG, M16 and M28). Cytosolic Ca^{2+} levels in Fura-2-loaded cells were monitored as the fluorescence ratio at 340 and 380 nm (F340 / F380). In 'double pulse' experiments, KCl-driven depolarization and Bay K 8644 application failed to induce changes in the F340 / F380 ratio of control melanocytes, and only minor increases could be recorded in JG cells. However, both stimuli elicited consistent increases of F340 / F380 in the M28 and M16 melanoma ma cell lines, demonstrating the functional expression of L-type $Ca_v1.2$ channels. (A) Average F340 / F380 data points from six to 12 cells recorded in a single experiment, as indicated. Standard deviation values are represented as error bars every 50 points, for clarity. (B) Fold increase of the F340 / F380 ratio values induced by paired-KCl and Bay K 8644 pulses. Values are represented as means ± SD (n = 37 for melanocytes, n = 37 for JG, n = 17 for M28, n = 21 for M16).*

The following different experimental paradigms were used to demonstrate the functional expression of high and low voltage-activated channels. KCl-mediated depolarization did not induce detectable changes in the cytosolic Ca^{2+} levels in melanocytes, with only small elevations in melanoma JG cells. In contrast, high K^+ triggered consistent increases of the F340/F380 ratio in $Ca_v1.2$-expressing M16 and M28 cells. The addition of Bay K 8644 (an L-type channel activator) resulted in equivalent increases of F340/F380 in M16 and M28 cells, indicating that L-type $Ca_v1.2$ channels were the main carriers of depolarization-mediated Ca^{2+}-influx (Figure 12 A,B). All M16 and M28 melanoma cells responded to the high K^+ and Bay K 8644 challenges, even when showing individual differences.

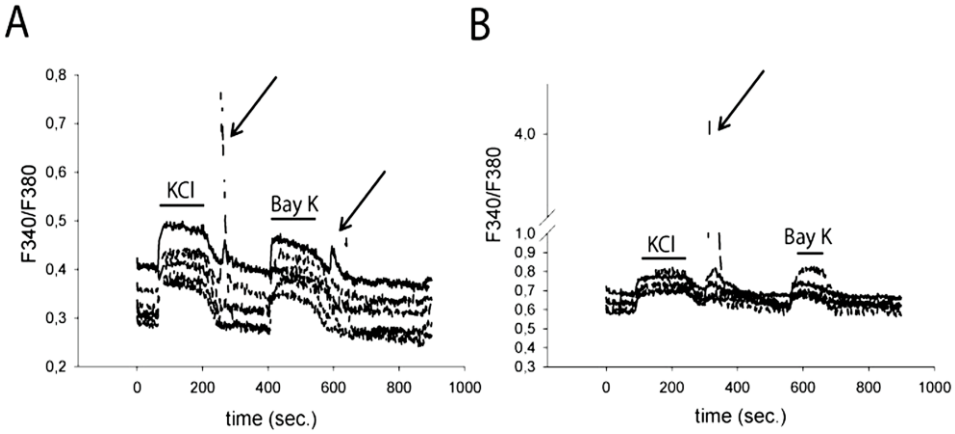

Figure 13. *Panel A and B shows cytosolic Ca^{2+} increases in melanoma cells, secondary to membrane depolarization and / or L type channels activation-induced elevations*

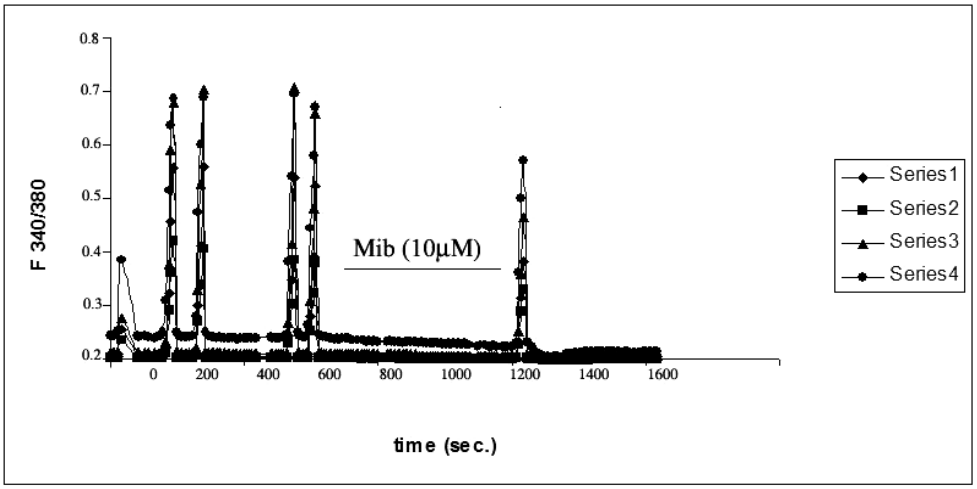

Figure 14. *Oscillation of intracellular calcium in M16 cells at resting membrane potential.*

Often, either the depolarizing or the pharmacological stimuli triggered secondary increases of the intracellular Ca^{2+}, suggesting a coupling of L-type channels to the intracellular Ca^{2+} reservoirs (Figure 13 A, B). Moreover, M16 cells at normal resting membrane potential also showed intracellular calcium oscillations which were largely decreased with the use of Mibefradil (Figure 14).

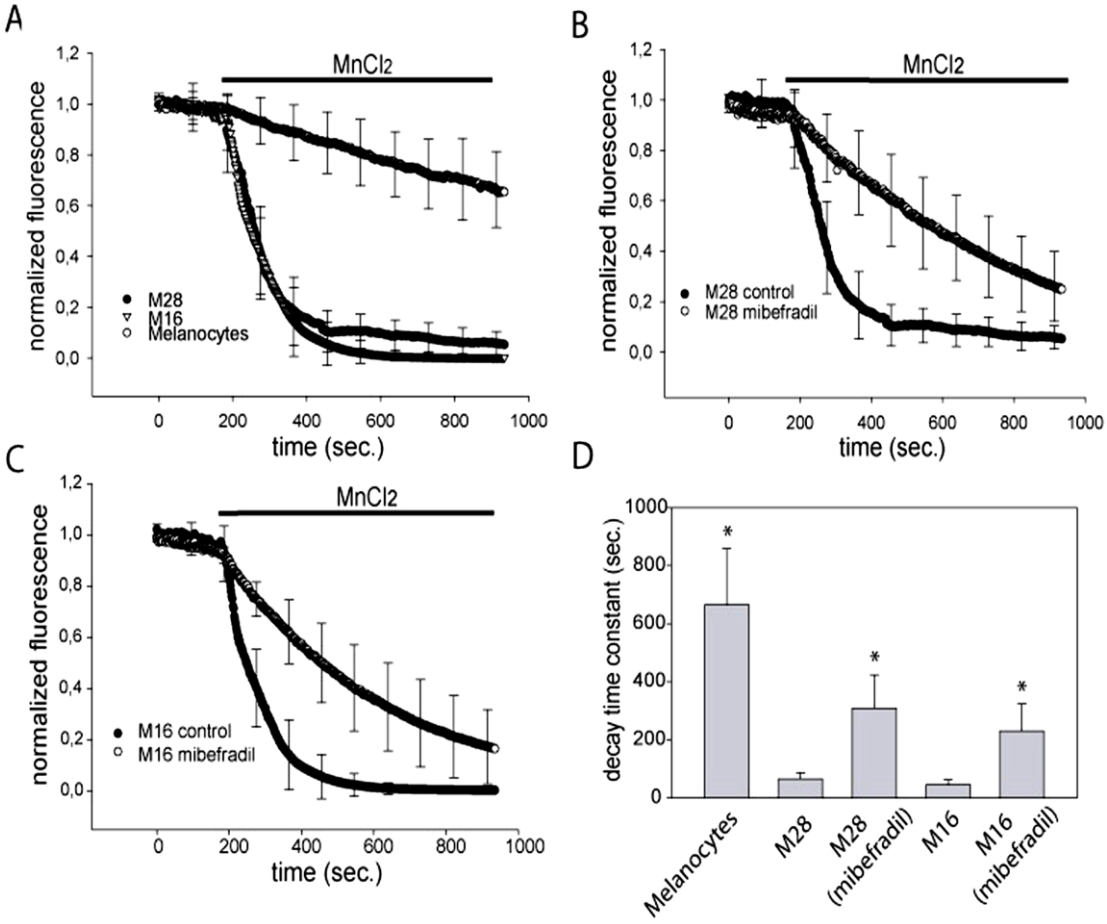

Figure 15. *Basal Mn^{2+} influx and its inhibition by Mibefradil. Fura-2-loaded cells were exposed to 200 µM $MnCl_2$ dissolved in a Ca^{2+}-free Ringer solution, as indicated. The Mn^{2+}-induced decrease of the normalized Fura-2 fluorescence was recorded at the isosbestic (Ca^{2+} independent) excitation wavelength (360 nm). (A) Comparison of the Mn^{2+}-induced quenching of control normal melanocytes (open circles), M28 (closed circles) and M16 (open triangles) Fura-2-loaded cells. (B) Mn^{2+}-induced quenching of Fura-2 fluorescence in M28 melanoma cells in the absence (closed circles, same curve as in A) and presence of Mibefradil (open circles), displaying a much slower time course. (C) Mn^{2+}-induced quenching of Fura-2 fluorescence in M16 melanoma cells in the absence (closed circles, same curve as in A) and presence (open circles) of Mibefradil*

*(10μM), which again slowed down of the quenching. Traces shown in (A–C) were obtained by averaging three independent experiments. (D) Quantification of the Mn^{2+}-induced quenching rate of all analyzed cell types as the time taken for the fluorescence signal to decay to 67% of the initial value (decay time constant). Histogram bars represent mean ± SD values from at least three independent experiments (n = 20 for melanocytes, n = 28 for M28 cells, n = 29 for M28 cells in the presence of Mibefradil, n = 40 for M16 cells, n = 27 for M16 cells in the presence of Mibefradil). *Statistical significance of P < 0.001 achieved by application of the Mann– Whitney rank sum test (means compared: melanocytes versus M28 cells, M28 cells versus M28 cells in the presence of Mibefradil, M16 cells versus M16 cells in the presence of Mibefradil).*

4. Constitutive Ca^{2+} influx: Mn^{2+} quenching at the FURA-2 isosbestic point

The function of low voltage-activated Ca^{2+}-channels was confirmed by measuring the rate of Mn^{2+} influx into the cells, following the approach first described by Jacob in 1990 (see Methods). A rapid quenching of the FURA-2 fluorescence (excitation at the Ca^{2+}-insensitive excitation wavelength of 360 nm) resulted from 200 μM Mn^{2+} perfusion in the two tested melanoma cell lines, M16 and M28, in contrast to a 10-fold slower decay of the fluorescence in control normal melanocytes (figure 15 A,D). This result is consistent with the increased expression of T-type channels in melanoma cells, compared with melanocytes. Furthermore, when we included the T-type channel blocker Mibefradil in the perfusate for M16 and M28 melanoma cells, the rate of fluorescence quenching by Mn^{2+} was four- to five-fold slower, indicating the participation of T-type channels in the constitutive influx of divalent ions (15B,C).

5. Role for T-type channels in melanoma cell cycle progression

We further studied the effects of T-type channel blockers on the viability of melanoma JG cells by analyzing the DNA content after propidium iodide staining using flow cytometry. T-type channel blocker Kurtoxin induced a significant increase of the percentage of cells at the G1 phase, while reducing the percentage of cells at the S phase, which indicates cell cycle arrest (Figure 16A). To ascertain a direct role of Ca_v3 channels in the regulation of cell cycle progression, we performed a set of siRNA-mediated $Ca_v3.1$ knockdown experiments in M16 cells and $Ca_v3.2$ knockdown experiments in JG cells. Q-PCR demonstrated a 58% reduction of $Ca_v3.1$ transcripts in M16 cells and a 63% reduction of

$Ca_v3.2$ transcripts in JG cells compared with the cells transfected with control siRNA (Figure 16D). These reduced levels of $Ca_v3.1$ and $Ca_v3.2$ genes induced cell cycle arrest at the G1 and S phases (Figure 16B,C), in a pattern similar to that induced by Kurtoxin, albeit to a lesser extent.

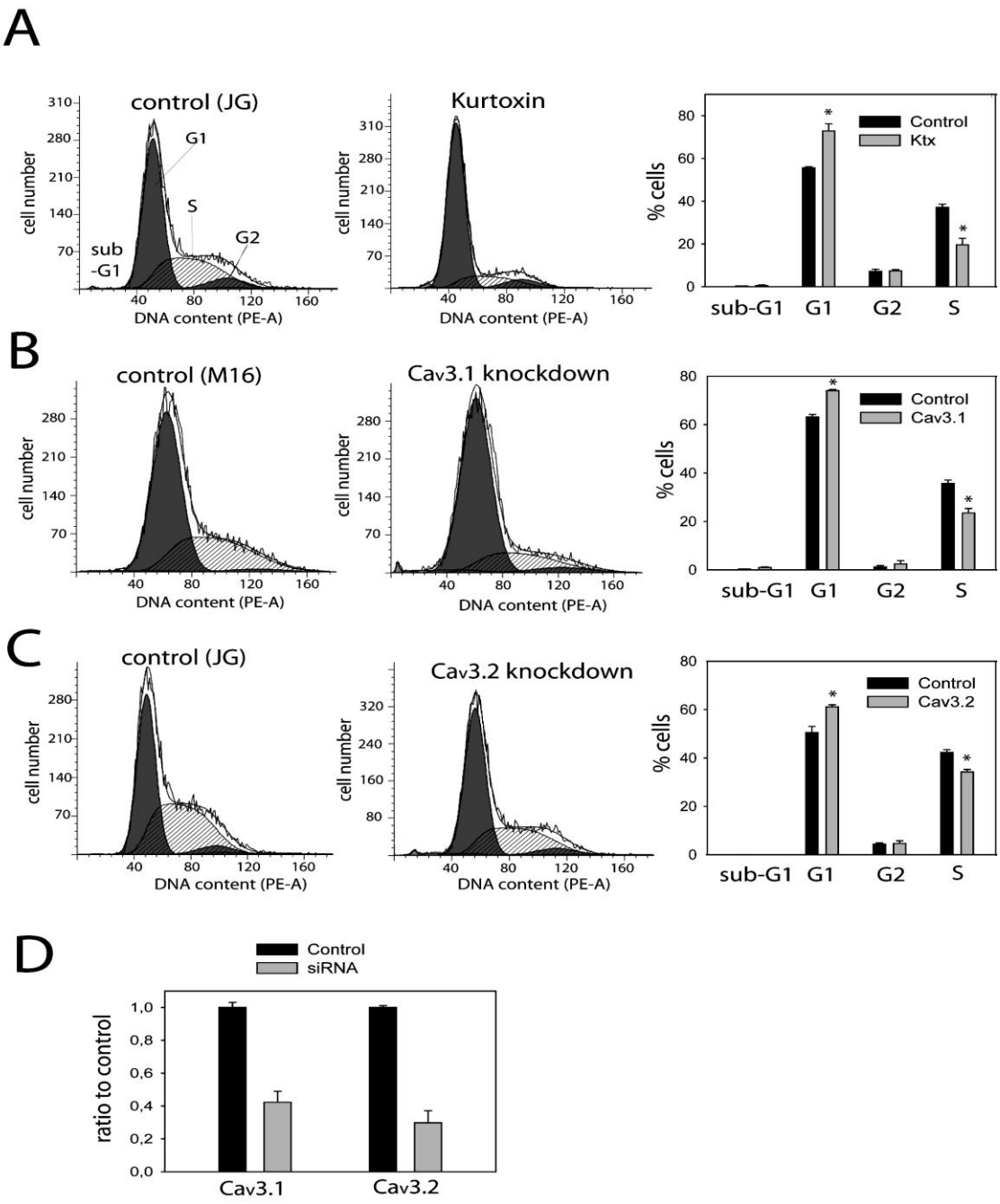

Figure 16. *Flow cytometry analysis and cell cycle distribution of JG and M16 melanoma cells: effect of T-type channel pharmacological blockade and gene silencing. (A) JG cells were incubated with 250 nM Kurtoxin for 24 h. Kurtoxin treatment slowed down the cell cycle by concomitantly increasing the percentage of cells at the G1 phase and decreasing*

*the percentage of proliferating (S phase) cells. (B) siRNA-mediated $Ca_v3.1$ knockdown halted the progression of cell cycle from G1 to S phase of M16 melanoma cells. (C) Similarly, siRNA mediated $Ca_v3.2$ knockdown in JG melanoma cells promoted cell cycle arrest at the G1 and S phases. (D) Q-PCR analysis of the level of $Ca_v3.1$ and $Ca_v3.2$ knockdown in M16 and JG cells, respectively, for the experiments displayed in (B) and (C). (A–C, left and center) Graphs display the cell cycle profiles of representative experiments.(A–C, right) Histograms for the mean values (±SEM)(n=3) of the different cell cycle phases using flow cytometric analysis. *Significant differences related to control group (P < 0.05).*

6. Cell proliferation in hypoxia

Having shown that hypoxia regulates T-type channel expression, and that T-type channels are directly involved in the melanoma cell cycle progression, we next examined the effect of hypoxia on the cell cycle parameters.

A 2% O_2 atmosphere (applied for 24 h) had opposite effects on the growth rate, depending on the melanoma cell type: the percentage of proliferating M16 cells was reduced (Figure 17A) whereas the percentage of proliferating JG cells was increased (Figure 17B). These opposite effects of hypoxia on the proliferation rate of M16 and JG cells correlate with the opposite effects of hypoxia on T-type channel expression in these cell types (Figure 10).

To further elucidate the relationship between hypoxia, T-type channels expression and proliferation rate, we silenced $Ca_v3.1$ and $Ca_v3.2$ genes in JG cells subject to hypoxia. Under these conditions the $Ca_v3.1/Ca_v3.2$ expression ratio is increased by about 30-fold (Figure 10C). The transfection of $Ca_v3.1$ siRNA completely prevented its hypoxia mediated up-regulation and, in fact, the $Ca_v3.1$ transcripts were reduced to a 57% of the normoxia levels (Figure 18A). In comparison, the $Ca_v3.2$ transcripts were reduced to 30% of the normoxia levels in the JG cells transfected with $Ca_v3.2$ siRNA (Figure 18A). Both siRNAs were able to reverse the hypoxia-mediated effects on cell cycle parameters and or $Ca_v3.2$ knockdown, the percentage of cells arrested at the G1/S phase was significantly higher than in JG cells grown in normoxia (figure 18B).

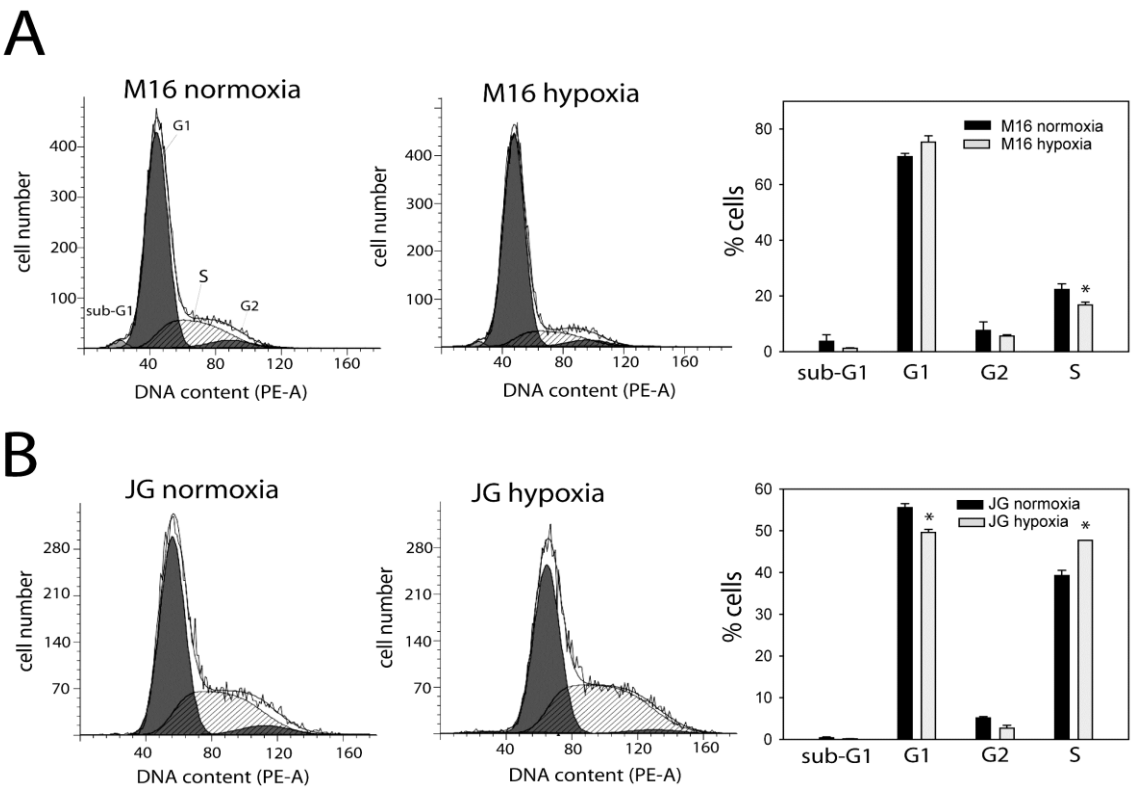

Figure 17. *Flow cytometry analysis and cell cycle distribution of JG and M16 melanoma cells: effect of hypoxia. (A, Left and center graphs) Representative profiles for M16 cells grown in normoxia and 2% O_2, respectively. Hypoxia induced a small increase of the percentage of cells in the G1 phase, and a concomitant reduction of cells in the proliferative S phase. (B, Left and center graphs) Representative profiles for JG cells grown in normoxia and 2% O_2, respectively. Hypoxia induced G1-S progression, contrary to the effect in M16 melanoma cells. (A–B, right) Histograms summarize data for cell cycle parameters in M16 and JG melanoma cells, respectively. *Significant differences related to control group ($P < 0.05$).*

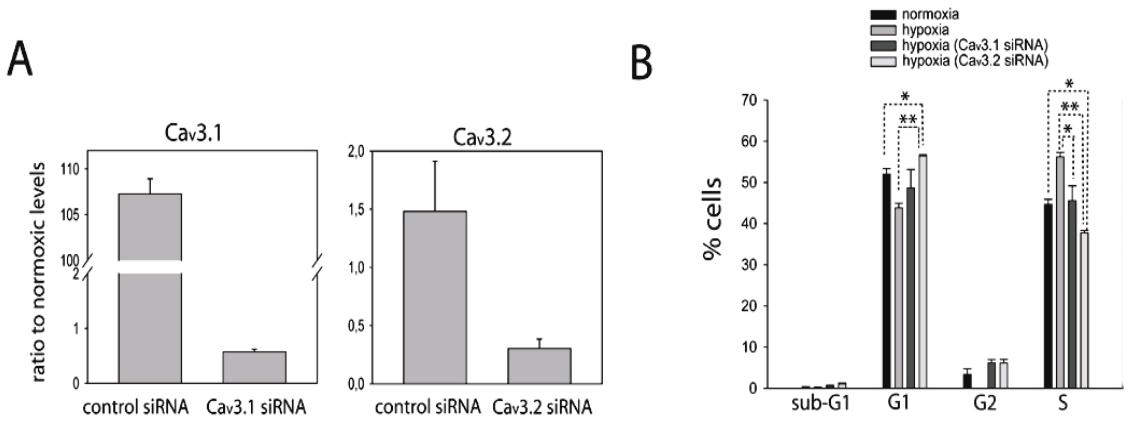

Figure 18. *The knockdown of $Ca_v3.1$ and $Ca_v3.2$ T type channels prevents hypoxia-induced JG melanoma cell proliferation.*

7. Effect of the pharmacological blockade of VGCCs on viability of melanoma cells

To investigate a possible role of VGCCs in melanoma cell proliferation and survival, we examined the effect of VGCC blockade on cell viability. We performed WST-1 metabolic assays on a selection of melanoma cell lines (M16, JG, M28) treated with some of the most specific VGCC blockers available: the neurotoxins Kurtoxin (T-type channel blocker), ω-Agatoxin IVA (P-Q type channel blocker), ω-Conotoxin GVIA (N-type channel blocker), rSNX-482 (R-type channel blocker) and the Dihydropyridines Nimodipine and Nifedipine (L-type channel blockers).

After treatment for 24 hours, Kurtoxin had the strongest effect and reduced the viability of all melanoma cells by an average of 38–41%. Kurtoxin treatment was non-effective in control normal melanocytes (non-significant 3% reduction of viability, consistent with the lack of expression of T-type channels in these cells. In contrast, L-type channel blockers Nimodipine and Nifedipine negatively affected the viability of both control normal melanocytes (11 and 6%, respectively) and melanoma cells (12–15 and 8–10%, respectively. The rest of the VGCC channel blockers also had a moderate effect on control normal melanocytes and melanoma cells (2–11% reduction of viability) (Figure 19).

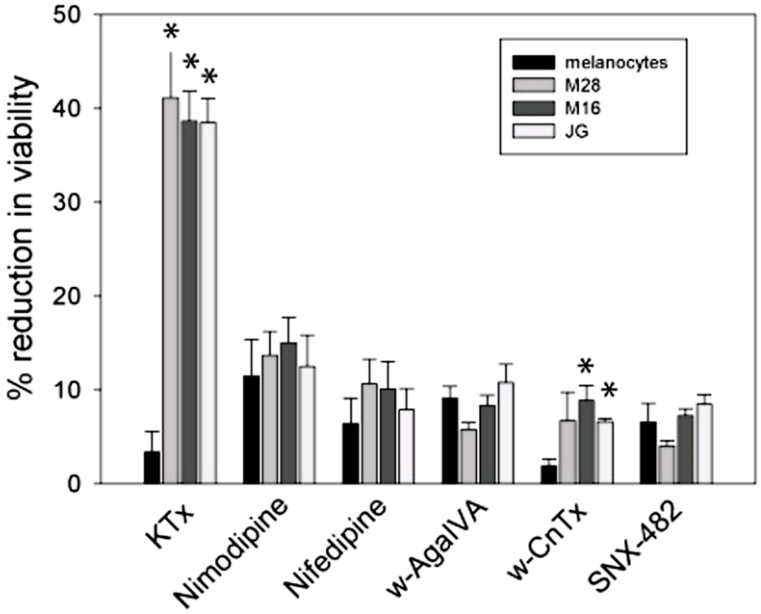

Figure 19. *Effect of VGCC pharmacological blockers on cell viability. The viability of melanoma cells was measured using the WST-1 proliferation assay. Absorbance values at 440 nm, obtained from cells subjected to the different treatments, are expressed as the percent reduction with respect to control untreated cells. T-type channel blocker Kurtoxin (KTx, 250 nM) did not significantly affect the viability of control normal melanocytes, consistent with the lack of expression of T-type channels in these cells (Figures 8 and 9). In contrast, Kurtoxin induced a similar reduction of viability in all cell lines tested (M28, M16 and JG, values ranging from 38 to 41% reduction in viability). Blockers specific for L-type (Nimodipine and Nifedipine, 10 µM), P-Q-type (ω-Aga-IVA, 500 nM), N-type (ω-Cntx, 1 µM) and R-type (SNX-482, 250 nM) channels had a moderate effect on the viability of melanocytes and melanoma cell lines, ranging from 6 to 15% reduction. Three to four independent experiments were performed per cell type and treatment, using parallel controls and triplicate measurements of each. *Significant differences related to control (melanocytes), $P < 0.01$.*

Chapter 2

T-Type calcium channel blockers and gene silencing induce endoplasmic reticulum stress and inhibit constitutive autophagy in human cutaneous melanoma-derived cell lines

1. Effect of Mibefradil and Pimozide on cellular viability

The experiments shown in the previous section suggested that T-type channel blockade might be a valid approach to tackle melanoma progression. We thus decided to test the effect on melanoma cells of T-type channel blockers which have been or are currently used in clinical practice, such as the anti-hypertensive/anti-anginal Mibefradil (banned by the Food and Drug Administration (USA) in 1998 due to interactions with certain hypolipemic drugs, but reintroduced in 2008, 2009 and 2010 for the treatment of breast, prostate and glioma tumours), and the neuroleptic Pimozide.

We first studied the effect of these clinically relevant T-type VGCC blockers on melanoma cell viability, by performing a concentration-dependency study: the human melanoma cell lines M9, M29, M16, M17, JG, M28, M36 were exposed to increasing concentrations of Mibefradil for 24 h at 37°C and, and the activity of the mitochondrial dehydrogenase enzyme was measured by the MTT metabolic assay (Figure 20A). Parallel experiments were performed with Pimozide (Figure 20B). Both Mibefradil and Pimozide reduced cell survival in a concentration-dependent manner in all tested cell lines. In primary tumor-derived cell lines and slow and medium growing metastatic melanoma cell lines, the EC_{50} for Mibefradil on survival ranged from 6.1 to 7.0 μM; in the same cells, the EC_{50} for Pimozide was from 4.3 to 5.9 μM. Fast-growing metastatic melanoma cell lines showed a higher sensitivity to both drugs, with Mibefradil EC_{50} values between 2.8 to 3.1 μM, and Pimozide EC_{50} values between 2.3 to 2.8 μM. Having tested that Mibefradil and Pimozide were effective in reducing the viability of melanoma cells, we next wondered if the main parameter contributing to viability loss was the proliferation of the cells, like for Kurtoxin at 24 hours treatments. In fact, under phase contrast microscopy, the appearance of shrunk and floating cells in the culture dishes treated with drug concentrations > 1 μM suggested that there was a significant cell death.

2. Mibefradil induces cell cycle arrest and a reduction of the proliferation rate

Based on the preliminary assays where we observed a strong growth inhibitory effect of Mibefradil and Pimozide in a panel of melanoma cells, we tried to determine the molecular mechanisms underlying the anti-proliferative activity of these drugs, by flow cytometry analysis and BrdU labelling. We chose M16 and JG melanoma cells as two

A

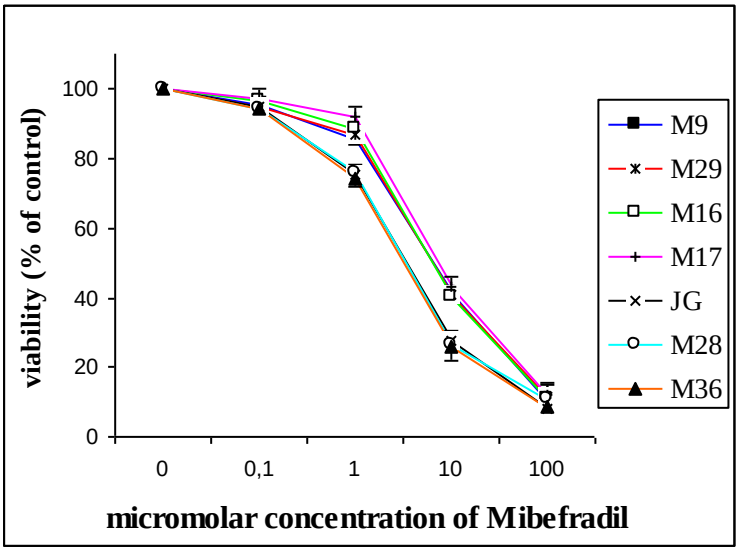

B

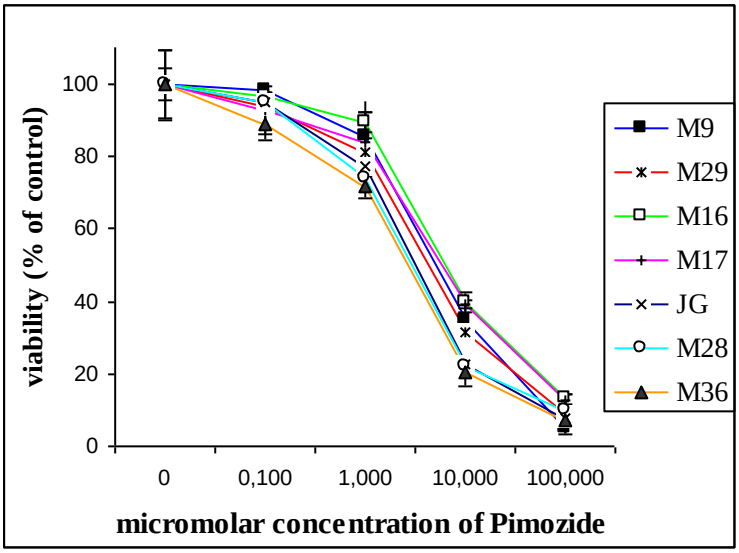

Figure 20. *Mibefradil and Pimozide induce a decrease in cell viability in a panel of melanoma cell lines. Melanoma cells from either primary or metastatic tumours (see table 9) were treated with increasing concentrations of Mibefradil (panel A) and Pimozide (panel B) for 24 h.Cell viability was assessed by 3-(4,5- dimethylthiazol-2-yl)-2,5-diphenyltetrazolium bromide assay. Results are expressed as mean ± SE percentage of the control values.*

representative cell lines for further study, because they displayed a differential profile of VGCCs expression, in addition to a differential proliferation rate. M16 is a medium proliferating malignant melanoma cell strongly expressing $Ca_v3.1$ T-type channels, and

JG is a fast growing malignant melanoma cell line strongly expressing the $Ca_v3.2$ isoform (Table 9, Figure 8).

Earlier, we had found that 250 nM Kurtoxin induced a decrease in the percentage of JG cells in the S phase (Figure 16A). This result encouraged us to check the effect of other pharmacological blockers of T-type channels on human melanoma cells. M16 and JG cells were treated with Mibefradil and Pimozide for 24 hours, and the DNA content was analysed by propidium iodide staining and flow cytometry (Figure 21). We found that Mibefradil and Pimozide not only induced a decrease in the number of cells at the S phase, but remarkably, also induced a dramatic augmentation of the number of cells in the sub-G1 phase, hallmark of apoptotic cell death, in line with our light microscopy observations reported above.

To complement the analysis of the T-type channel blockers antiproliferative effect, BrdU incorporation assays were performed in two representative cell lines. Both M16 and JG melanoma cells treated with Mibefradil and Pimozide for 24 hours presented a clear decrease in the anti-BrdU staining compared with untreated cells (Figure 22).

As the treatment of M16 and JG cells with Mibefradil and Pimozide induced cell cycle arrest at the G1 phase, we next assessed the effect of Mibefradil and Pimozide on cell cycle regulatory molecules involved in G1 to S phase progression. Consistent with our previous observation, the expression of cyclin D1, a CDK kinase regulator that induces the G1-S transition, was found down-regulated when the cells were treated with either T-type channel blocker for 24 hrs (Figure 23).

3. Mibefradil and Pimozide trigger apoptosis

We set on to explore the molecular pathways leading to Mibefradil/Pimozide- induced cell death. The two representative melanoma cell lines (M16, JG) were treated with Mibefradil and Pimozide for 24 hrs, and nuclei morphology was determined by Hoechst 33258 staining. As expected, both T-type channel blockers prompted a drastic decrease in the number of total nuclei, in parallel to a relative increase in the number of pycnotic nuclei (Figure 24)

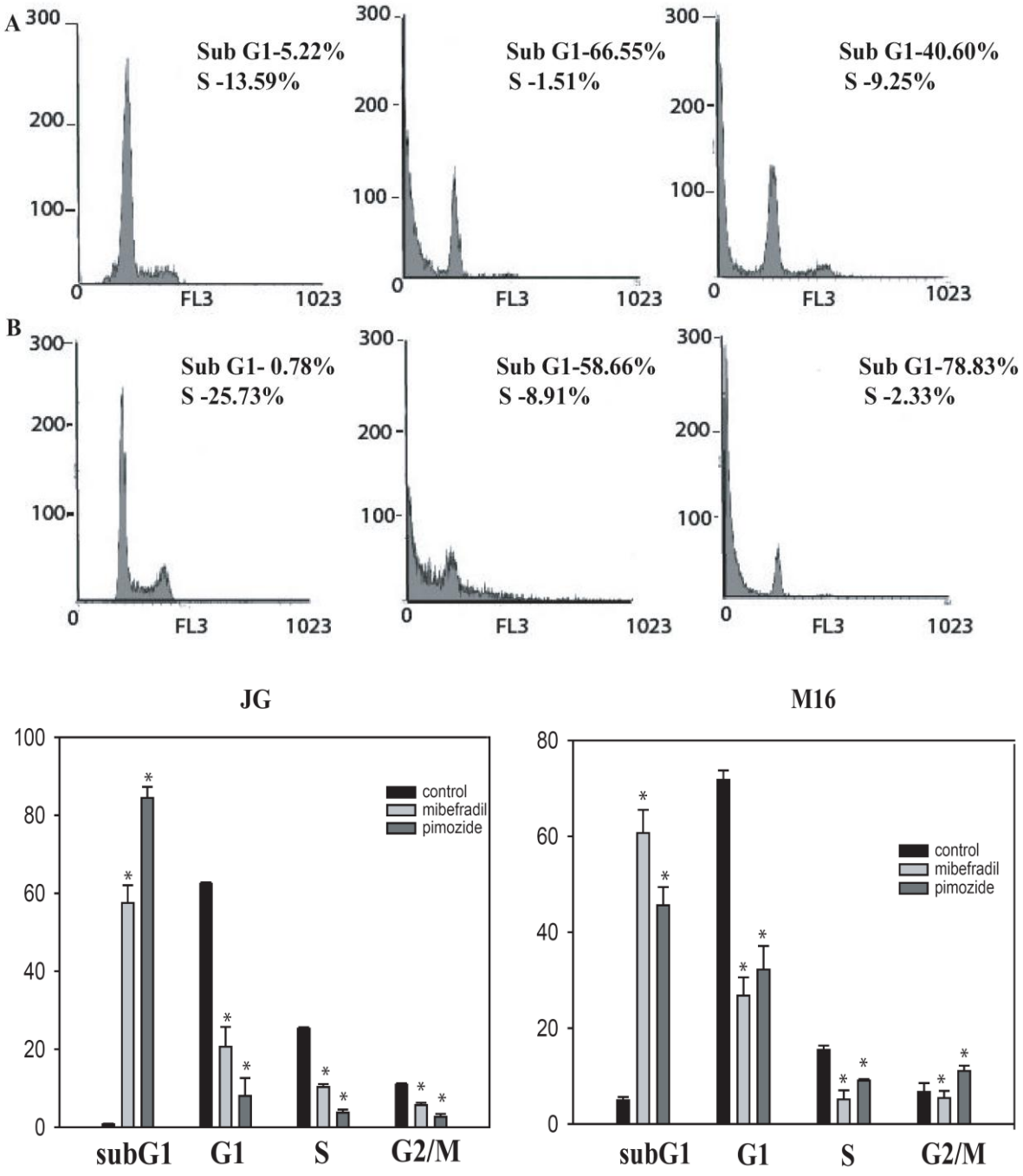

Figure 21. *Flow cytometry analysis and cell cycle distribution of JG and M16 cells treated with Mibefradil and Pimozide.M16 (panel A) and JG cells (panel B) were incubated with 10μM Mibefradil and Pimozide for 24 h after which DNA content was analysed by propidium iodide staining and flow cytometry. These drugs slowed down the cell cycle arrest by concomitantly increasing the percentage of cells at the sub G1 phase and decreasing the percentage of proliferating (S phase) cells. Histograms display the cell cycle profiles of representative experiments.(figure A and B).Graphs represent mean values (±SEM)(n=3) of the different cell cycle phases using flow cytometric analysis.*Significant differences related to control group (P < 0.05).*

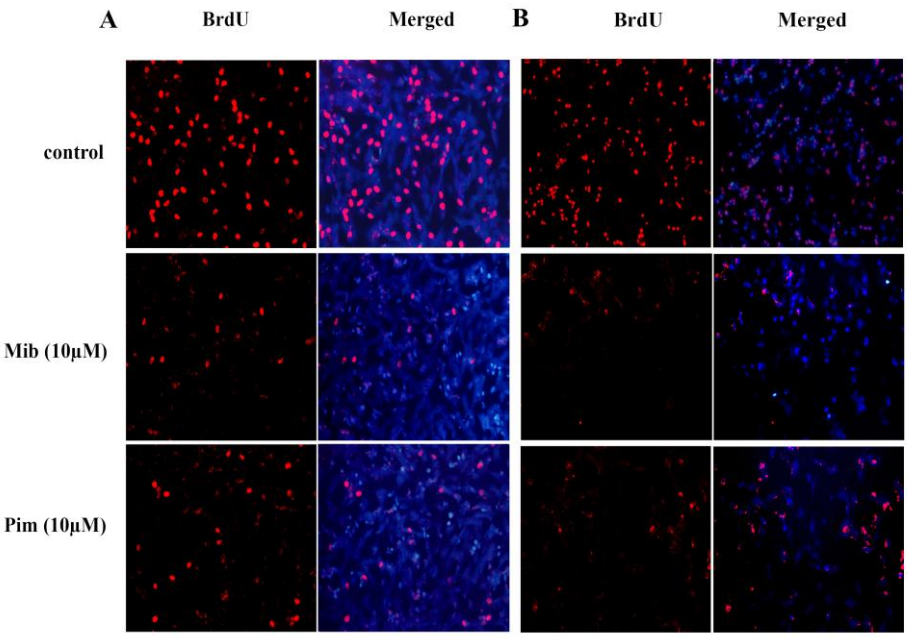

Figure 22. *Mibefradil and Pimozide decrease proliferation of melanoma cells. M16 (panel A) and JG cells (panel B) were incubated with Mibefradil (10µM) and Pimozide (10µM) for 24 hrs. Proliferating cells showing 5-bromodeoxyuridine incorporation are bright red in colour, nuclei are counter stained with Hoechst 33258.Less number of BrdU positive treated cells indicate that Mibefradil and Pimozide inhibits proliferation in both the cell lines.*

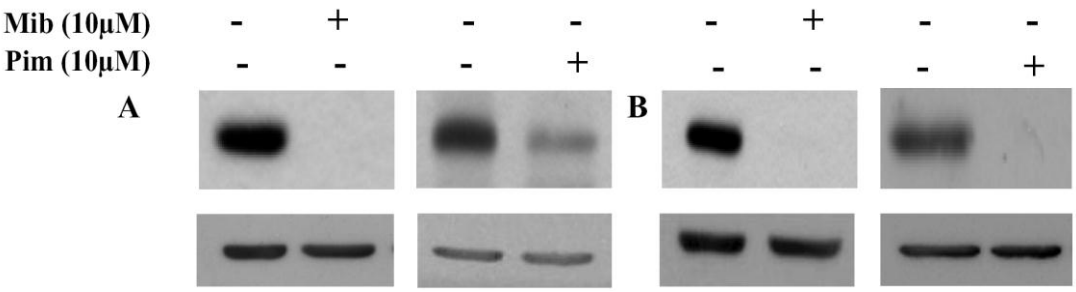

Figure 23. *Mibefradil and Pimozide induce downregulation of Cyclin D1 in M16 and JG cells. Whole cell lysate of M16 and JG cells treated with Mibefradil and Pimozide for 24 hrs were analysed by western blotting. Panel A shows prominent downregulation of Cyclin D1 expression in M16 cells treated with Mibefradil and Pimozide.Panel B shows similar effect of the above mentioned drugs in JG cells. .β actin was used as loading control.*

Next, we assessed the involvement of caspases by Western blot. In M16 and JG cell lines, Mibefradil or Pimozide triggered the cleavage of initiator procaspase 9 and effector procaspase 3 (Figure 25). These results pointed to the engagement of the intrinsic or

mitochondrial death pathway, which is often accompanied by the release of proapoptotic factors such as cytochrome c into the cytoplasm and subsequent binding to Apaf-1, resulting in apoptosome activation of Caspase 9 and subsequent cleavage (and activation) of Procaspase 3.

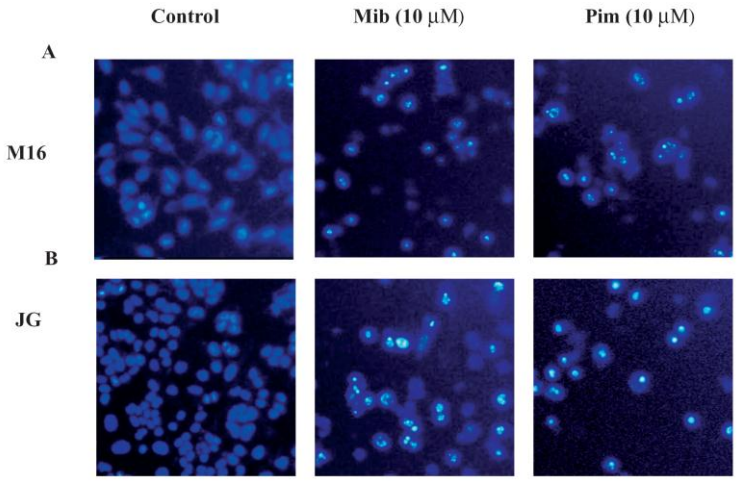

Figure 24. *M16 (panel A) and JG (panel B) cells incubated with Mibefradil and Pimozide for 24 hrs were stained with Hoechst 33258.Deep pycnotic apoptotic nuclei were visible in the treated cells indicating apoptosis.*

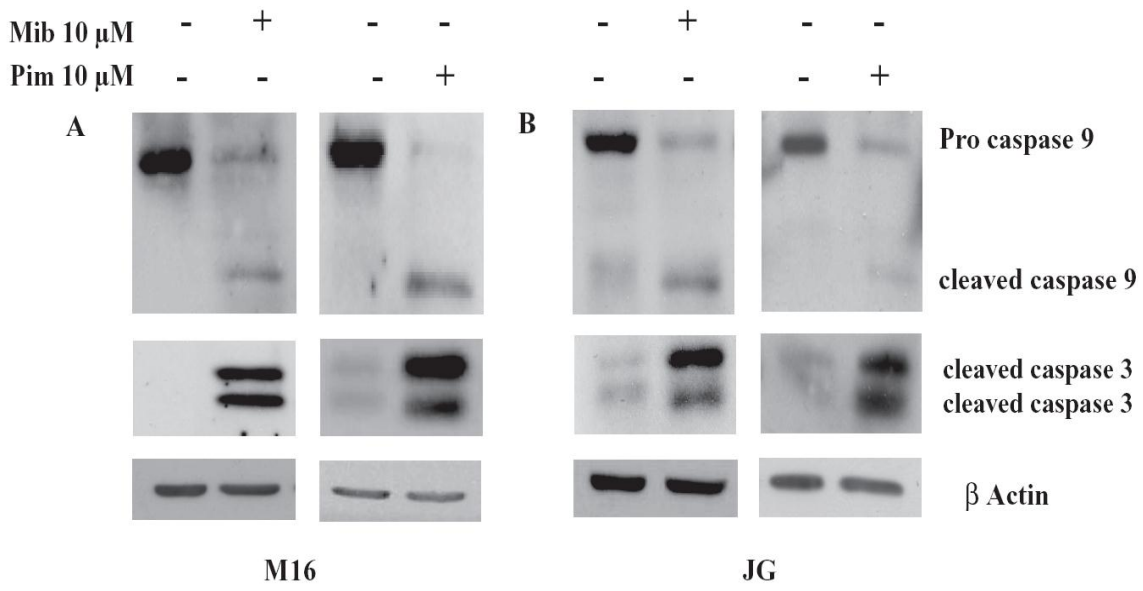

Figure 25. *Mibefradil and Pimozide trigger apoptosis by caspase processing in melanoma cells. M16(panel A) and JG cells(panel B) were exposed to 10 μM of Mibefradil and Pimozide for 24 hrs.Total protein extracts were subjected to Western blot analysis to monitor the expression of processed caspase 3 and caspase 9. β actin was used as loading control.*

4. T-type calcium channel blockers and RNAi-mediated gene silencing of $Ca_v3.1$ and $Ca_v3.2$ channels induce endoplasmic reticulum stress

During certain stages of tumorigenesis, Ca^{2+}-homeostasis deregulation together with an inhospitable environment compromise the protein folding function in the ER and unleash the Unfolded Protein Response. That way, the UPR is an adaptive response and their markers are associated to malignity and recurrence in a number of tumors, including melanoma[212.] Nonetheless, a sustained UPR may promote either apoptotic death or cell survival throughout a macroautophagic process, depending on the cell type and stimuli strength. As T-type channels have been suggested to couple Ca^{2+} influx to ER Ca^{2+} storage[213] we examined whether T-type Ca^{2+} channel blockers would cause a disruption of Ca^{2+} homeostasis at the ER, ultimately leading to the observed apoptosis. To our knowledge, no studies have addressed this question previously. A number of articles had already been published indicating ER stress as a driver of malignancy in melanoma tumors[147]. In our study, we also checked that untreated M16, JG and M28 cells displayed some degree of ER stress, which was absent in untransformed melanocytes. An RT-PCR analysis of total RNA, showed a basal level of splicing of the XBP-1 transcription factor in untreated melanoma cells, which was absent in untransformed melanocytes (Figure 26B).GRP78, another marker of UPR is also upregulated in melanoma cells in comparison to the untransformed melanocytes (26A).

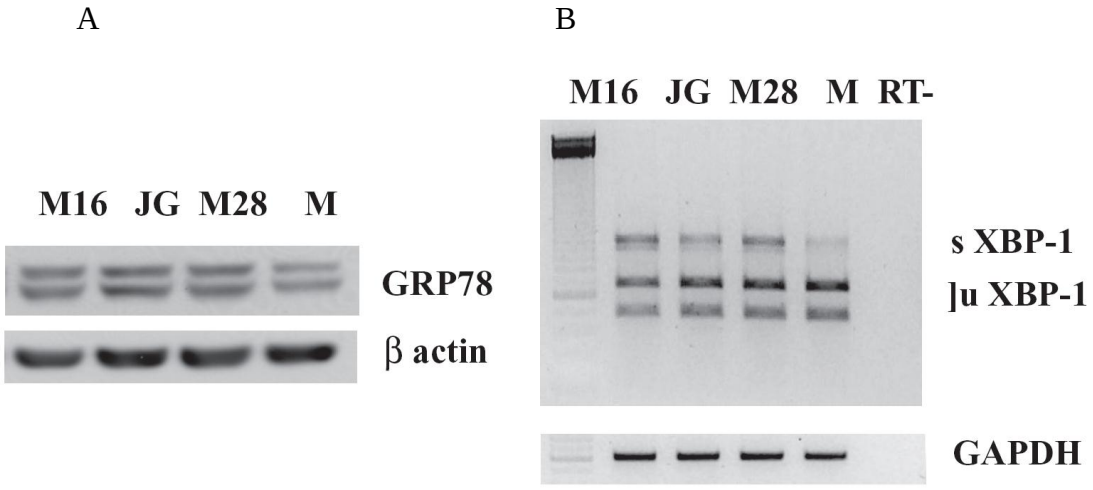

Figure 26. *Melanoma cells express some degree of ER stress which is absent in control normal melanocytes. Western blot of total protein lysate of human control melanocytes and melanoma cells (M16, JG, M28) shows an upregulation of GRP78 in melanoma cells in comparison to the*

control melanocytes (panel A). β actin was used as loading control. RT-PCR analysis of untreated melanocytes and melanoma cells (M16, JG, M28) shows upregulation of spliced (s) XBP-1in comparison to control normal melanocytes (panel B). Here GAPDH was used as loading control and M stands for melanocytes.

In order to evaluate a putative effect of Mibefradil and Pimozide on the ER, the induction of GRP78/αBIP, a well-characterized UPR molecular chaperone, was determined in a series of time-course experiments. Cells treated with Thapsigargin, a classical inhibitor of the SERCA pump, were used as a positive control. Mibefradil and Pimozide induced a clear up-regulation of GRP78 in M16 and JG cells treated for 4, 8, 16 and 24 hrs. (Figure 27 A,B,E,F), remaining stable at all time points.

We further examined which ones out of the three branches of the UPR were activated by T-type channel blockers. Activation of ER-resident transmembrane protein and transcription factor ATF6 induces the expression of XBP-1 mRNA[135-138] Another ER-resident transmembrane protein, IRE1α has an endoribonuclease domain, by which it splices a 26 nucleotide fragment out of the XBP-1 mRNA (frame-shift splice variant of XBP-1 mRNA) when activated. The generated frame-shift splice variant (sXBP-1) codes for a transcription factor that induces the expression of ER chaperones. Mibefradil-treated M16 and JG cells showed a robust splicing of XBP-1 at all time points (making a clear difference with the sXBP-1 levels present in untreated cells), along a consistent decrease of unspliced native XBP-1 (Figure 27 C-D). Pimozide-treated melanoma cells also showed an enhanced XBP-1 splicing at 4 and 8 hrs time points. Thus both T-type channel blockers induced the activation of the IRE1α pathway of the UPR (Figure 27 G-H).

As mentioned above, during prolonged or severe ER stress the cytoprotective, adaptive UPR can switch from a pro-apoptotic response to initiate cell death. Therefore, we questioned whether the UPR-mediated apoptotic pathway was taking part in the Ca^{2+} channel blockers-induced melanoma cell death. The transcription factor GADD153/CHOP has been shown to play a central role by altering the balance of pro- and anti-apoptotic Bcl-2 proteins, to promote apoptosis[139]. GADD153 levels were undetectable in untreated melanocytes or melanoma cells. However, exposure of JG and M16 melanoma cells to T-type channel blockers induced the up-regulation of

GADD153/CHOP, which was detectable at 4 and 8 hrs during Mibefradil application (Figure 27 A-B), and at 8 and 16 hours in the presence of Pimozide (Figure 27 E-F).

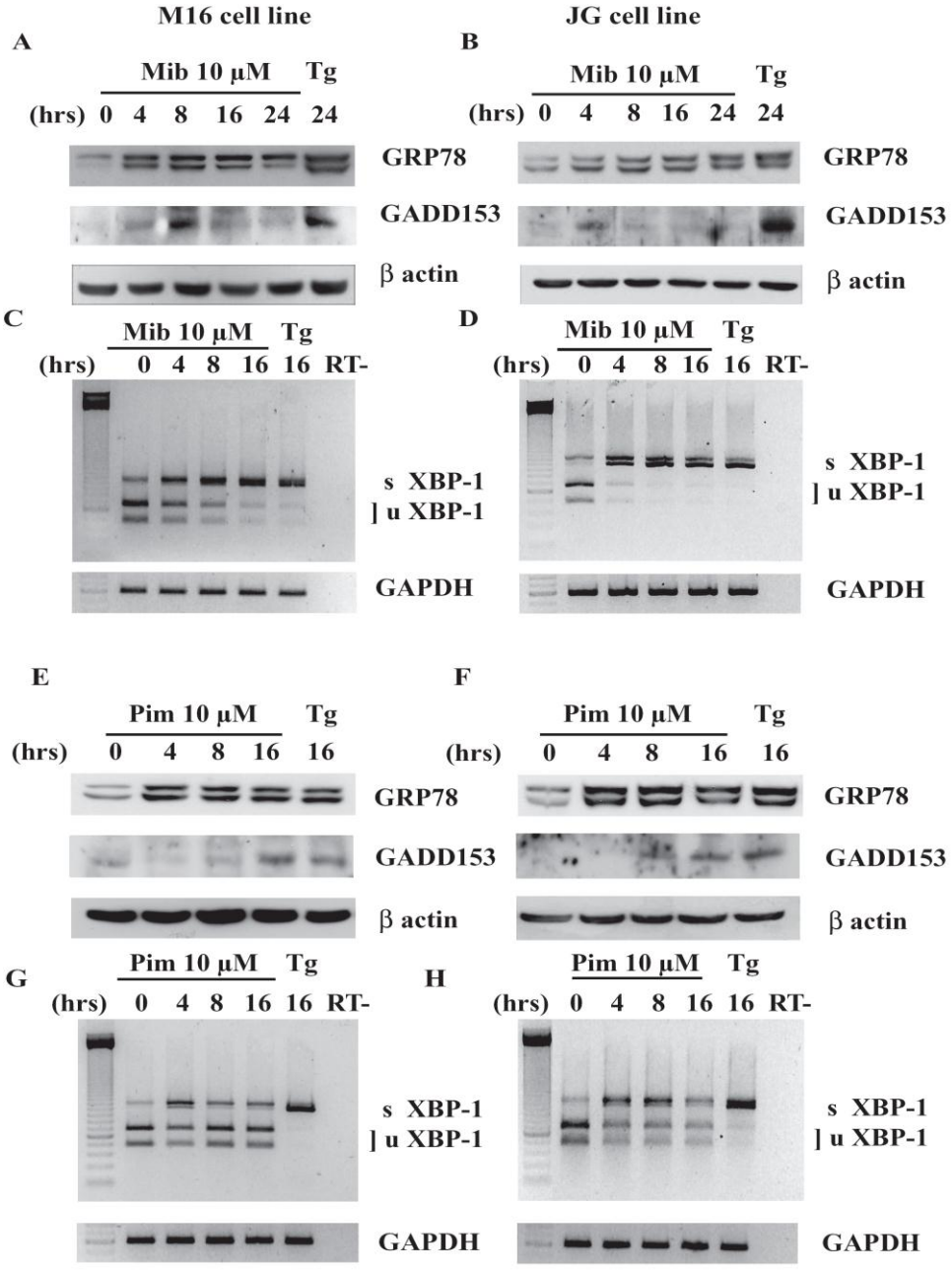

Figure 27. *Mibefradil and Pimozide induce ER stress in M16 and JG cells. Western blotting of the whole cell lysates of M16 cells and JG cells treated with Mibefradil (panel A and B respectively) for 4, 8, 16 and 24 hrs show upregulation of GRP78 and GADD153. Similarly Pimozide also induces similar upregulation of GRP78 and GADD153 in M16 (panel E) and JG (panel F) cells. β actin was used as loading control for western blot analysis of protein sample. RT-PCR analysis of M16 (panel C) and JG (panel D) cells treated with Mibefradil show*

upregulation of spliced (s) XBP-1 at 4,8,16 hrs. Pimozide also shows similar upregulation of spliced XBP-1 in M16 (panel G) and JG (panel H) cells. In all the experiments cells treated with Thapsigargin were used as positive control. For RT-PCR analysis GAPDH was used as loading control.

Earlier, we had shown that Kurtoxin induced a decrease in the proliferation of JG cells (Figure 16A). To further investigate the effects of Kurtoxin on the ER of melanoma cells, we treated JG cells with 250 nM of Kurtoxin for 4, 8, 16 and 24 hrs. Like for Mibefradil or Pimozide treatments, we found increased GRP78 protein levels (Figure 28A); the up-regulation of GRP78 reached a maximum at 8 hrs into the treatment with Kurtoxin, followed by a slow decline at 16 and 24 hrs. In addition, we observed the time dependent splicing of XBP-1 at all time points (Figure 28 B), indicating that Kurtoxin-induced ER stress also involves the IRE1α signalling pathway of UPR, like for Mibefradil or Pimozide. In contrast, we detected only a very mild up-regulation of GADD153 after 16 and 24 hrs. application of Kurtoxin (Figure 28A); this result is consistent with the flow cytometry analysis of DNA content of Kurtoxin-treated JG cells, in which no significant increase in the percentage of cells in the sub-G1 phase was visible at 24 hours treatments (Figure 16A).

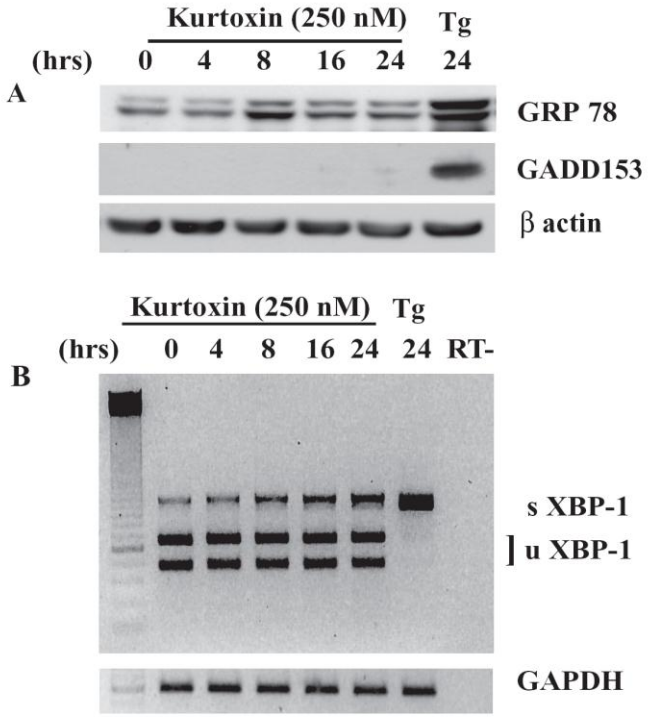

Figure 28. *Kurtoxin induces endoplasmic reticulum stress in JG cells. Western blot of total protein lysate of JG Cells treated with Kurtoxin for 4, 8, 16 and 24 hrs (panel A) shows*

upregulation of GRP78 without any upregulation of GADD153 expression.ß actin was used as loading control.RT PCR analysis of total RNA extract (panel B) shows time dependent upregulation of spliced XBP-1 (sXBP-1). Here GAPDH was used as loading control.

Leaving the expression of GADD153 aside, the coincidence of effects of the structurally unrelated Mibefradil and Pimozide on the one hand, and the peptide neurotoxin Kurtoxin in the other, seemed to point steadily to T-type channels as the real targets of the pharmacological blockade-mediated effects in the ER. In an attempt to elucidate a direct role for specific T-type channel isoforms, we transfected M16 cells with short interfering RNAs (siRNAs) specific for $Ca_v3.1$ and $Ca_v3.2$ T-type channels, and JG cells with $Ca_v3.2$ siRNA; we monitored the level of channel knockdown by Q-PCR, achieving knock down comprised between 79 and 80% (Figure 33E). The attained western blot results showed that the silencing of both $Ca_v3.1$ and $Ca_v3.2$ isoforms associates to the splicing of XBP-1, and to the up-regulation of GRP78 and GADD153 proteins, thus mimicking the effects of Mibefradil and Pimozide (Figure 33).

5. Melanoma cells display a basal autophagy which is inhibited by T-type channel blockers and T-type channels gene silencing

A sustained UPR has been linked to the development of macroautophagy, an adaptative cell mechanism which deals with the accumulation of protein aggregates resulting from ER stress[143-147].

Initially, we examined the putative unfolding of an autophagic process in melanoma cells by staining them with LysoTracker® Red DND-99 , an acidotropic autofluorescent compound which accumulates into acidic compartments like lysosomes and autolysosomes and thus can be used as a marker of macroautophagy[244]. The images displayed in Figure 31 show that, when M16 and JG melanoma cells were challenged with Mibefradil or Pimozide, the number of acidic vesicles (displaying a punctuated fluorescence) was dramatically augmented. These results prompted us to examine the expression of 2 key mediators of canonical macroautophagy at the protein level, using antibodies specific for the inducible genes Beclin1 (Atg6) and Atg5 in Western blot assays, in control normal melanocytes and melanoma cells. At the peak of the UPR (8 hrs.), none of T-type channel blockers had induced the expression of Beclin1

significantly, and that did not happen for the whole time course (0-16 h or 0-24 h depending on the experiments) (Figure 30). Regarding Atg5, Mibefradil induced a slight decrease at the 4 h time point and no further changes (Figure 30A-B), whereas Pimozide triggered a mild increase of both Atg5 levels and assembly of the Atg5-Atg12 complex (figure 30C-D).

Since these results did not show the induction of a canonical autophagy by the blockers, we further analyzed the conversion of LC3 (Atg8) from the soluble form (LC3-I) to the autophagosomal-associated lipidated form (LC3-II), which can be taken as an indirect measurement of the number of autophagosomes[214]. These data showed that, while in melanocytes LC3-II remained undetectable at all times (Figure 29A) in M16 and JG melanoma cells LC3-II was increased in a time dependent manner by treatment with Mibefradil (Figure 30A-B), Pimozide (Figure 30C-D) and Kurtoxin (Figure 32C). Importantly, the untreated controls at 0 time point also showed that the LC3-II/I ratio was constitutively increased in M16 cells and JG cells (to a minor extend), compared to control melanocytes, in which the LC3-II form was absent. The conversion of LC3-I to LC3-II correlates to the number of autophagosomes formed in the cells [214].

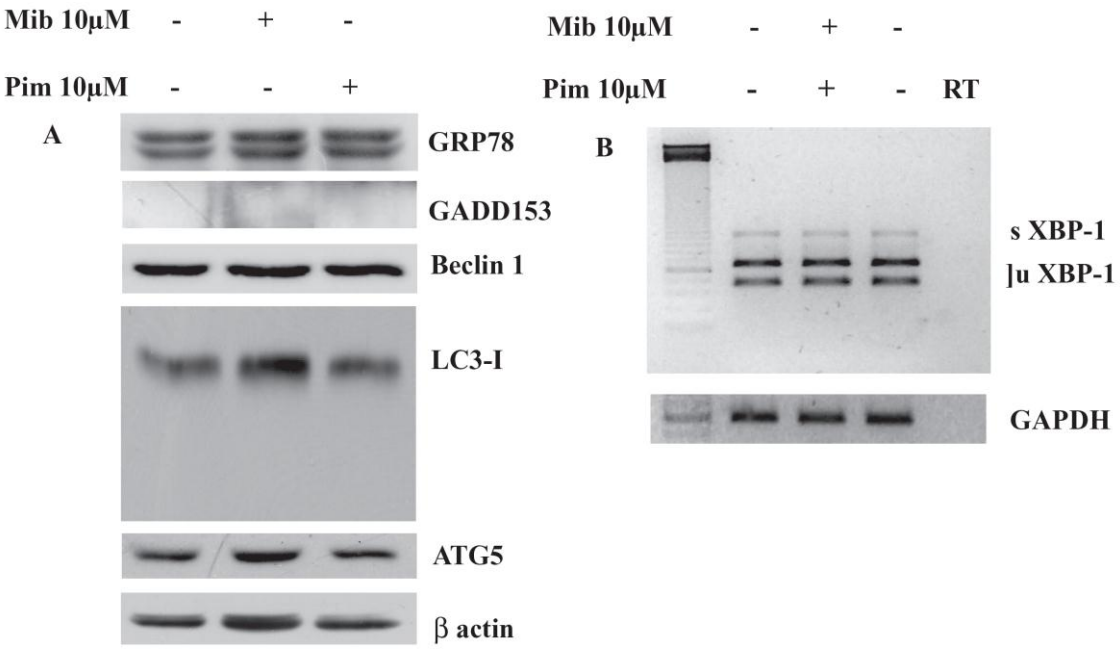

Figure 29. *Mibefradil and Pimozide induce no endogenous LC3 conversion and autophagosome formation in melanocytes. Western blot of total protein lysate of human control melanocytes treated for 6 hrs show no LC3 II formation, no change in expression of GRP78, GADD153, ATG5*

or Beclin 1 (panel A). Here β actin was used as loading control. RT-PCR analysis of melanocytes treated with Mibefradil and Pimozide (panel B) show no induction of spliced (s) XBP-1. Here GAPDH was used as loading control.

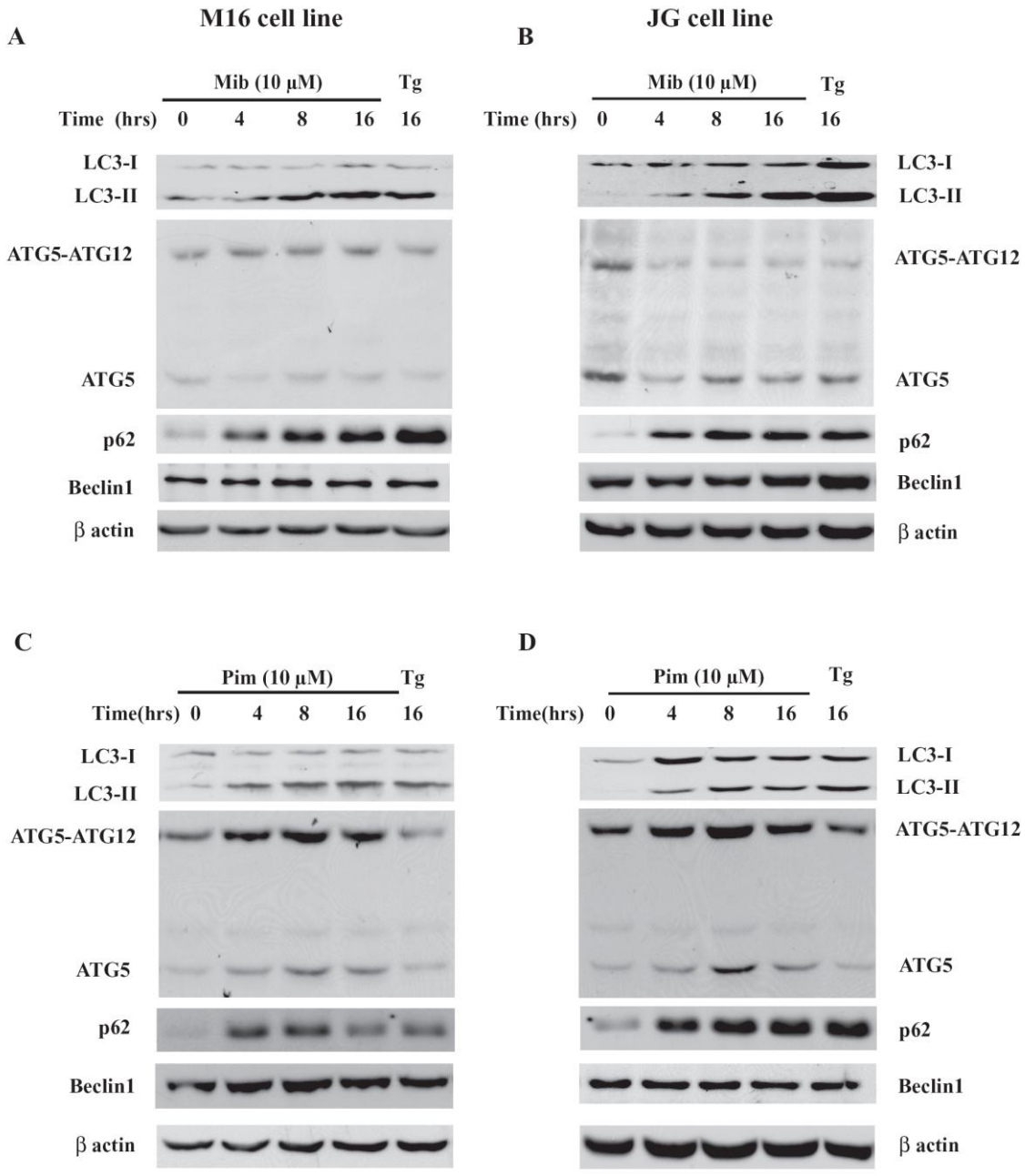

Figure 30. *Effect of Mibefradil and Pimozide on autophagic flux. Western blot analysis of whole cell lysates of M16 cells treated with Mibefradil (Panel A) and Pimozide (Panel C) and JG cells treated with Mibefradil (panel B) and Pimozide (panel D) for 4,8,16 hrs show consistent upregulation of LC3-II and marked accumulation of p62 without any prominent change in expression of Beclin 1 or ATG5. Here β actin was used as loading control.*

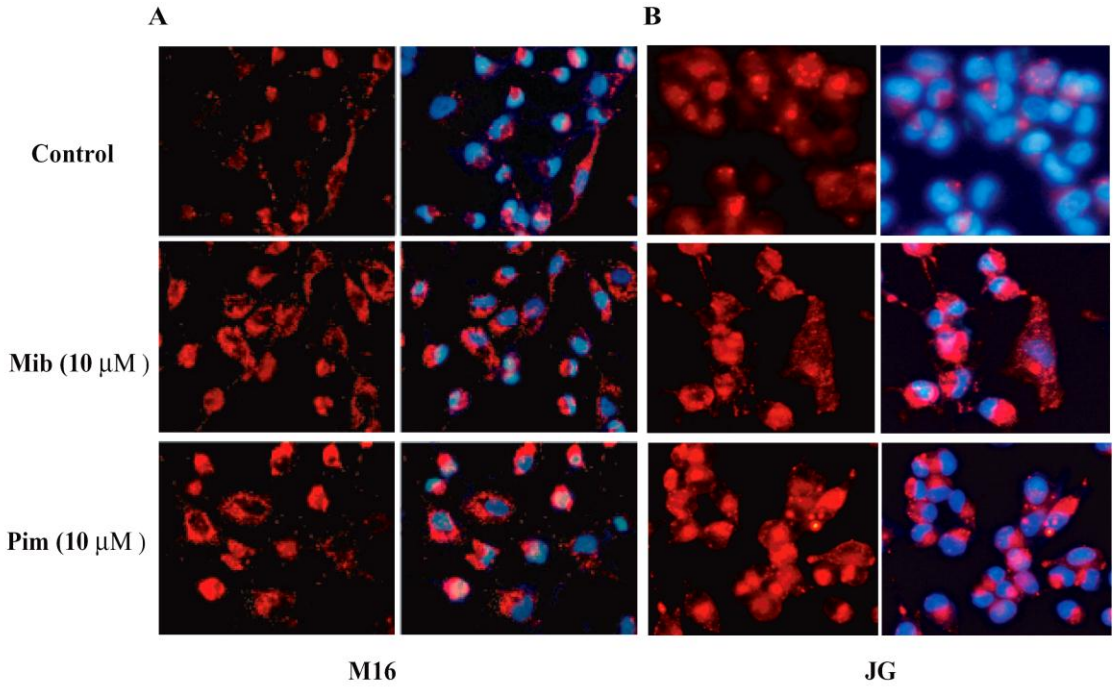

Figure 31*. Mibefradil and Pimozide induce formation of acidic vesicular organelles in M16 and JG cells 6 hrs after the treatment. Melanoma cells were incubated with LysoTracker® Red DND 99 for two minutes. Cells were washed with phosphate buffer saline and fluorescent micrographs were obtained using an inverted fluorescence microscope. Nuclei were counterstained with Hoechst 33258 stain. Mibefradil and Pimozide treatment in M16 (panel A) and JG cells (panel B) indicate accumulation of acidic vesicles in untreated control cells, which is further increased in presense of Mibefradil and Pimozide.*

However, it can reflect either an increased or a decreased autophagic flux, according to the following paradigm: if the LC3-II/I ratio is further enhanced by addition of a late-stage inhibitor of macroautophagy, the primary increase is considered to be the result of an increased autophagy; conversely, an elevated LC3-II/I ratio which is not augmented by addition of an autophagy inhibitor, is interpreted as the result of a reduced autophagic flux and subsequent accumulation of autophagosomes[215]. To distinguish between these two possibilities, we applied Mibefradil and Pimozide in M16 (Figure 32A) and JG cells (Figure 32B), and Kurtoxin (Figure 32C) in JG cells, in the absence or presence of Bafilomycin A1, which is a established inhibitor of autophagosomal-lysosomal fusion. In all cases the intensity of the LC3-II band was not further increased by Bafilomycin A1, indicative of suppression of autophagy rather than enhancement of lysosomal clearance.

The p62/SQSTM1 protein facilitates autophagic degradation of ubiquitinated proteins and constitutes one of the best known mammalian autophagy specific substrates[165-167]. As p62 degrades upon autophagy stimulation and accumulates when autophagy is inhibited, the p62 levels can also be used as markers of autophagic flux. Consistent to LC3-I to LC3-II conversion in presense or in absence of Bafilomycin A1, the examination of the p62 protein by Western Blott revealed a significant increase of the p62 at 4, 8 and 16 hours upon treatment with Mibefradil (Figure 30A-B) or Pimozide (Figure 30C-D).

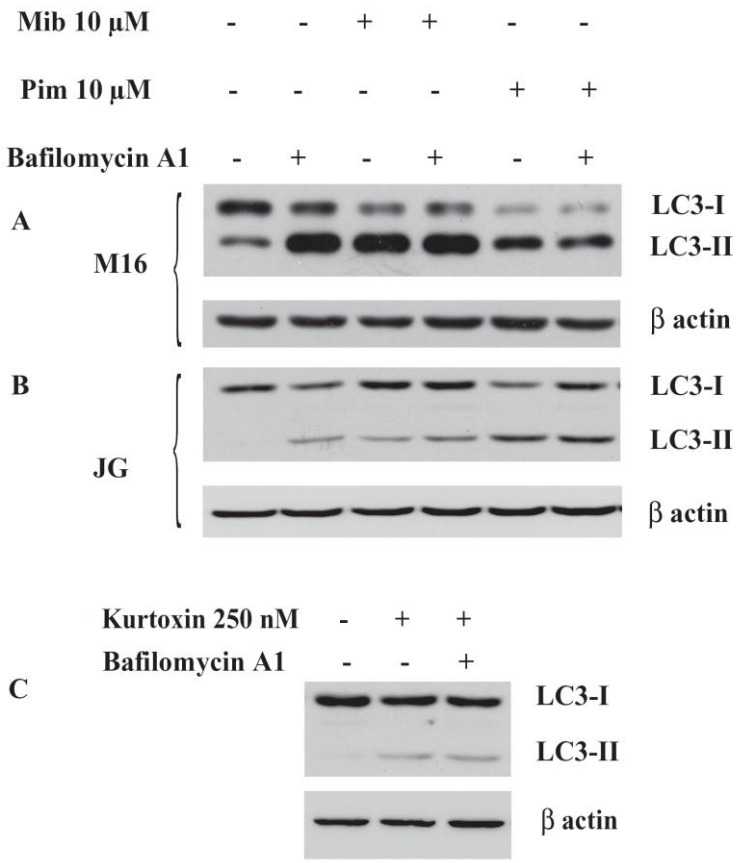

Figure 32. *T-type calcium channel blockers induce autophagy inhibition in human melanoma cell. Western blot of total protein lysate of M16 cells treated with Mibefradil and Pimozide (panel A) for 6 hrs show accumulation of LC3-II which was not further increased in presence of Bafilomycin A1, an inhibitor of autophagosome lysosome fusion indicating that increase in LC3-II was not due to increased degradation of autophagosomes but due to augmented formation of autophagosomes. Western blott JG cells treated with Mibefradil, Pimozide (panel B) for 6 hrs and Kurtoxin (panel C) for 24 hrs also shows similar autophagy inhibition. Here β- actin was used as loading control.*

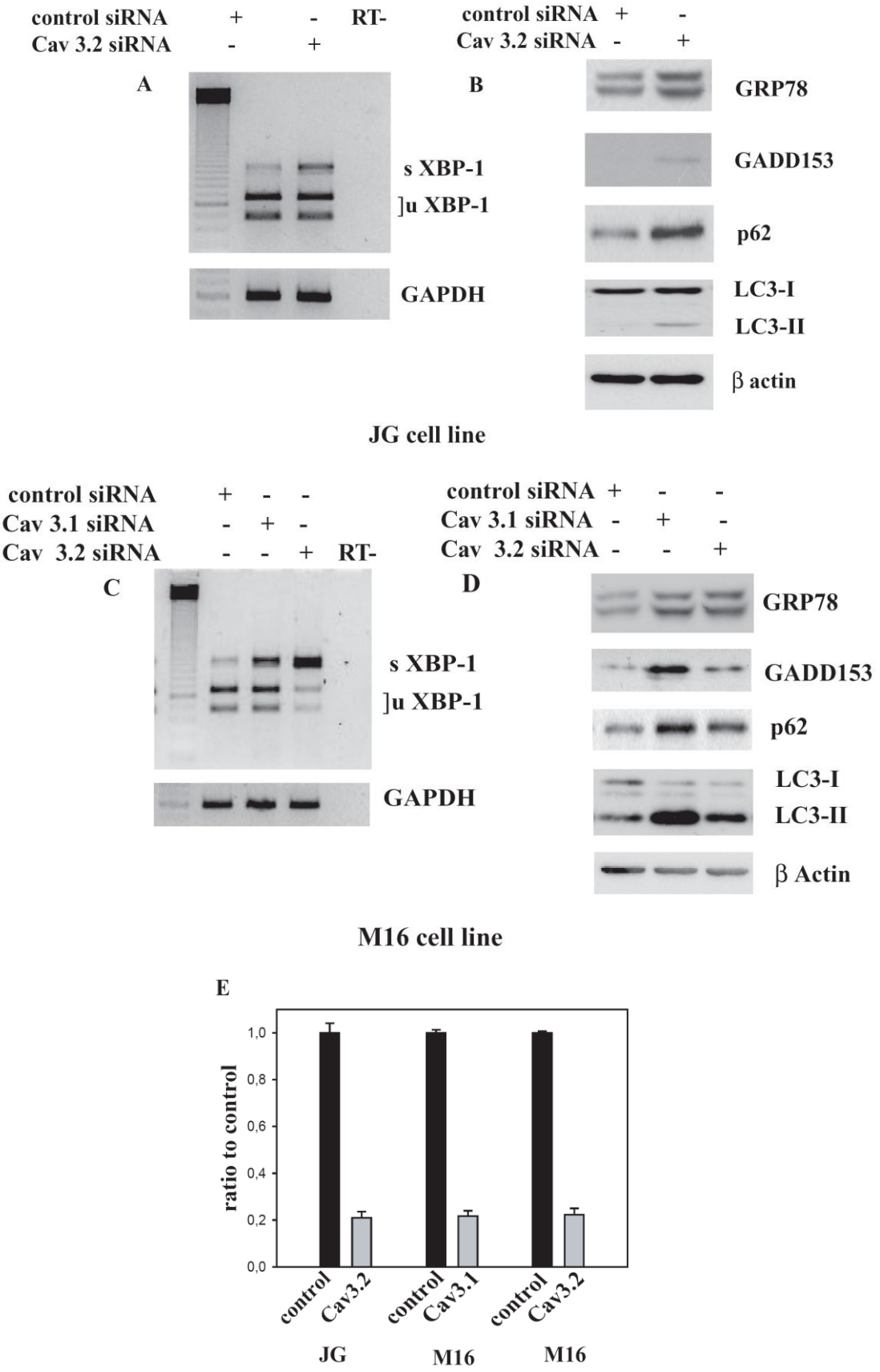

Figure 33. *Knock down of $Ca_v3.1$ and $Ca_v3.2$ induces endoplasmic reticulum stress and autophagy inhibition in melanoma cells. Western blotting of total cell lysates of JG cells*

transfected with siRNA for $Ca_v3.2$ shows upregulation of GRP78, GADD153 and accumulation of LC3-II and p62 indicating ER stress and autophagy inhibition simultaneously (panel B). Cells transfected with non-specific control siRNA were used as negative control. β actin was used as loading control. RT-PCR analysis shows induced splicing of XBP-1 in JG cells transfected with siRNA for $Ca_v3.2$ (panel A). Here GAPDH was used as loading control. Knock down of $Ca_v3.1$ and $Ca_v3.2$ induces similar effect in M16 cells (panel C, D). Q-RT PCR analysis of M16 and JG cells transfected with siRNA for $Ca_v3.1$ and $Ca_v3.2$ shows around 79-80 % decrease in expression of the above said isoforms of T-type calcium channels (panel E).

Finally, we investigated a likely causative link between ER stress and autophagy inhibition with the use of Salubrinal, a small molecule that protects cells from ER stress induced apoptosis by selectively activating the eIF2α branch of the UPR pathway[233]. In JG cells treated with Mibefradil and Pimozide, the co-application of Salubrinal significantly reduced the expression of LC3-II at the 6 hrs time point, suggesting that the PERK-eIF2α signalling pathway of the UPR is determinant for the accumulation of autophagosomes in melanoma cells treated with T-type channel blockers (Figure 34). These data highlight a functional link between ER stress and autophagy.

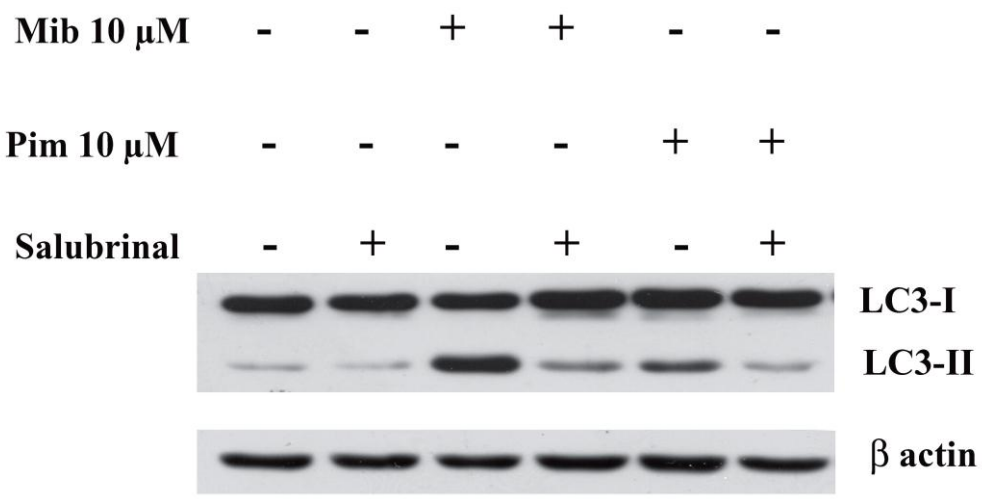

Figure 34. *PERK-eIF2α signalling pathway of ER stress plays an important role in accumulation of autophagosomes in JG human melanoma cells. Western blot of whole cell lysate of JG cells treated with Mibefradil and Pimozide for 6 hrs show accumulation of LC3-II which was decreased in presense of Salubrinal, an inhibitor of eIF2α dephosphorylation. Here β actin was used as loading control.*

Analogously to the preceding section, we aimed to identify the molecular targets of the drug-mediated autophagy inhibition by gene silencing of the specific T-type channel isoforms expressed in M16 and JG melanoma cells. The effects of knockdown of $Ca_v3.1$ and $Ca_v3.2$ on melanoma cell autophagy were investigated by Western blot analysis of LC3 and p62 proteins. In M16 cells, both the knockdown of $Ca_v3.1$ and $Ca_v3.2$ channels rendered an increase of the LC3-II/I ratio and a parallel increase of the p62 band intensity (Figure 33d). In JG cells, the knockdown of $Ca_v3.2$ channels induced a similar LC3-I/II conversion and p62 accumulation effect (Figure 33b). Thus, the knockdown of either T-type channel isoform mimicked the Mibefradil/Pimozide/Kurtoxin-mediated inhibition of the basal autophagy present in melanoma cells, suggesting that T-type channel pharmacological blockers exert its effects on melanoma autophagy by targeting these two T-type channel isoforms.

Discussion

VGCCs are expressed in different tumours and the role they play in cancer progression is a lively field of research. In the present study we have performed a comprehensive analysis of the expression of the different VGCC families in a variety of melanoma tumours and cell lines. We have found that human melanoma cells express VGCCs from three different families: (i) high voltage-activated L-type channels, which require significant depolarization to open and thus are widely distributed in excitable tissues; (ii) high voltage-activated N-type, P-Q type and R-type channels, classically involved in neurotransmitter and hormone release; and (iii) low voltage-activated T-type channels, which can operate at potentials near the typical membrane potentials of most cells.

1. Expression of L-type channels

Our results show that transcripts for $Ca_v1.2$ were undetectable in control normal melanocytes and strongly expressed in all melanoma cells except for JG and M17 skin metastasis (Figure 8). In contrast, the $Ca_v1.3$ isoform was ubiquitously expressed in control normal melanocytes and all melanoma cells. It should be taken into account that L-type channels are functionally diverse. Whereas $Ca_v1.2$ channels are characterized by a high threshold and slow kinetics of activation, $Ca_v1.3$ channels have been shown to be mid threshold activating and to display faster activation kinetics[216, 217]. These properties would enable $Ca_v1.3$ channels to operate at voltages near the resting membrane potential, mediating oscillatory Ca^{2+} entry along with T-type channels. Even though the viability assays presented in Figure 19 are not suggestive of a principal role for L-type channels in proliferation or survival, it should be taken into account that dihydropyridine actions are channel state-dependent[218], and that $Ca_v1.3$ are less sensitive than other L-type channels to dihydropyridines[216]. These considerations, together with the lack of $Ca_v1.2$ expression in untransformed melanocytes and the up-regulation of $Ca_v1.2$ channels by hypoxia in JG melanoma cells, encourage further investigation of the role of L-type channels in the melanoma cell physiology.

2. Expression of N-type, P-Q type and R-type channels

Experimental evidence shows that melanocytes display a variety of neuroendocrine functions and release neurotransmitters, neuropeptides and hormones, and this production is stimulated by ultraviolet radiation and different biological factors[219]. On the other hand, the role of VGCCs Ca_v1 and Ca_v2 family members in neurosecretion is well established,

particularly in the chromaffin and pheochromocytoma neurosecretory cells[220]. Our results show that both control normal melanocytes and melanoma cells (primary tumours and metastasis) express Ca_v2 channels, although the expression profile of the individual isoforms is variable (Figure 8). As for Ca_v1 channels, data from the viability assays rules out a direct participation of Ca_v2 channels in cell cycle regulation. However, the ability to correlate qualitative or quantitative changes in Ca_v2 expression with the neuroendocrine activity of tumours may shed light on how melanocyte transformation may be accompanied by neuroendocrine differentiation[221].

3. Expression of T-type channels

Our finding regarding the up-regulation of T-type channels in melanoma cells was expected, as a role for T-type channels in cancer cell proliferation has already been established[77, 75, 222]. The relevance of T-type channel expression in melanoma cells is highlighted by the fact that Ca_v3 isoforms may be selectively up-regulated in moderate hypoxic conditions (Figure 10) which approach the real hypoxic environment of skin and the high oxygen demand in metastasis. The effect of Kurtoxin in reducing the percentage of proliferating melanoma cells (Figure 16A) further suggests a relevant role for $Ca_v3.1$ and $Ca_v3.2$ channels in cell cycle control[97]. Nonetheless, the stronger effect of Kurtoxin on the viability of melanoma cells as measured by a colorimetric assay (Figure 19) also suggests that these T-type channels play an additional role in cell homeostasis maintenance. In line with this, it has been shown that T-type channel blockers are inducers of autophagy in PC12 cells[224].

The Ca^{2+}-imaging experiments displays in Figure 15 indicate that cultured melanoma cells display a basal Ca^{2+} influx which can be reduced by Mibefradil. This result is consistent with the occurrence of T-type channel window currents, providing the pattern of Ca^{2+} signalling required for cell cycle progression. Ca^{2+} transients are evident during certain stages of mitotic progression and these signals are transduced principally by direct binding of Ca^{2+} to intracellular receptors such as calmodulin[225]. A few models have been put forward to explain the role of T-type channels in promoting transient elevations of cytosolic Ca^{2+}, acting in concert with K^+ channels[223].

The precise signalling mechanisms for specific T-type channel subunits remain unknown[69]. In this regard, our finding about the counter-balanced expression of $Ca_v3.1$

and the other Ca_v3 channels (Figure 8) and the linkage between $Ca_v3.1$ expression and a low proliferation rate (Table 9) is intriguing. On one hand, we have shown that melanoma JG or M28 cells (expressing mainly $Ca_v3.2$ channels in normoxia) display a faster proliferation rate compared with $Ca_v3.1$-expressing M16 cells (Figure 11). Furthermore, other cell lines expressing $Ca_v3.1$ channels are either average-proliferating (M17) or slow proliferating (M9 and M29) (Table 9). On the other hand, the siRNA experiments show a direct involvement of both $Ca_v3.1$ and $Ca_v3.2$ isoforms in the proliferation of M16 and JG cells, respectively, as the percentage of cells in the S phase is decreased upon silencing of either gene (Figure 16B-C). Importantly, hypoxia experiments point in the same direction. In JG cells, in which both $Ca_v3.1$ and $Ca_v3.2$ are up-regulated by low O_2, the percentage of cells in the S phase is increased. In contrast, M16 cells under hypoxia experience a down-regulation of both $Ca_v3.1$ and $Ca_v3.2$ T-type channels and consequently are arrested at the G1 and S phases (Figure 17). The reversal of hypoxic effects on cell proliferation by $Ca_v3.1$ and $Ca_v3.2$ gene silencing (Figure 18B), further confirms the pivotal role of these T-type channels in the control of the cell cycle. Altogether, our data suggest that, whereas both $Ca_v3.1$ and $Ca_v3.2$ channels promote the progression of the melanoma cell cycle, $Ca_v3.1$ channels associate to slow cycling and are induced in environmentally stressful conditions.

4. Dual effect of T-type channel pharmacological blockers on melanoma cells viability: decreased cell proliferation and increased apoptosis

Up to this point we had found that the knockdown of $Ca_v3.1$ and $Ca_v3.2$ T-type channels slows down the progression of the melanoma cell cycle and that Kurtoxin, the most specific T-type channel blocker available up to date, also decreases the viability of melanoma cells by affecting the proliferating rate. The results encouraged us to check the effect of clinically used, well known T-type channel blockers such as Mibefradil and Pimozide, on human melanoma cells. For that purpose and, in an attempt to achieve some conclusions regarding the T-type channel isoforms involved in the pharmacological blockade effects, we selected out 2 metastatic cell lines showing a differential pattern of T-type channels expression: while JG cells only expressed the $Ca_v3.2$ isoform, M16 cells additionally expressed the $Ca_v3.1$ isoform. We had earlier shown that the expression of $Ca_v3.1$ is low or undetectable in fast-growing metastatic melanoma cell lines where expression of $Ca_v3.2$ is prominent (Table 9, Figure 8B). Our data showed that, at 24 hours

treatments, both Mibefradil and Pimozide affected cellular viability and that, for the fast-growing melanoma cell lines (JG, M28, M36), the EC_{50} value was lower in comparison to EC_{50} value for slow-growing cell lines from primary tumors (M9) or metastatic melanoma (M29, M17 or JG). These data suggests that the effect of both drugs is proliferation state-dependent.

The PI/FACS (cell cycle) analysis revealed that Mibefradil and Pimozide not only affected melanoma cells proliferation, but that they also induced a powerful apoptotic process, that was cross-checked by Hoechst staining and caspase 3 and 9 activation assays. This dual aspect of clinical T-type channel blockers immediately raise the question of why the effects on cell death were not seen by application of Kurtoxin. We can provide two possible explanations: (1) T-type channel blockade by 10 μM Mibefradil or Pimozide would be more effective than T-type channel blockade by 250 nM Kurtoxin. Although Chuang et al. (1998)[97] reported a nearly 95% blockade of $Ca_v3.1$ and an 85% blockade of $Ca_v3.2$ at 350 nM Kurtoxin (expressing recombinant channels in *Xenopus* oocytes), they found that the blockade was strongly voltage-dependent. In comparison, data available for Mibefradil and Pimozide, with EC_{50} values for T-type channels blockade in the high nM range[234, 235], suggest that at the applied 10 μM concentration, the blockade would be complete for the 3 T-type channel isoforms. (2) Numerous "unspecific" effects other than T-type channels blockade have been reported for Mibefradil and Pimozide, including L-type and N-type Ca^{2+} channel blockade, Na^+ and K^+ channel blockade and Cl^- channel blockade[236, 237, 231].

5. T-type calcium channel blockers induce ER stress and non-adaptive UPR in melanoma cells

Regardless of the identity of the molecular targets for the structurally unrelated Mibefradil and Pimozide we had decided to investigate the pathways leading to apoptosis of melanoma cells.

Endoplasmic reticulum (ER) stress and subsequent unfolded protein response (UPR) are primarily an adaptive response, aiming to restore ER homeostasis and protect the cell from the accumulation of unfolded or misfolded proteins. There are ample evidences that most melanoma tumours have some degree of ER stress at the early stage of their

development. Several of the metabolic consequences of ER stress, such as increased glycolysis and high lactic acid dehydrogenase (LDH), are readily apparent in patients with melanoma. Indeed, LDH levels in sera are the single most powerful predictor of prognosis in metastatic disease[238]. As discussed by others, adaptation to ER stress may be a key driver of malignancy and resistance to therapy[239]. There are also evidences of constitutive activation of the UPR in cultured melanoma even in the absence of additional ER stress induction[142]. Our results also show that there is a certain level of splicing of XBP-1 in melanoma cells in comparison to melanocytes (Figure 26B) and an upregulation of GRP78 in melanoma cells in comparison to the melanocytes (figure 26A). A sustained UPR has been linked to autophagy induction, a survival response dealing with the degradation of protein aggregates[144]. Nonetheless, if the stress is such that overwhelms the adaptive response, the UPR may convey into apoptosis[212]. For these reasons, both the pharmacological inhibition and induction of UPR have been investigated as anti-tumoral strategies[240, 212].

Previously Bertolesi et. al. (2002) had found a correlation between T-type current blockade and cell death (by either apoptosis or necrosis) produced by Mibefradil and Pimozide in retinoblastoma Y79 cells and adrenocarcinoma MCF7 epithelial cells[82], although no specific pathways were examined. In our study we have found, for the first time in any cell type, that the three T-type channel blockers Mibefradil, Pimozide and Kurtoxin induce splicing of XBP-1 (sXBP-1) (Figure 27 and 28), a marker for the coordinated action of active ATF6 and IRE1α. The early appearance of sXBP-1 mRNA during the first 4 hrs of treatment with Mibefradil and Pimozide, and the level of the splicing, were comparable to those induced by Thapsigargin, a classical inducer of ER stress. The up-regulation of GRP78 and GADD153/CHOP were also prominent in the early hours of treatment with Mibefradil and Pimozide. In the light of the data obtained from viability and apoptotic assays at 24 h treatments, these results emphasize that Mibefradil and Pimozide induce a pro-apoptotic branch of the ER stress pathway. The regulation of this effect may be via induction of the pro-apoptotic transcription factor GADD153 and subsequent activation of the ER-localized caspase-12; the activated ER stress death pathway, in concert with the mitochondrial death pathway, would trigger the so called intrinsic pathway of caspase activation (including the observed cleavage of caspases 9 and 3) (Figure 25), cytoskeleton breakdown and nuclear fragmentation, leading to the final demise of the cell. Particularly, the up-regulation of GADD153 in

Mibefradil and Pimozide-treated cells, also suggests that PERK-mediated eIF2α phosphorylation and transcriptional activation of ATF4 may be triggered, since this signalling pathway plays a dominant role in the induction of GADD153[241, 242]. In this regard, it has been shown that induction of ATF4 and GADD153 by ER stress is nearly completely attenuated in PERK null cells and $eIF2\alpha^{S51A}$ cells (containing a mutation at serine 51 phosphorylation site in the murine eIF2α gene)[134].

Previous studies have claimed that the mammalian UPR is linked to the inhibition Cyclin D1 translation and of cell cycle progression[226]. This was also the case for Mibefradil and Pimozide effects in our study (Figure 23).

6. The knockdown of $Ca_v3.1$ and $Ca_v3.2$ channels mimics the effects of T-type channel pharmacological blockade

Our experiments show that the siRNA-mediated gene silencing of $Ca_v3.2$ channels in JG cells and $Ca_v3.1$ or $Ca_v3.2$ channels in M16 cells also leads to the up-regulation of GRP78 and GADD153 and to the splicing of XBP-1 (Figure 33). These results unveil a more specific link between $Ca_v3.1$/$Ca_v3.2$ isoforms of T-type calcium channel and ER calcium homeostasis, resulting in the activation of the IRE1α pathway. In line with this, we have recorded in M16 cells oscillations in the intracellular calcium levels which were reduced by Mibefradil, indicating a crosstalk between cytoplasmic and ER Ca^{2+} levels (Figure 14). However, the application of Kurtoxin induced only minor up-regulation of pro-apoptotic GADD153 (Figure 28) and, consistently, melanoma cells did not undergo an apoptotic process in the presence of this neurotoxin at 24 h treatments. Given the fact that $Ca_v3.1$ and $Ca_v3.2$ knockdown up-regulated GADD153 in melanoma cells (albeit apoptosis was not assessed), we believe that it is likely that Kurtoxin (at 250 nM) induces only a partial blockade of $Ca_v3.1$ and $Ca_v3.2$ in the tested melanoma cells, as pointed out in the preceding section.

7. T-type calcium channels blockade or gene silencing inhibits the constitutive autophagy present in melanoma cells

There are emerging evidences supporting the idea that the ER status plays an important role in the process of macroautophagy and that, conversely, a constitutive, house-keeping

autophagy is critical for maintaining ER homeostasis[245-247]. Recent articles indicate that the IRE1α-JNK pathway and the PERK or ATF6 pathway are required for autophagy activation after ER stress [143-147]. In addition, it has been reported that basal autophagy activation is a relevant determinant for tumor aggressiveness and response to therapy in melanoma [180]. Since we had found a high level of sXBP-1 in untreated melanoma cells in comparison to control normal melanocytes (Figure 26B) and an upregulation of GRP78 (26A) we were suspicious about the presence of basal autophagy in melanoma cells. Consistently, the detection of the autophagosomal-associated LC3-II protein, which was further enhanced by co-application of Bafilomycin A1, demonstrated that M16 and JG were displaying a significant (albeit different) activation of macroautophagy (Figure 32), contrarily to control melanocytes (Figure 29A). In addition, a basal level of macroautophagy in melanoma cells could be seen by the presence of a high number of acidic vacuoles stained with LysoTracker® Red DND-99 (Figure 31).

As pointed above, upon sustained ER stress-stimuli the UPR may trigger a macroautophagic process. However, the apoptotic death induced by Mibefradil and Pimozide was difficult to reconcile with the activation of autophagy, which is an adaptive response by nature. Initially, we addressed this issue by using the same tools that had uncovered the presence of basal autophagy (Figure 32). To our surprise, these results initially seemed to show that the T-type channel blockers were enhancing the autophagy in M16 and JG melanoma cells, as they were inducing a prominent increase of the LC3-II form, in parallel to an increase in the labelling of acidic compartments by LR, indicative of the accumulation of autophagic vacuoles (AV). However, an increased number of AV is not always the consequence of an enhanced autophagy, but may also result from the failed elimination of autophagic debris, that is, from the blockade of the autophagic flow. When we monitored the level of autophagic substrate p62/SQSTM1 (Figure 30) and we additionally applied the Mizushima paradigm for LC3-I-II conversion in the presence of Bafilomycin A1 (Figure 32), it became clear that T-type channel blockers were inhibiting, rather than enhancing, the constitutive autophagy of melanoma cells. Because of the obvious accumulation of AVs such inhibition must occur at a late stage of the macroautophagic process, by preventing the fusion of autophagosomes with lysosomes. Importantly, not only Kurtoxin was able to mimic the effects of Mibefradil and Pimozide regarding LC3-I-II conversion in the presence of Bafilomycin A1 (Figure 32), but the knockdown of $Ca_v3.2$ in JG cells and of either $Ca_v3.1$ or $Ca_v3.2$ in M16 cells also showed

on LC3-I-II conversion and p62 increased levels (Figure 33), reassuring that the blockade of autophagic flow by T-type channel blockers was targeting T-type channels and, particularly, the $Ca_v3.1$ and $Ca_v3.2$ isoforms.

Our results also show the activation of the pro-apoptotic UPR branch in response to T-type channel blocker-mediated ER-stress, and that this is linked to autophagosome accumulation, and not to their biogenesis. During ER stress, eIF2α phosphorylation by PERK reduces protein synthesis and alleviates cell from death[232]. Here, we demonstrate that Salubrinal, a selective inhibitor of the eIF2α dephosphorylation[233], reduces LC3-I-II conversion during Mibefradil or Pimozide treatment (Figure 34). On a first glance, these results would appear conflicting with the known role of eIF2α phosphorylation in inducing autophagy. One can speculate that both the magnitude and duration of eIF2α phosphorylation might be important factors in adjusting the autophagic response to ER stress. However, we rather take the results using Salubrinal as a further proof that the LC3 I-II conversion in the presence of T-type channel blockers is a reflex of autophagy inhibition, rather than autophagy induction. Importantly, this result also allows establish a chronological sequence of events, by virtue of which ER stress anticipates autophagy inhibition, and it is the likely cause of it.

Indeed, our study demonstrates that the T-type channel blockade-mediated melanoma cell death associated to the accumulation of AVs is the result of inhibited, rather than exacerbated autophagy. T-type channels blockade apparently inhibit the formation of autophagolysosomes through the fusion of AV and lysosomes, thereby reducing the turnover of AV. Although autophagic vacuolization by itself is not lethal, it primes cells for death accompanied by a loss in the mitochondrial membrane potential, relocation of cytochrome C from mitochondria to the cytosol and activation of Caspases[151, 199, 174]. We have checked how a disabled autophagy in melanoma cells is linked to cell death via the up-regulation of the pro-apoptotic UPR branch and a common final pathway involving biochemical features of apoptosis. Irrespective of the detailed molecular pathways linking disabled autophagy to mitochondrial apoptosis, the results attained in this work add to the growing suspicion that type 1 (apoptotic) and type 2 (autophagic) cell deaths are somehow interwoven.

Recent studies have demonstrated that inhibition of macroautophagy induces apoptosis in cancer cells [182-186]. Conversely, inhibition of apoptosis also induces macroautophagy in a reciprocal manner[173-176]. Moreover, many currently used chemotherapeutical agents induce the proliferation of autophagosomes *in vitro*, which is likely to represent a protective mechanism of cancer cells against the stress induced by cytotoxic agents. Conversely, inhibition of autophagy by various lysosomotropic agents has been shown to sensitize tumour cells to chemotherapy[180, 182, 184-189]. These findings suggest that apoptosis and macroautophagy are two complementary reciprocally regulated pathways for regulating the cell fate between death and survival. Targeting the autophagy regulation of cancer cells is a therapeutic strategy yet to be properly designed and, in fact, it is becoming obvious that such approaches will need to be tailored for every kind of tumour and stage of tumorigenesis.

Melanoma incidence has increased in last four decades and diverse therapies targeting specific molecules involved in melanoma progression are under evaluation [228, 229, 230]. The involvement of pathophysiological Ca^{2+} signalling in cancer promises new therapeutic strategies. There are a growing number of publications describing the expression of Ca^{2+} channel types in cancer, and the functional consequences of channel blockade on tumour parameters such as growth, migration or invasion. In this Thesis we present seminal data demonstrating the expression of a wide range of VGCCs in melanoma cells and the involvement of T-type channels in cell cycle control. We also show that human melanoma cells experience basal levels of adaptive UPR and macroautophagy, and that T-type channel blockers induce a caspase-dependent melanoma cell death through a sustained ER-stress and subsequent inhibition of the constitutive macroautophagy present in these cells. Finally, we identify T-type $Ca_v3.1$ and $Ca_v3.2$ channels as the targets for clinically used T-type channel blockers, by a gene silencing approach. Thus, our findings provide putative markers of melanoma progression, and the rationale for possible pharmacological therapies using T-type channel blockers, alone or in combination therapies, against melanoma progression.

Conclusions

1. Human melanoma cells and normal melanocytes express a diversity of voltage-gated calcium channels, including members of the Ca_v1 family (L-type) and Ca_v2 family (N-type, P/Q-type and R-type). Importantly, the expression of Ca_v3 family members (T-type) is detectable only in melanoma cells, in which mediates a constitutive influx of divalent cations in the absence of membrane depolarization, but not in normal untransformed melanocytes.

2. The expression of the $Ca_v3.1$ and $Ca_v3.2$ isoforms of T-type channels is mutually exclusive to a certain extent. $Ca_v3.1$ channels are prominently expressed in melanoma cell lines displaying a low or average proliferation rate, whereas $Ca_v3.2$ channels are the main T-type channel isoform in melanoma cell lines displaying a *fast* proliferation rate.

3. Both T-type $Ca_v3.1$ and $Ca_v3.2$ channels are involved in the melanoma cell cycle progression. Gene silencing of either isoform results in a significant degree of cell cycle arrest, as evidenced by increased percentage of cells at the G1 phase and decreased percentage of cells at the S-phase.

4. Moderate hypoxia (1% O_2) may induce the selective up-regulation of the T-type $Ca_v3.1$ isoform and, to a lesser extent, of the $Ca_v3.2$ isoform. These effects are dependent on the melanoma cell type. The hypoxia-mediated up-regulation of T-type channels is associated with an increased proliferation rate of the involved melanoma cell lines.

5. The application of the T-type channel blocker Kurtoxin, affects melanoma viability in a negative way, by promoting cell cycle arrest. In contrast, synthetic T-type channel pharmacological blockers with a therapeutic pedigree in cardiovascular and nervous system diseases, Mibefradil and Pimozide respectively, affect negatively the viability of melanoma cells at two levels: (1) by promoting cell cycle arrest; and (2) by inducing the intrinsic apoptosis pathway.

6. The melanoma cell death process triggered by T-type channel blockers Mibefradil and Pimozide is mediated by the induction of endoplasmic reticulum stress and

associated unfolded protein response, followed by inhibition of the constitutive autophagy present in these cells.

7. The knockdown of T-type $Ca_v3.1$ and $Ca_v3.2$ channels in melanoma cells also induces the unfolded protein response, and inhibits the constitutive autophagy. Thus, these T-type channel subtypes are the likely targets of T-type channel blockers, regarding the reported effects on melanoma cells homeostasis and viability.

Publications

Das A, Pushparaj C, Bahí N, Sorolla A, Herreros J, Pamplona R, Vilella R, Matias-Guiu X, Martí RM, Cantí C (2012) Functional expression of voltage-gated calcium channels in human melanoma; Pigment Cell Melanoma Res. 25(2):200-12

References

1. Clark WH, Jr., Tucker MA and Goldstein AM (1995) Parenchymal-stromal interactions in neoplasia.Theoretical considerations and observations in melanocytic neoplasia. Acta.Oncol. 34(6): 749-7571

2. Kaddu S, Smolle J, Zenahlik P, Hofmann-Wellenhof R, Kerl H.(2002) Melanoma with benign melanocytic naevus components: reappraisal of clinicopathological features and prognosis. Melanoma Res 12(3): 271-278

3. Weatherhead SC, Haniffa M and Lawrence CM (2007) Melanomas arising from naevi and de novo melanomas--does origin matter? Br J Dermatol 156(1): 72-76

4. Yovino J (2005) Thaller S Potential for development of malignant melanoma with congenital melanocytic nevi. J Craniofac Surg 16(5): 871-873

5. Jen M, Murphy M, Grant-Kels JM Childhood melanoma (2009) Clin Dermatol 27(6): 529-536

6. Yakov Chudnovsky, Paul A. Khavari, and Amy E. Adams (2005) Melanoma genetics and the development of rational therapeutics The Journal of Clinical Investigation 115 (4) (813-824)

7. Thompson JF, Scolyer RA, Kefford RF (2005) Cutaneous melanoma. Lancet 365 (9460): 687-701

8. Breslow A (1970) Thickness, cross-sectional areas and depth of invasion in the prognosis of cutaneous melanoma. *Ann Surg* **172**(5)**:** 902-908

9. Clark WH, Jr., From L, Bernardino EA, Mihm MC (1969) The histogenesis and biologic behavior of primary human malignant melanomas of the skin. *Cancer Res* **29**(3)**:** 705-727

10. Houghton AN, Polsky D (2002) Focus on melanoma. *Cancer Cell* **2**(4)**:** 275-278

11. Rigel DS, Carucci JA (2000) Malignant melanoma: prevention, early detection, and treatment in the 21st century. CA Cancer J Clin 50(4): 215-236; quiz 237-240

12. Vanessa Gray Schopfer, Claudia Wellbrock, Richard Marais (2007) Melanoma biology and new targeted therapy. Nature 445, 851-857

13. Jennings L, Murphy GM (2000) Predicting outcome in melanoma: where are we now? Br J Dermatol 161(3): 496-503

14. Gogas H, Eggermont AM, Hauschild A, Hersey P, Mohr P, Schadendorf D, Spatz A, Dummer R (2009) Biomarkers in melanoma. Ann Oncol 20 Suppl 6: vi8-13

15. Jemal A, Siegel R, Ward E, Hao Y, Xu J, Thun MJ (2009) Cancer statistics CA Cancer J Clin 2009; **59**(4)**:** 225-249

16. Marrett LD, King WD, Walter SD (1992) Use of host factors to identify people at high risk for cutaneous malignant melanoma CMAJ 147 (4)**:** 445-453

17. Claus Garbe, Ulrike Leiter (2009) Melanoma epidemiology and trends Clinics in Dermatology 27, 3-9

18. Cox J.L, Lancaster T and Carlson C.G. (2002) Changes in the motility of B16F10 melanoma cells induced by alterations in resting calcium influx. Melanoma Res. 12, 211–219.

19. Deli T, Varga N, Adam A et al.(2007) Functional genomics of calcium channels in human melanoma cells. Int. J. Cancer 121, 55–65.

20. Glass-Marmor L, Penso J, and Beitner R (1992) Ca^{2+} induced changes in energy metabolism and viability of melanoma cells.Br. J. Cancer 81, 219–224.

21. Oka M, Kikkawa U. (2005) Protein kinase C in melanoma.Cancer Metast Rev 24:287–300.

22. Demaurex N, Distelhorst C (2003) Apoptosis—the calcium connection. Science 300 :65-67

23. Allen DH, Lepple-Wienhues A, Cahalan MD (1997) Ion channel phenotype of melanoma cell lines. J Membr Biol 155:27–34.

24. MJ Berridge, MD Bootman, P Lipp (1998) Calcium—a life and death signal, Nature 395; 645–648.

25. MJ Berridge, P Lipp, MD Bootman (2000) The versatility and universality of calcium signalling, Nat. Rev. Mol. Cell Biol. 1;11–21.

26. M.J.Berridge, M.D. Bootman, H.L. Roderick (2003) Calcium signalling: dynamics, homeostasis and remodelling, Nat. Rev. Mol. Cell Biol. 4 517–529.

27. Michiaki Yamakage, Akiyoshi Namiki (2001) Calcium channels-basic aspects of their structure, function and gene encoding; anesthetic action on the channels - a review. Can J Anesth. 49: 2 (151–164)

28. Dolphin AC (2006) A short history of voltage-gated calcium channels. Br J Pharmacol.147 (Suppl 1): S56–S62.

29. Catterall WA (2000) Structure and regulation of voltage-gated Ca^{2+} channels. Annu .Rev. Cell Dev. Biol. 2000 16, 521–555

30. Bito H, Deisseroth, K & Tsien, RW (1997) Ca^{2+} dependent regulation in neuronal gene expression. Curr. Opin. Neurobiol; 419–429.

31. Ertel EA et.al. (2000) Nomenclature of voltage-gated calcium channels Neuron 25, 533–535

32. Spitzer NC, Gu X & Olson E (1994) Action potentials, calcium transients and the control of differentiation of excitable cells. Curr.Opin.Neurobiol.,4,70–77.

33. Marshall J., Dolan B.M., Garcia E.P., Sathe S., Tang X., Mao Z. & Blair L. A. (2003) Calcium channel and NMDA receptor activities differentially regulate nuclear C/EBPb levels to control neuronal survival. Neuron, 39, 625–639.

34. Nicotera P. & Orrenius S. (1998) The role of calcium in apoptosis. Cell Calcium, 23, 173–180.

35. Weick JP, Groth RD, Isaksen AL & Mermelstein PG (2003) Interaction with PDZ proteins are required for L-type calcium channels to activate cAMP response element-binding protein-dependent gene expression.J. Neurosci., 23, 3446–3456.

36. Toescu EC, Verkhratsky A & Landfield PW (2004) Ca^{2+} regulation and gene expression in normal brain aging. Trends Neurosci., 27, 614–620.

37. Dolmetsch RE, Pajvani U, Fife K, Spotts JM, Greenberg ME (2001) Signaling to the nucleus by an L-type calcium channel-calmodulin complex through the MAP kinase pathway. Science 294:333–339.

38. C R Kahl, A R Means (2003) Regulation of cell cycle progression by calcium / calmodulin - dependent pathways, Endocr. Rev. 24 719–736.

39. MJ Berridge (1995) Calcium signaling and cell proliferation, Bioessays 17 491–500.

40. Richard S, Neveu D, Carnac G, Bodin P, Travo P, Nargeot J (1992) Differential expression of voltage-gated Ca^{2+} currents in cultivated aortic myocytes. Biochem Biophys Acta.10; 1160(1):95-104.

41. Guo W, Kamiya K, Kodama I, Toyama J. (1998) Cell cycle-related changes in the voltage-gated Ca^{2+} currents in cultured newborn rat ventricular myocytes. J Mol Cell Cardiol. 30(6):1095-103.

42. Kuga T, Kobayashi S, Hirakawa Y, Kanaide H, Takeshita A (1996) Cell cycle--dependent expression of L- and T-type Ca^{2+} currents in rat aortic smooth muscle cells in primary culture. Circ Res. 79(1):14-9.

43. Panner, A, Cribbs LL, Zainelli GM, Origitano TC, Singh, S, Wurster RD (2005) Variation of T-type calcium channel protein expression affects cell division of cultured tumor cells. Cell Calcium 37:105–119.

44. DM Rodman, K Reese, JL Cribbs et.al. (2005) Low voltage- activated (T-type) calcium channels control proliferation of human pulmonary artery myocytes, Circ. Res. 96 864–872

45. N Akaike, H Kanaide, T Kuga, M Nakamura, J Sadoshima, H Tomoike (1989) Low-voltage-activated calcium current in rat aorta smooth muscle cells in primary culture, J. Physiol. 416 (1989) 141–160.

46. PA Boyden, CD Jack (1995) Ion channel function in disease, Cardiovasc.Res. 29. 312–318.

47. Marino AA et. al. (1994) Association between cell membrane potential and breast cancer. Tumour Biol. 15, 82–89

48. Prevarskaya N, Skryma R, Shuba Y (2010) Ion channels and the hallmarks of cancer. Trends Mol Med; 16:107–121

49. Zhang, WM. et. al. (2008) Endothelin-1 enhances proliferation of lung cancer cells by increasing intracellular free Ca^{2+} Life Sci. 82, 764–771

50. Brereton HM, Harland ML, Froscio M., Petronijevic T, Barritt GJ (1997) Novel variants of voltage-operated calcium channel alpha 1-subunit transcripts in a rat

liver-derived cell line: deletion in the IVS4 voltage sensing region. Cell Calcium 22, 39–52.

51. Li Y et al. (2007) FSH stimulates ovarian cancer cell growth by action on growth factor variant receptor. Mol. Cell Endocrinol. 267, 26–37

52. Yukihiro S, Posner GH, Guggino SE (1994) Vitamin D3 analogs stimulate calcium currents in rat osteosarcoma cells. J Biol Chem 269:23889–23893

53. Barry ELR, Gesek FA, Froehner SC, Friedman PA (1995) Multiple calcium channel transcriptions in rat osteosarcoma cells: selective activation of a1D isoform by parathyroid hormone. Proc Natl Acad Sci USA 92:10914–10918

54. Leipziger J, Fisher KG, Greger R (1994) Voltage-dependent Ca^{2+} influx in the epithelial cell line HT29: simultaneous use of intracellular Ca^{2+} measurements and nystatin perforated patch-clamp technique.Pflugers Arch 426:427–432

55. Bou-Hanna C, Berthon B, Combettes L, Claret M, Laboisse CL (1994) Role of calcium in carbachol- and neurotensin-induced mucin exocytosis in a human colonic goblet cell line and cross-talk with the cyclic AMP pathway. Biochem J 299(Suppl 2):S579–S585

56. Reinlib L, Mikkelsen R, Zahniser D, Dharmsathaphorn K, Donowitz M (1989) Carbachol-induced cytosolic free Ca^{2+} increases in T84 colonic cells seen by microfluorimetry. Am J Physiol 257:G950– G960

57. Wang XT, Nagaba Y, Cross HS, Wrba F, Zhang L and Guggino SE (2000) The mRNA of L-type calcium channel elevated in colon cancer: protein distribution in normal and cancerous colon. Am. J. Pathol. 157, 1549–1562.

58. Khazaie K, Schirrmacher V, Lichtner RB (1993) EGF receptor in neoplasia and metastasis. Cancer Metastasis12:255–274

59. Aaronson SA (1991) Growth factors and cancer. Science 254:1146–1153

60. Maa M-C, Leu T-H, McCarley DJ, Schatzman RC, Parsons SJ (1995) Potentiation of epidermal growth factor receptor-mediated oncogenesis by c-Src: implications for the etiology of multiple human cancers. Proc Natl Acad Sci USA 92:6981–6985

61. Hu XQ, Singh N, Mukhopadhyay D, Akbarali HI (1998) Modulation of voltage dependent Ca^{2+} channels in rabbit colonic smooth muscle cells by c-Src and focal adhesion kinase. J Biol Chem 273:5337–5342

62. Grassi C, D'Ascenzo M, Torsello A, Martinotti G, Wolf F, Cittadini A & Azzena GB (2004) Effects of 50 Hz electromagnetic fields on voltage gated Ca2+ channels and their role in modulation of neuroendocrine cell proliferation and death. Cell Calcium, 35, 307–315.

63. Green ME, Barrett FC, Bultynck G, Shamah SM, Dolmetsch RE (2007) The Tumor Suppressor eIF3e Mediates Calcium-Dependent Internalization of the L-Type Calcium Channel $Ca_V1.2$; Neuron 55(4): 615–632.

64. Zhang, L et. al. (1997) Gene expression profiles in normal and cancer cells. Science **276**, 1268–1272

65. Grafton, GL, Stokes L, Toellner KM, Gordon J (2003) A non-voltage-gated calcium channel with L-type characteristics activated by B cell receptor ligation. Biochem. Pharmacol. 66, 2001–2009.

66. Kotturi MF, Carlow DA, Lee JC, Ziltener HJ, Jefferies WA (2003) Identification and functional characterization of voltage-dependent calcium channels in T lymphocytes. J. Biol. Chem. 278, 46949–46960.

67. Latour I, Louw DF, Beedle AM, Hamid J, Zamponi GW (2004) Expression of T-type calcium channel splice variants in human glioma. Glia 48: 112-119

68. Lu F, Chen H, Zhou C, Liu S, Guo M, Chen P, Zhuang H, Xie D, Wu S (2008)T-type Ca^{2+} channel expression in human esophageal carcinomas: a functional role in proliferation. Cell Calcium 43: 49-58

69. Mariot P, Vanoverberghe K, Lalevee N, Rossier MF, Prevarskaya N (2002) Overexpression of an alpha 1H ($Ca_v3.2$) T-type calcium channel during neuroendocrine differentiation of human prostate cancer cells. J Biol. Chem. 277:10824–1083

70. CF Chen, MJ Corbley, TM Roberts, P Hess (1988) Voltage-sensitive calcium channels in normal and transformed 3T3 fibroblasts, Science 239 1024–1026.

71. JM Caffrey, AM Brown, MD Schneider (1987) Mitogens and oncogenes can block the induction of specific voltage-gated ion channels, Science 236 570–573.

72. MW Strobeck, M Okuda, H Schwartz, K Fukasawa (1999) Morphological transformation induced by activation of the mitogen-activated protein kinase pathway requires suppression of the T-type Ca^{2+} channel, J. Biol. Chem. 274 15694 –15700.

73. T Ueki, M Toyota, T Sohn, CJ Yeo, JP Issa, RH Hruban, M Goggins (2000) Hypermethylation of multiple genes in pancreatic adenocarcinoma, Cancer Res. 60 1835–1839.

74. L Shen, N Ahuja, Y Shen, NA Habib, M Toyota, A Rashid, JP Issa (2002) DNA methylation and environmental exposures in human hepatocellular carcinoma, J. Natl. Cancer Inst. 94 755–761.

75. Toyota M, Ho C, Ohe-Toyota M, Baylin SB, Issa JP (1999) Inactivation of CACNA1G, a T-type calcium channel gene by aberrant methylation of its 5' CpG island in human tumors. *Cancer Res* 59: 4535-4541

76. Taylor JT, Huang L, Pottle JE, Liu K, Yang Y, Zeng X, Keyser BM, Agrawal KC, Hansen JB, Li M (2008) Selective blockade of T-type Ca^{2+} channels suppresses human breast cancer cell proliferation. Cancer Lett 267: 116-124

77. Gray LS, Perez-Reyes E, Gomora JC, Haverstick DM, Shattock M, McLatchie L, Harper J, Brooks G, Heady T, Macdonald TL (2004) The role of voltage gated T-type Ca^{2+} channel isoforms in mediating "capacitative" Ca^{2+} entry in cancer cells. Cell Calcium 36: 489-497

78. Leuranguer V, Bourinet E, Lory P, Nargeot J (1998) Antisense depletion of beta-subunits fails to affect T-type calcium channels properties in a neuroblastoma cell line. Neuropharmacology 37: 701-708

79. Wyatt CN, Page KM, Berrow NS, Brice NL, Dolphin AC (1998) The effect of overexpression of auxiliary Ca^{2+} channel subunits on native Ca^{2+} channel currents in undifferentiated mammalian NG108-15 cells. J Physiol 510 (Pt 2): 347-360

80. Assandri R, Egger M, Gassmann M, Niggli E, Bauer C, Forster I, Gorlach A (1999) Erythropoietin modulates intracellular calcium in a human neuroblastoma cell line. J Physiol 516 (Pt 2): 343-352

81. Hirooka K, Bertolesi GE, Juhasz AE, Haynes LW, Barnes S (2002) T-Type calcium channel alpha1G and alpha1H subunits in human retinoblastoma cells and their loss after differentiation. J Neurophysiol 88: 196-205

82. Bertolesi GE, Shi C, Elbaum L, Jollimore C, Rozenberg G, Barnes S, Kelly ME (2002) The Ca^{2+} channel antagonists Mibefradil and Pimozide inhibit cell growth via different cytotoxic mechanisms. Mol Pharmacol 62: 210-219

83. Wang YQ, Brooks G, Zhu CB, Yuan WZ, Li YQ, Wu XS (2002) Functional analysis of the human T-type calcium channel alpha 1H subunit gene in cellular proliferation] Yichuan Xuebao 29: 659-665

84. Huang JB, Kindzelskii AL, Clark AJ, Petty HR (2004) Identification of channels promoting calcium spikes and waves in HT1080 tumor cells: their apparent roles in cell motility and invasion. Cancer Res 64: 2482-2489

85. Harkins AB, Cahill AL, Powers JF, Tischler AS, Fox AP (2003) Expression of recombinant calcium channels support secretion in a mouse pheochromocytoma cell line. J Neurophysiol 90: 2325-2333

86. Del Toro R, Levitsky KL, Lopez-Barneo J, Chiara MD (2003) Induction of T-type calcium channel gene expression by chronic hypoxia. J Biol Chem 278: 22316-22324

87. Lesouhaitier O, Chiappe A, Rossier MF (2001) Aldosterone increases T-type calcium currents in human adrenocarcinoma (H295R) cells by inducing channel expression. Endocrinology 142: 4320-4330

88. Zhuang H, Bhattacharjee A, Hu F, Zhang M, Goswami T, Wang L, Wu S, Berggren PO, Li M (2000) Cloning of a T-type Ca^{2+} channel isoform in insulin-secreting cells. Diabetes 49: 59-64

89. ME Williams, MS Washburn, M Hans, A Urrutia, PF Brust, P Prodanovich, MM Harpold, KA Stauderman (1999) Structure and functional characterization of a novel human low-voltage activated calcium channel, J. Neurochem. 72 791–799.

90. Paz MF et al.(2003) Genetic unmasking of epigenetically silenced tumor suppressor genes in colon cancer cells deficient in DNA methyl transferases. Hum.Mol.Genet. 12, 2209–2219

91. Wei Li W, Zhang SL, Wang N, Zhang B, Li M (2011) Blockade of T-Type Ca^{2+} Channels Inhibits Human Ovarian Cancer Cell Proliferation. Cancer Investigation, 29:339–346

92. Heo JH, Seo HN, Choe YJ, Kim, S, Oh CR, Kim YD, Rhim, H, Choo DJ, Kim J, Lee JY (2008) T-type Ca^{2+} channel blockers suppress the growth of human cancer cells. Bioorg Med Chem Lett 18:3899–3901.

93. Mergler S, Wiedenmann B, Prada J (2003) R-Type Ca^{2+} channel Activity Is Associated with Chromogranin A Secretion in Human Neuroendocrine Tumor BON Cells J. Membrane Biol. 194, 177–186

94. Li Y et. al. (2007) FSH stimulates ovarian cancer cell growth by action on growth factor variant receptor. Mol. Cell Endocrinol. 267, 26–37

95. Graus F, Lang B, Pozo-Rosich P et. al. (2002) P/Q type calcium channel antibodies in paraneoplastic cerebellar degeneration with lung cancer. Neurology 59:764-766

96. Monstad SE, Drivsholm L, Storstein A, Aarseth JH, Haugen M, Lang B, Vincent B, Vedeler CA (2002) Voltage-Gated Calcium Channel (VGCC) Antibodies Related to the Prognosis of Small-Cell Lung Cancer; Journal of clinical oncology 22

97. Chuang RS, Jaffe H, Cribbs L, Perez-Reyes E, Swartz KJ (1998) Inhibition of T-type voltage-gated calcium channels by a new scorpion toxin. Nat Neurosci 1:668–674.

98. SS Sidach, IM Mintz (2002) Kurtoxin, a gating modifier of neuronal high- and low threshold ca channels, J. Neurosci. 22 2023–2034.

99. Utako Yokohama et.al. (2006) (Multiple transcripts of Ca^{2+} channel α1-subunits and a novel spliced variant of the α1C-subunit in rat ductus arteriosus *Am J Physiol Heart Circ Physiol* 290: H1660–H1670

100. Mishra SK and Hermsmeyer K (1994) Selective inhibition of T-type Ca^{2+} channels by Ro 40-5967. *Circ Res* 75:144–148.

101. Lacinova´ L, Klugbauer N, and Hofmann F (2000) Regulation of the calcium channel α (1G) subunit by divalent cations and organic blockers. *Neuropharmacology* 39:1254–1266.

102. Mullins ME, Horowitz BZ, Linden DH, Smith GW, Norton RL, and Stump J (1998) Life-threatening interaction of Mibefradil and beta-blockers with dihydropyridine calcium channel blockers. *JAMA (J Am Med Assoc)* 280:157–158.

103. http://www.accessdata.fda.gov/scripts/opdlisting/oopd/OOPD_Results_2.cfm

104. P. Lijnen, R. Fagard, V. Petrov (1999) Mibefradil induced inhibition of proliferation of human peripheral blood mononuclear cells, J. Cardiovasc. Pharmacol. 33 595–604.

105. R Schmitt, JP Clozel, N Iberg, FR Buhler (1995) Mibefradil prevents neointima formation after vascular injury in rats. Possible role of the blockade of the T-type voltage-operated calcium channel, Arterioscler. Thromb. Vasc. Biol. 15 1161–1165.

106. JA Chemin, A Monteil, S Dubel, J Nargeot, P Lory (2001) The α1I T-type calcium channel exhibits faster gating properties when overexpressed in neuroblastoma/glioma NG 108–115, Eur. J. Neurosci.14 1678–1686

107. Taylor JT, Rider B, Huang L, Keyser B, Agrawal K, Li M (2004) A selective T-type calcium channel antagonist inhibits breast cancer cell growth (abstract). FASEB A996

108. Galizzi JP, Fosset M, Romey G, Laduron P, and Lazdunski M (1986) Neuroleptics of the diphenylbutylpiperidine series are potent calcium channel inhibitors. *Proc Natl Acad Sci USA* **83:**7513–7517

109. Enyeart JJ, Biagi BA, Day RN, Sheu SS, and Maurer RA (1990) Blockade of low and high threshold channels by diphenylbutylpiperidine antipsychotics linked to inhibition of prolactin gene expression. *J Biol Chem* **265:**16373–16379

110. Armoult CVM and Florman HM (1998) Pharmacological properties of the T-type Ca^{2+} current of mouse spermatogenic cells. *Mol Pharmacol* **53:**1104–1111

111. JS Strobl, Z Melkoumian, VA Peterson, H Hylton (1998) The cell death response to gamma-radiation in MCR-7 cells is enhanced by a neuroleptic drug, Pimozide, Breast Cancer Res. Treat. 51 83–95

112. GL Lee, WN Hait (1985) Inhibition of growth of C6 astrocytoma cells by inhibition of calmodulin, Life Sci. 36 (1985) 347–354

113. Neifeld JP, Tormey DC, Baker MA, Meyskens FL Jr, Taub RN (1983) Phase II trial of the dopaminergic inhibitor Pimozide in previously treated melanoma patients. Cancer Treat Rep.67(2):155-7

114. WF McCalmont, TN Heady, JR Patterson, MA Lindenmuth ,DM Haverstick, L S Gray, TL Macdonald (2004) Design, synthesis and biological evaluation of novel T-type calcium channel antagonists, Bioorg. Med. Chem. Lett. 14 3691–3695

115. C Armoult, J Lemos, H Florman (1997) Voltage-dependent modulation of T-type calcium channels by protein tyrosine phosphorylation, EMBO J. 16 1593–1599

116. R Scott, J Wootton, D Dolphin (1990) Modulation of neuronal T-type calcium channel currents by photoactivation of intracellular guanosine 5´-O (3-thio) triphosphate, Neuroscience 38 285–294

117. K Talavera, M Staes, A Janssens, G Droogmans, B Nilius (2004) Mechanism of arachidonic acid modulation of the T-type Ca^{2+} channel α1G, J. Gen. Physiol. 124 225–238

118. Z Wang, M Estacion, LJ Mordan (1993) Ca^{2+} influx via T-type channel modulates PDGF-induced replication of mouse fibroblasts, Am. J.Physiol. 265 C1239–C1246.

119. Jensen RL, Wurster RD (2001) Calcium channel antagonists inhibit growth of subcutaneous xenograft meningiomas in nude mice. Surg. Neurol. 55, 275–283

120. Yoshida J, Ishibashi T, Nishio M (2003) Antiproliferative effect of Ca^{2+} channel blockers on human epidermoid carcinoma A431 cells. European Journal of Pharmacology 472, 23–31, 2003

121. Yoshida J, Ishibashi T, Nishio M (2004) Antitumor effects of amlodipine, a Ca2+ channel blocker, on human epidermoid carcinoma A431 cells in vitro and in vivo. European Journal of Pharmacology 492, 103–112, 2004

122. Yoshida J, Ishibashi T, Nishio M (2007) G1 cell cycle arrest by amlodipine, a dihydropyridine Ca^{2+} channel blocker, in human epidermoid carcinoma A431 cells. Biochemical Pharmacology 73, 943–953

123. Lee YS, Sayeed MM, Wurster RD (1994) Inhibition of cell growth and intracellular Ca^{2+} mobilization in human brain tumor cells by Ca^{2+} channel antagonists. Mol. Chem. Neuropathol. 22, 81–95.

124. Taylor JM, Simpson RU (1992) Inhibition of cancer cell growth by calcium channel antagonists in the athymic mouse. Cancer Res. 52, 2413– 2418

125. Green DR (2005) Apoptotic pathways: ten minutes to dead. Cell; 121:671–4

126. Degterev A, Yuan J (2008) Expansion and evolution of cell death programmes. Nat Rev Mol Cell Biol 2008; 9:378–90

127. Adams JM (2003) Ways of dying: multiple pathways to apoptosis. Genes Dev 2003; 17:2481–95

128. Jensen, RL, Peter M, Wurster RD (2000) Calcium channel antagonist effect on in vitro meningioma signal transduction pathways after growth factor stimulation. Neurosurgery 46,692– 702

129. R Rizzuto, M Brini, M Murgia, T Pozzan (1993) Microdomains with high Ca^{2+} close to IP_3-sensitive channels that are sensed by neighbouring mitochondria Science 262(5134):744-7

130. Arnaudeau S, Kelley WL, Walsh JV Jr, Demaurex N (2001) Mitochondria recycle Ca^{2+} to the endoplasmic reticulum and prevent the depletion of neighbouring endoplasmic reticulum regions. 276(31):29430-9

131. G Hajnoczky, LD Robb-Gaspers, LD Seitz, AP Thomas (1995) Decoding of cytosolic calcium oscillations in the mitochondria Cell 82(3):415-24

132. G Hajnoczky, G Csordas, M Yi (2002) Old players in a new role: mitochondria-associated membranes, VDAC, and ryanodine receptors as contributors to calcium signal propagation from endoplasmic reticulum to the mitochondria. Cell Calcium 32(5-6):363-77

133. P Pacher, G Hajnoczky (2001) Propagation of the apoptotic signal by mitochondrial waves. EMBO J. 20(15):4107-21

134. Oyadomari S, Mori M (2004) Roles of CHOP/GADD153 in endoplasmic reticulum stress Cell Death Differ 11,381-389

135. DG Breckenridge, M Germain, JP Mathai, M Nguyen, GC Shore (2003) Regulation of apoptosis by endoplasmic reticulum pathways, Oncogene 22 8608–8618.

136. R Rizzuto, P Pinton, M Chami, G Szabadkai, PJ Magalhaes, F Di Virgilio, T Pozzan (2003) Calcium and apoptosis: facts and hypotheses, Oncogene 22 8619–8627.

137. RV Rao, HM Ellerby, DE Bredesen (2004) Coupling endoplasmic reticulum to the cell death program, Cell Death Diff. 11 372–380.

138. Kaufman RJ (1999) Stress signaling from the lumen of the endoplasmic reticulum: coordination of gene transcriptional and translational controls. Genes Dev13: 1211–1233

139. Rao RV, Hermel E, Castro-Obregon S, Del Rio G, Ellerby LM, Ellerby HM and Bredesen DE (2001) Coupling endoplasmic reticulum stress to the cell death program. Mechanism of caspase activation. J. Biol. Chem. 276: 33869–33874

140. Liu H, Bowes III RC, van de Water B, Sillence C, Nagelkerke JF and Stevens JL (1997) Endoplasmic reticulum chaperones GRP78 and calreticulin prevent oxidative stress, Ca^{2+} disturbances, and cell death in renal epithelial cells. J.Biol. Chem. 272: 21751–21759

141. Rao R, Poksay K, Castro-Obregon S, Schiilling B, Row RH, dcl Rio G, Gibson BW, Ellerby HM and Bredesen DE (2004) Molecular components of a cell death pathway activated by endoplasmic reticulum stress. J. Biol. Chem. 279:177–187

142. Peter Hersey, Xu Dong Zhang (2008) Adaptation to ER stress as a driver of malignancy and resistance to therapy in human melanoma. Pigment Cell Melanoma Res. 21; 358–367

143. Yorimitsu T, Nair U, Yang Z, Klionsky DJ (2006) Endoplasmic reticulum stress triggers autophagy Biol. Chem. 281: 30299–30304.

144. Høyer-Hansen M, Bastholm L, Szyniarowski P, Campanella M, Szabadkai G, Farkas T et. al. (2007) Control of macroautophagy by calcium, calmodulin-dependent kinase kinase-b and Bcl-2. Mol Cell 25: 193–205.

145. Kouroku Y, Tanida I, Ueno T, Isoai A, Kumagai H et. al. (2007) ER stress (PERK/eIF2α phosphorylation) mediates the polyglutamine-induced LC3

conversion, an essential step for autophagy formation. Cell Death Differ14: 230–239.

146. M Høyer-Hansen, M Jaattela (2007) Connecting endoplasmic reticulum stress to autophagy by unfolded protein response and calcium. Cell Death Differ 14, 1576–1582

147. Kroemer G, Mariño G, Levine B (2010) Autophagy and the Integrated Stress Response. Mol. Cell 40; 280-293.

148. Mijaljica D, Prescott M, Devenish RJ (2011) Microautophagy in mammalian cells: revisiting a 40-year-old conundrum. Autophagy.7(7):673-82.

149. Arias E, Cuervo AM (2011) Chaperone-mediated autophagy in protein quality control. Curr Opin Cell Biol.23(2):184-9

150. Levine B, Klionsky DJ (2004) Development by self-digestion: molecular mechanisms and biological functions of autophagy. Dev Cell 6: 463–477.

151. Kroemer G, Jaattela (2005) M. Lysosomes and autophagy in cell death control. Nat Rev Cancer 5: 886–897.

152. Codogno P, Meijer AJ (2005) Autophagy and signaling: their role in cell survival and cell death. Cell Death Differ12 (Suppl 2): 1509–1518.

153. Sabatini DM (2006) mTOR and cancer: insights into a complex relationship. Nat Rev Cancer 6: 729–734

154. Fader CM, Sanchez D, Furlan M and Colombo MI (2008) Induction of autophagy promotes fusion of multivesicular bodies with autophagic vacuoles in k562 cells. Traffic 9, 230–250.

155. Hay JC (2007) Calcium: a fundamental regulator of intracellular membrane fusion? EMBO Rep. 8, 236–240.

156. Decuypere JP, Bultynck G, Parys JB (2011) A dual role for Ca^{2+} in autophagy regulation Cell Calcium.50(3):242-50

157. Demarchi F, Bertoli C, Copetti T, Tanida I, Brancolini C et.al. (2006) Calpain is required for macroautophagy in mammalian cells. J Cell Biol175: 595–605.

158. Yousefi S, Perozzo R, Schmid I, Ziemiecki A, Schaffner T, Scapozza L et. al. (2006) Calpain-mediated cleavage of Atg5 switches autophagy to apoptosis. Nat Cell Biol 8:1124–1132

159. Handerson T, Pawelek, J. (2003) β1, 6-branched oligosaccharides and coarse vesicles: a common and pervasive phenotype in melanoma and other human cancers. Cancer Res ; 63: 5363.

160. Handerson T, Berger A, Harigopol M, et. al. (2007) Melanophages reside in hypermelanotic aberrantly glycosylated tumor areas and predict improved outcome in primary CMM. J Cutan Pathol ; 34: 667.

161. Jensen, RL, Origitano TC, Lee YS, Weber M, Wurster RD (1995) In vitro growth inhibition of growth factor-stimulated meningioma cells by calcium channel antagonists. Neurosurgery 36, 365– 373.

162. Mizushima N (2010) The role of the Atg1/ULK1 complex in autophagy regulation. Current Opinion in Cell Biology 22:132–139

163. Ogata M, Hino S, Saito A, Morikawa K, Kondo S, Kanemoto S et. al. (2006) Autophagy is activated for cell survival after endoplasmic reticulum stress. Mol. Cell Biol. 26: 9220–9231.

164. Moscat J and Diaz-Meco MT (2009) P62 at the crossroads of autophagy, apoptosis, and cancer. Cell 137, 1001–1004.

165. Bjorkoy G, Lamark T, Brech A, Outzen H, Perander M, Overvatn A, Stenmark H and Johansen T (2005) P62/SQSTM1 forms protein aggregates degraded by

autophagy and has a protective effect on huntingtin-induced cell death. J. Cell Biol. 171, 603–614.

166. Pankiv S. et al. (2007) P62/SQSTM1 binds directly to Atg8/LC3 to facilitate degradation of ubiquitinated protein aggregates by autophagy. J. Biol. Chem. 282, 24131–24145.

167. Ichimura Y. et al. (2008) Structural basis for sorting mechanism of p62 in selective autophagy. J. Biol. Chem. 283, 22847–22857.

168. Yue Z, Jin S, Yang C, Levine AJ, Heintz N (2003) Beclin 1, an autophagy gene essential for early embryonic development, is a haploinsufficient tumor suppressor. Proc Natl Acad Sci U S A100:15077–82.

169. Qu X, Yu J, Bhagat G, et.al. (2003) Promotion of tumorigenesis by heterozygous disruption of the Beclin 1 autophagy gene. J Clin Invest; 112:1809–20.

170. Kondo Y, Kanzawa T, Sawaya R, Kondo S. (2005) The role of autophagy in cancer development and response to therapy. Nat Rev Cancer ; 5:726–34.

171. Feng Z, Zhang H, Levine AJ, Jin S.(2005) The coordinate regulation of the p53 and mTOR pathways in cells. Proc Natl Acad Sci U S A ; 102 : 8204–9.

172. Arico S, Petiot A, Bauvy C et al. (2001) The tumor suppressor PTEN positively regulates macroautophagy by inhibiting the phosphatidylinositol 3-kinase/protein kinase B pathway. J Biol Chem 276:35243–6.

173. Boya P, Gonzalez-Polo RA, Casares N et. al. (2005) Inhibition of macroautophagy triggers apoptosis. Mol Cell Biol 25:1025–40.

174. Lum JJ, Bauer DE, Kong M et. al. (2005) Growth factor regulation of autophagy and cell survival in the absence of apoptosis. Cell; 120:237–48.

175. Maiuri MC, Zalckvar E, Kimchi A, Kroemer G (2007) Self-eating and selfkilling: crosstalk between autophagy and apoptosis. Nat Rev Mol Cell Biol 8:741–52.

176. White E, DiPaola RS (2009) The double-edged sword of autophagy modulation in cancer. Clin Cancer Res; 15:5308–16.

177. Miracco C, Cevenini G, Franchi A et.al. (2010) Beclin 1 and LC3 autophagic gene expression in cutaneous melanocytic lesions Hum Pathol.41(4):503-12

178. Lazova R, Pawelek J. (2009) Why do melanomas get so dark? Exp Dermatol; in press.

179. Lazova R, Klump V, Pawelek J (2010) Autophagy in cutaneous malignant melanoma. J Cutan Pathol.37(2):256-68

180. Ma X, H Piao S, Wang D et.al (2011) Measurements of tumor cell autophagy predicts invasiveness, resistance to chemotherapy, and survival in melanoma. Clin Cancer Res;17:3478-89

181. Degenhardt K, Mathew R, Beaudoin B, Bray K, Anderson D, Chen G et. al. (2006) Autophagy promotes tumor cell survival and restricts necrosis, inflammation, and tumorigenesis. Cancer Cell; 10:51–64.

182. Han J, Hou W, Goldstein L A, Lu C, Stolz D B, Yin X M et. al. (2008) Involvement of protective autophagy in TRAIL resistance of apoptosis-defective tumor cells. J Biol Chem; 283:19665–77.

183. Shacka JJ, Klocke BJ, Roth KA (2006) Autophagy, bafilomycin and cell death: the "a-B-cs" of plecomacrolide-induced neuroprotection.Autophagy 2:228–30.

184. Amaravadi RK, Yu D, Lum JJ, Bui T, Christophorou MA, Evan G et. al. (2007) Autophagy inhibition enhances therapy-induced apoptosis in a Mycinduced model of lymphoma. J Clin Invest 117:326–36.

185. Li J, Hou N, Faried A, Tsutsumi S, Kuwano H (2010) Inhibition of autophagy augments 5-fluorouracil chemotherapy in human colon cancer in vitro and in vivo model. Eur J Cancer 46:1900–9.

186. Carew JS, Medina EC, Esquivel JA 2nd, Mahalingam D, Swords R, Kelly K et al. (2010) Autophagy inhibition enhances vorinostat-induced apoptosis via ubiquitinated protein accumulation. J Cell Mol Med 14:2448–59.

187. Wu Z, Chang PC, Yang JC, Chu CY, Wang LY, Chen NT, et. al. (2010) Autophagy blockade sensitizes prostate cancer cells towards Src family kinase inhibitors. Genes Cancer ; 1:40–9.

188. Ruiz-Irastorza G, Ramos-Casals M, Brito-Zeron P, Khamashta MA (2010) Clinical efficacy and side effects of antimalarials in systemic lupus erythematosus: a systematic review. Ann Rheum Dis 69:20–8.

189. Rosenfeld MR, Grossman SA, Brem S, Mikkelsen T, Wang D, Piao S et. al. (2010) Pharmacokinetic analysis and pharmacodynamic evidence of autophagy inhibition in patients with newly diagnosed glioblastoma treated on a phase I trial of hydroxychloroquine in combination with adjuvant temozolomide and radiation (ABTC 0603). J Clin Oncol 28:15s.

190. Ding WX, Ni HM, Gao W, Chen X, Kang JH, Stolz DB, et. al. (2009) Oncogenic transformation confers a selective susceptibility to the combined suppression of the proteasome and autophagy. Mol. Cancer Ther. 8:2036–45.

191. Hara T, Nakamura K, Matsui M, Yamamoto A, Nakahara Y, Suzuki-Migishima R, Yokoyama M, Mishima K, Saito I, Okano H, Mizushima N (2006) Suppression of basal autophagy in neural cells causes neurodegenerative disease in mice. Nature 15 ; 441 (7095):885-9.

192. Komatsu M et. al. (2006) Loss of autophagy in the central nervous system causes neurodegeneration in mice. *Nature* 441, 880–884

193. Pua HH, Dzhagalov I, Chuck M, Mizushima N & He YW (2007) A critical role for the autophagy gene *Atg5* in T cell survival and proliferation. *J. Exp. Med.* 204, 25–31

194. Takacs-Vellai K. et. al. (2005) Inactivation of the autophagy gene *bec-1* triggers apoptotic cell death in *C. elegans*. Curr. Biol. 15, 1513–1517.

195. Ganley IG, Wong PM, Gammoh N, Jiang X (2011) Distinct autophagosomal-lysosomal fusion mechanism revealed by Thapsigargin-induced autophagy arrest. Mol Cell. 42(6):731-43.

196. Katayama M, Kawaguchi T, Berger MS, Pieper RO (2007) DNA damaging agent-induced autophagy produces a cytoprotective adenosine triphosphate surge in malignant glioma cells. Cell Death Differ 2007; 14:548–58.

197. Carew JS, Nawrocki ST, Kahue CN, Zhang H, Yang C, Chung L et al. (2007) Targeting autophagy augments the anticancer activity of the histone deacetylase inhibitor SAHA to overcome Bcr-Abl-mediated drug resistance. Blood 110:313–22.

198. Gonzalez-Polo RA. et al. (2005) The apoptosis/autophagy paradox: autophagic vacuolization before apoptotic death. J. Cell Sci. **118**, 3091–3102 (2005).

199. Kroemer G, Galluzzi L, Brenner C (2007) Mitochondrial membrane permeabilization in cell death. Physiol.Rev. **87**, 99–163.

200. Rubinsztein DC, Gestwicki JE, Murphy, LO & Klionsky DJ (2007) Potential therapeutic applications of autophagy. Nature Rev. Drug Discov.**6**, 304–312.

201. Zhineng J. Yang, Cheng E. Chee, Shengbing Huang et. al. (2011) The Role of Autophagy in Cancer: Therapeutic Implications Mol Cancer Ther 10:1533-1541

202. Sorolla, A, Yeramian A, Dolcet X et. al. (2008) Effect of proteasome inhibitors on proliferation and apoptosis of human cutaneous melanoma-derived cell lines. Br. J. Dermatol. 158, 4 96–504.

203. Jacob R (1990) Agonist-stimulated divalent cation entry into single cultured human umbilical vein endothelial cells. J. Physiol. (Lond.) 421, 55–77.

204. Kaku U, Lee TS, Arita M, Hadama T, Ono K (2003) The gating and conductance properties of $Ca_v3.2$ low-voltage-activated T-type calcium channels. Jpn. J. Physiol. 53, 165–172.

205. Jiang CC, Chen LH, Gillespie S, Wang YF, Kiejda KA, Zhang XD, Hersey P (2007) Inhibition of MEK sensitizes human melanoma cells to endoplasmic reticulum stress-induced apoptosis. Cancer Res 67:9750–9761.

206. Nakamura M, Gotoh T, Okuno Y, Tatetsu H, Sonoki T, Uneda S, Mori M, Mitsuya H, Hata H (2006) Activation of the endoplasmic reticulum stress pathway is associated with survival of myeloma cells. Leuk Lymphoma 47:531–539.

207. Loechner KJ, Salmon WC, Fu J, Patel S and McLaughlin JT (2009) Cell cycle-dependent localization of voltage-dependent calcium channels and the mitotic apparatus in a neuroendocrine cell line (AtT-20). Int. J. Cell Biol. 487959, 1–12.

208. Silver DL, Pavan WJ (2006) The origin and development of neural crest-derived melanocytes. In Melanocytes to Melanoma, Vol. I, V.J. Hearing, and S.P. Leong, eds. (Totowa, NJ: Humana Press), pp. 3–26.

209. Evans RM, Zamponi GW (2006) Presynaptic calcium channels integration centres for neuronal signaling pathways. Trends Neurosci. 29, 617–624.

210. Bedogni B, Powell MB (2006) Skin hypoxia: a promoting environmental factor in melanomagenesis. Cell Cycle 5, 1258–1261.

211. Pluteanu F, Cribbs LL (2009) T-type calcium channels are regulated by hypoxia/reoxygenation in ventricular myocytes. Am. J. Physiol. Heart Circ. Physiol. 297, H1304–h1313.

212. Wang G, Yang ZQ, Zhang K (2010) Endoplasmic reticulum stress response in cancer: molecular mechanism and therapeutic potential. Am J Transl Res.1;2 (1) : 65-74.

213. Rossier MF (2006) T channels and steroid biosynthesis: in search of a link with mitochondria. Cell Calcium 40 (2):155-64.

214. Kabeya Y, Mizushima N, Ueno T, Yamamoto A, Kirisako T, Noda T, Kominami E, Ohsumi Y, Yoshimori T (2000) LC3, a mammalian homologue of yeast Apg8p, is localized in autophagosome membranes after processing. EMBO J. 1; 19 (21) : 5720-8.

215. Mizushima N, Yoshimori T (2007) How to interpret LC3 immunoblotting. Autophagy 3:542-5.

216. Koschak A, Reimer D, Huber I, Grabner M, Glossmann H, Engel J, Striessnig J (2001) α1D ($Ca_v1.3$) subunits can form L-type calcium channels activating at negative voltages. J. Biol. Chem. 276, 22100–22106.

217. Lipscombe D, Helton TD and Xu W (2004) L-type calcium channels: the low down. J. Neurophysiol. 92, 2633–2641.

218. Triggle DJ (2003) 1,4-Dihydropyridines as calcium channel ligands and privileged structures. Cell. Mol. Neurobiol. 23, 293–303.

219. Slomisnky A (2009) Neuroendocrine activity of the melanocyte. Exp. Dermatol. 18, 760–763.

220. Marcantoni A, Baldelli P, Hernandez-Guijo JM, Comunanza V, Carabelli V and Carbone E (2007) L-type Ca^{2+} channels in adrenal chromaffin cells: role in pace-making and secretion. Cell Calcium 42, 397–408.

221. Eyden B, Pandit D and Banerjee SS (2005) Malignant melanoma with neuroendocrine differentiation: clinical, histological, immunohistochemical and ultrastructural features of three cases. Histopathology 47, 402–409.

222. Taylor JT, Zeng XB, Pottle JE, Lee K, Wang AR, Yi SG, Scruggs JA, Sikka SS *and* Li M (2008) Ca^{2+} signaling and T-type calcium channels in cancer cell cycling. World J. Gastroenterol. 14, 4984–4991.

223. Panner A, Wurster RD (2006) T-type calcium channels and tumour proliferation. Cell Calcium 40, 253–259.

224. Williams A, Sarkar S, Cuddon P et al. (2008) Novel targets for Huntington's disease in an mTOR-independent autophagy pathway. Nat. Chem. Biol. 4, 295–305.

225. Kahl CR, Means AR (2003) Regulation of cell cycle progression by calcium/calmodulin-dependent pathways. Endocr. Rev. 24, 719–736.

226. Brewer JW, Hendershot LM, Sherr CJ, Diehl JA (1999) Mammalian unfolded protein response inhibits Cyclin D1 translation and cell-cycle progression**.** Proc Natl Acad Sci U S A. 96(15):8505-10.

227. Kwong L, Chin L, Wagner SN (2007) Growth factors and oncogenes as targets in melanoma: lost in translation? Adv. Dermatol. 23, 99–129.

228. Mayorga ME, Sanchis D, Perez de Santos AM et. al. (2006) Antiproliferative effect of STI571 on cultured human cutaneous melanoma-derived cell lines. Melanoma Res. 16, 127–135

229. Yeramian A, Sorolla A, Velasco A et. al. (2011) Inhibition of activated receptor tyrosine kinases by Sunitinib induces growth arrest and sensitises melanoma cells to Bortezomib by blocking Akt pathway. Int. J. Cancer 130, 967–978.

230. Martinez-Alonso M, Llecha N, Mayorga ME et. al. (2009) Expression of somatostatin receptors in human melanoma cell lines: effect of two different somatostatin analogues, octreotide and SOM230, on cell proliferation. J. Int. Med. Res. 37, 1813–1822.

231. Nilius B, Prenen J, Kamouchi M, Viana F, Voets T, and Droogmans G (1997) Inhibition by Mibefradil, a novel calcium channel antagonist, of Ca^{2+} and volume activated Chloride channels in macrovascular endothelial cells. *Br J Pharmacol* 121:547–555.

232. Moretti L, Cha YI, Lu B (2007) Switch between apoptosis and autophagy: radiation- induced endoplasmic reticulum stress? Cell Cycle; 6: 793-8.

233. Boyce M, Bryant KF, Jousse C, Long K, Harding HP, Scheuner D, Kaufman RJ, Ma D, Coen DM, Ron D, Yuan J (2005) A selective inhibitor of eIF2α dephosphorylation protects cells from ER stress. Science ; 307:935-9.

234. Martin RL, Lee JH, Cribbs LL, Perez-Reyes E, Hanck DA (2000) Mibefradil block of cloned T-type calcium channels. J Pharmacol Exp Ther.; 295(1):302-8.

235. Santi CM, Cayabyab FS, Sutton KG, McRory JE, Mezeyova J, Hamming KS, Parker D, Stea A, Snutch TP (2002) Differential inhibition of T-type calcium channels by neuroleptics. J Neurosci. 15; 22(2):396-403.

236. Liu JH, Bijlenga P, Occhiodoro T, Fischer-Lougheed J, Bader CR, Bernheim L. (1999) Mibefradil (Ro 40-5967) inhibits several Ca^{2+} and K^{+} currents in human fusion-competent myoblast. Br J Pharmacol; 126(1): 245-50.

237. McNulty MM, Hanck DA (2004) State-dependent Mibefradil block of Na^{+} channels. Mol. Pharmacol. 66(6):1652-61.

238. Keilholz U, Suciu S, Bedikian AY, Punt, CJ, Gore M, Kruit W, Pavlick AC., Spatz A, Gilles E, Eggermont AM (2007) LDH is a prognostic factor in stage IV melanoma patients (pts) but is a predictive factor only for bcl2 antisense treatment efficacy: Re-analysis of GM301 and EORTC18951 randomized trials. American Society of Clinical Oncology Meeting, Abstract 8552, 485s.

239. Rutkowski DT, Kaufman RJ (2007) That which does not kill me makes me stronger: adapting to chronic ER stress. Trends Biochem Sci. 32(10):469-76.

240. Li X, Zhang K, Li Z (2011) Unfolded protein response in cancer: the physician's perspective. J Hematol Oncol. Feb 23;4:8

241. Scheuner D, Song B, McEwen E, Liu C, Laybutt R, Gillespie P, Saunders T, Bonner-Weir S and Kaufman RJ (2001) Translational control is required for the unfolded protein response and in vivo glucose homeostasis. Mol. Cell 7:1165–1176.

242. Harding HP, Novoa II, Zhang Y, Zeng H, Wek R, Schapira M, Ron D (2000) Regulated translation initiation controls stress-induced gene expression in mammalian cells. Mol. Cell 6: 1099–1108.

243. Okada T, Yoshida H, Akazawa R, Negishi M and Mori K (2002) Distinct roles of activating transcription factor 6 (ATF6) and double-stranded RNA-activated protein kinase-like endoplasmic reticulum kinase (PERK) in transcription during the mammalian unfolded protein response. Biochem. J. 366: 585–594 2007

244. Klionsky DJ, Cuervo AM, Seglen PO (2007) Methods for monitoring autophagy from yeast to human. Autophagy 3(3):181-206

245. Brinda Ravikumar, Sovan Sarkar, Janet E. Davies et.al. (2010) Regulation of mammalian autophagy in physiology and pathophysiology *Physiol Rev*. 90: 1383–1435

246. Noboru Mizushima and Daniel J. Klionsky (2007) Protein Turnover Via Autophagy: Implications for Metabolism Annual Review of Nutrition ; 27:19-40.

247. Robin Mathew, Vassiliki Karantza-Wadsworth and Eileen White (2007) Role of autophagy in cancer Nat. Rev. Cancer 7; 961-967

248. Calfon M, Harding HP (2004) Marcie Calfon's & Heather Harding's protocol for detection of XBP-1 processing in mouse or human cells (http://saturn. med.nyu.edu /research/mp/ronlab/protocols/XBP-1.splicing.04.09.16.pdf).

249. Calfon M, Zeng H, Urano F, Till JH, Hubbard SR, Harding HP, Clark SG, Ron D (2002) IRE1 couples endoplasmic reticulum load to secretory capacity by processing the XBP-1 mRNA. Nature 415: 92–96